

The Henryk Niewodniczański
INSTITUTE OF NUCLEAR PHYSICS
Polish Academy of Sciences
152 Radzikowskiego str., 31-342 Kraków, Poland

www.ifj.edu.pl/reports/2004.html
Kraków, listopad 2004

Report No 1951/AP

**XXXVII Polish Seminar on Nuclear Magnetic Resonance
and Its Applications. Kraków, 1-2 December 2004**

ABSTRACTS

Organizing Committee:

<i>K. Banaś</i>	<i>P. Kulinowski</i>
<i>T. Banasik</i>	<i>S. Kwieciński</i>
<i>A. Birczyński</i>	<i>M. Labak</i>
<i>J. Blicharski</i>	<i>Z. T. Lalowicz</i>
<i>P. Borowiec</i>	<i>K. Majcher</i>
<i>S. Heinze-Paluchowska</i>	<i>M. Noga /secretary/</i>
<i>J. W. Hennel /chairman/</i>	<i>Z. Olejniczak</i>
<i>A. Jasiński /v-chairman/</i>	<i>T. Skórka</i>
<i>A. Korzeniowska</i>	<i>Z. Sulek</i>
<i>A. Krzyżak</i>	<i>W. Węglarz</i>

Sponsors:

Varian International AG
Bruker Polska Sp. z o.o
AMX-ARMAR AG

Addresses of the sponsors:

Varian International AG

mgr inż. W. Kośmider
ul. Skarbka 21
60-348 Poznań
tel. (061) 867 31 84
tel. kom. 602 287 918
e-mail: woko@polbox.com
www.varianinc.com

Bruker Polska Sp. z o.o

ul. Budziszewska 69
60-179 Poznań
tel. (061) 868 90 08
fax. (061) 868 90 96
e-mail: sekretariat@bruker.poznan.pl
www.bruker.poznan.pl

AMX-ARMAR AG

Anna Potrzebowska

ul. Bułgarska 12a
93-362 Łódź
tel. (042) 645 00 64

CONTENTS:

DTI STUDY OF PATIENTS WITH SPONDYLOTIC MYELOPATHY OF THE CERVICAL SPINAL CORD T. Banasik, M. Hartel, A. Kiełtyka, M. Konopka, T. Skórka, and A. Jasiński	11
EQUILIBRIUM AND NON-EQUILIBRIUM DIFFUSION MEASUREMENTS IN ZEOLITES BY NMR TECHNIQUES Krzysztof Banaś, Federico Brandani, Douglas M. Ruthven, Frank Stallmach, and Jörg Kärger	12
ONE-BOND CARBON-CARBON COUPLING CONSTANTS ($^1J_{CC}$) IN DERIVATIVES OF QUINOLIZINE. AN INFLUENCE OF THE PROTONATION Elżbieta Bednarek, Małgorzata Bechcicka, Krystyna Kamieńska-Trela, and Lidia Kania	13
NMR-BASED METHOD FOR THE LOCATION OF AMINO ACID MOIETIES IN BACTERIAL OLIGOSACCHARIDES Piotr Bernatowicz, Andrzej Ejchart, Gabriela Pastuch-Gawolek, Wiesław Szeja, Tomasz Lipiński, and Andrzej Gamian.....	15
^{19}F NMR SPECTRA OF CIPROFLOXACIN Antoni Bijak, Barbara Blicharska, and Paola Porcari	16
T_1 AND $T_{1\rho}$ PROTON RELAXATION TIMES OF STARCH Barbara Blicharska, Magdalena Hyjek, and Joanna Szymońska	17
NMR RELAXATION IN BIOPOLYMERS (CELLULOSE AND STARCH) Barbara Blicharska and Magdalena Hyjek.....	18
MAGNETIC ROTATIONAL RESONANCE AND CROSS RELAXATION IN GASES Jerzy S. Blicharski.....	19
INTERACTION OF FLAVONOID TOPOISOMERASES I AND II INHIBITORS WITH DNA OLIGOMERS Wojciech Bocian, Robert Kawęcki, Elżbieta Bednarek, Jerzy Sitkowski, Agnieszka Parcińska, and Lech Kozerski	20
INTERACTION OF THE CAMPTOTHECIN FAMILY WITH DNA OLIGOMERS Wojciech Bocian, Elżbieta Bednarek, Jerzy Sitkowski, Agnieszka Parcińska, and Lech Kozerski.....	21

NMR STUDY OF $SM_2CO_{17}H_x$ HYDRIDES Marta Borowiec, Czesław Kapusta, Małgorzata Jasiurkowska, Peter C. Riedi, and Jan Żukrowski	22
ARTIFACTS PRODUCED BY DENTAL MATERIALS IN MR IMAGING Amira Bryll, Andrzej Urbanik, Anna Jurczak, Maria Chomyszyn-Gajewska, Stanisław Sztuk, Małgorzata Szafirska, and Barbara Sobiecka	23
NON-CARTESIAN SAMPLING IN MRI: RADIAL AND SPIRAL SEQUENCES Katarzyna Cieślak, Katarzyna Suchanek, Mateusz Suchanek, Tadeusz Pałasz, Tomasz Dohnalik, and Zbigniew Olejniczak	24
“THROUGH SPACE” J-COUPPLINGS OF THE PERI-F ATOM TO THE CH_3 PROTONS IN A TETRAFLURO DERIVATIVE OF 9-METHYLTRIPTYCENE. STRENGTHENED EVIDENCE OF BLUE-SHIFTING HYDROGEN BOND I. Czernski, K. Kamińska-Trela, T. Ratajczyk, S. Szymanski, and J. Wojcik	25
NMR STUDIES OF 5β -SPIROST-25(27)-EN- $1\beta,2\beta,3\beta$ - 5β -TETROL AND ITS 25,27-DIHYDRO DERIVATIVE, NEW SAPOGENINS FROM CONVALLARIA MAJALIS L. Karolina Dąbrowska-Balcerzak, Edyta Pindelska, Jadwiga Nartowska, and Iwona Wawer.....	26
DETERMINATION OF THE AMPLITUDE OF SPIN MOTIONS BY THE ANALYSIS OF SIDE BANDS IN THE NMR SPECTRUM Artur Freda and Czesław Lewa	27
NMR DIFFUSION STUDIES USING ULTRAHIGH STATIC MAGNETIC FIELD GRADIENTS Franz Fujara.....	29
^{13}C -NMR STUDY OF MICROSTRUCTURE OF BUTYL ACRYLATE-METHYL METHACRYLATE COPOLYMERS Magdalena Gołąbek, Piotr Bujak, and Marek Matlengiewicz	30
NMR FINGERPRINT OF 2,5-DIHYDROXYPHENYLACETIC (HOMOGENITISIC) ACID Adam Gryff-Keller and Anna Kraska	31
INDIRECT NUCLEAR INTERACTIONS IN MPTSN SEMICONDUCTORS (M=TI, ZR, HF, TH) : ^{119}SN AND ^{195}PT MAS NMR STUDY Agnieszka Grykałowska and Bogdan Nowak	32
NMR OF HIGH-TEMPERATURE SUPERCONDUCTORS AND IN PULSED HIGH FIELD MAGNETS Jürgen Haase	33

DESIGN PRINCIPLES OF THE GRAPHICAL USER INTERFACE FOR MRI SYSTEM BASED ON THE MARAN DRX CONSOLE J.M. Haduch, T. Banasik, A. Jasiński, and T. Skórka.....	34
EFFECT OF ANTIBIOTICS ON FORMING OF WHEAT THYLAKOIDS AS OBSERVED IN REHYDRATED MEMBRANE LYOPHILIZATES USING PROTON MAGNETIC RELAXATION AND SORPTION ISOTHERM H. Harańczyk, A. Leja, and K. Strzałka.....	35
WATER BOUND IN ANTARCTIC LICHEN USNEA ANTARCTICA AS OBSERVED BY PROTON RELAXATION AND SORPTION ISOTHERM H. Harańczyk, A. Leja, and K. Strzałka.....	36
A SPECIALIZED PROBEHEAD FOR MR IMAGING OF SMALL OBJECTS <i>IN VIVO</i> . S. Heinze-Paluchowska, T. Skórka, A. Jasiński, P. Borowiec, J. Kiczek, P. Skóra, and R. Wiertel.....	37
DYNAMIC INVESTIGATIONS ON TROPICAMIDE AND ITS DEGRADATION PRODUCTS Franciszek Herold, Jerzy Kleps, Jacek Stefanowicz, and Andrzej Zimniak.....	38
REORIENTATIONAL MOTIONS OF THE NH ₃ LIGANDS IN [ZN(NH ₃) ₄](BF ₄) ₂ Łukasz Hetmańczyk, Wojciech Medycki, Edward Mikuli and Anna Migdał-Mikuli.....	40
CONFORMATIONAL ANALYSIS OF DIBENZO[E,H][1,4]DIOXONIN DERIVATIVES Krzysztof Jamroży, Edward Szneler, <u>Jacek Grochowski</u> , Paweł Serda, and Barbara Rys.....	42
PROTON NMR STUDIES OF MOLECULAR DYNAMICS IN POLYDIMETHYLSILOXANE Mariusz Jancelewicz, Hieronim Maciejewski, and Stefan Jurga.....	44
APPLICATION OF NMR SPECTROSCOPY FOR INVESTIGATION OF COMPLEXES OF RHODIUM SALTS WITH NITROGENOUS BASES Jarosław Jaźwiński.....	45
PROTON NMR STUDIES OF HARD DENTAL TISSUES UNDER FAST MAS Joanna Kolmas, Zofia Paszkiewicz, Anna Slosarczyk, and Waclaw Kołodziejcki.....	46
MOBILITY OF CD ₄ MOLECULES IN NANOSCALE CAGES OF ZEOLITES AS STUDIED BY DEUTERON NMR RELAXATION Agnieszka M. Korzeniowska, Zdzisław T. Lalowicz, and <u>Aleksander Gutsze</u>	47
DETERMINATION OF ROTATIONAL DIFFUSION TENSOR FROM RELAXATION DATA. CREATININE IN WATER SOLUTION Dmytro Kotsyubynskyy and Adam Gryff-Keller.....	48

NMR STUDY ON DIASTEREOMERIC DERIVATIVES OF 5-SUBSTITUTED CREATININES Hanna Krawczyk, Agnieszka Pietras, and Anna Kraska	49
DIPOLAR RELAXATION PROCESSES IN THE PRESENCE OF NEIGHBORING QUADRUPOLE SPINS. LaF_3 CRYSTALS AS AN EXAMPLE Danuta Kruk, Oliver Lips, Alexei Privalov, and Franz Fujara	50
^1H NMR STUDIES OF POLY(ϵ -CAPROLACTONE) – SODIUM MONTMORILLONITE NANOCOMPOSITES Justyna Krzaczkowska and Stefan Jurga.....	51
THE ANALYSIS OF ^{31}P MR SPECTRA OF PHOSPHOLIPIDS' EXTRACTS' OF BONE MARROW BLASTS' CELLS FROM PATIENTS WITH ACUTE LEUKEMIA (AL) Małgorzata Kuliszkiewicz-Janus, Mariusz Tuz, Marek Kiełbiński, and Stanisław Baczyński ...	52
BINARY MIXTURE OF HARD SPHERES AS A MODEL COLLOIDAL SYSTEM INVESTIGATED BY MOLECULAR COMPUTER SIMULATION Bartosz Kuroczycki, Michał Banaszak, and Stefan Jurga.....	55
APPLICATIONS OF ^{19}F MR SPECTROSCOPY TO DIAGNOSTIC AND THERAPY MONITORING OF BRAIN TUMOR ON A RAT MODEL <i>IN VIVO</i> M. Labak, Z. Sułek, K. Majcher, P.Grieb, T. Kryczka, and A. Jasiński	56
NMR STUDY OF $\text{Nd}_2\text{Fe}_{14}\text{B}_x$ HYDRIDES Andrzej Lemański, Małgorzata Jasiurkowska, Czesław Kapusta, Peter C. Riedi, Olivier Isnard, and Daniel Fruchart.....	57
INVESTIGATION OF TEMPERATURE CHANGES IN THE PROPERTIES OF RINGER'S SOLUTIONS BY ^1H NMR AND DENSITOVISCOMETRY D. Lewandowska, T. Klinkosz, and T. Podoski.....	58
^1H , ^{13}C AND ^{19}F NMR STUDIES OF GASEOUS AND LIQUID SEVOFLURANE Edyta Maciąga, Włodzimierz Makulski, Karol Jackowski, and Barbara Blicharska.....	60
FUNCTIONAL MAGNETIC RESONANCE IMAGING OF THE RAT SPINAL CORD K. Majcher, B. Tomanek, A. Jasinski, T. Foniok, U. I. Tuor, and G. Hess	61
MOLECULAR MOTION IN ETHYLENE/NORBORNENE COPOLYMERS Monika Makrocka-Rydzik, Bakyt Orozbaev, Stanisław Głowinkowski, and Stefan Jurga.....	63
TAUTOMERISM AND HYDROGEN BONDING OF PURINE ANALOGUES Radek Marek, Jaromír Toušek, Jiří Brus, Kateřina Maliňáková, Zdeněk Trávníček, and Michal Hocek	65

DO ZPV CORRECTIONS TO NMR SHIELDINGS CHANGE WITH THE CONFORMATION? THE DIMETHOXYMETHANE STUDY Wojciech Migda	66
MULTINUCLEAR CORRELATION $\delta_{C,H,\dots}^{EXP}$ VS. $\delta_{C,H,\dots}^{GIAO}$ AS A TOOL IN STEREOCHEMICAL ANALYSIS AND NMR SIGNAL ASSIGNMENT Ryszard B. Nazarski.....	68
UNIQUE INFORMATION ABOUT MOLECULAR DYNAMICS AND TIMESCALE OF MOLECULAR MOTIONS IN BIOPOLYMER OF LACTIDE AND ϵ -CAPROLACTONE USING SOLID-STATE NMR SPECTROSCOPY Alovidin Nazirov, Farhod Nozirov, Stefan Jurga	69
INTERACTION BETWEEN POLY(ACRYLIC ACID) AND A NONIONIC SURFACTANT. A RHEOLOGY AND SELF-DIFFUSION NMR INVESTIGATION Grzegorz Nowaczyk, Dimitris Vlassopoulos, and Stefan Jurga	70
NMR STUDY OF CMR EFFECT IN MANGANITES Colin J.Oates, Czesław Kapusta, Marcin Sikora, Dariusz Zając, Peter C.Riedi, Christine Martin, Cedric Yaicle, Antoine Maignan, Jose Maria DeTeresa, and M. Ricardo Ibarra	71
NON-MARKOVIAN PROCESSES OF MOLECULAR MOTIONS IN SOLIDS Marcin Olszewski and Nikolaj Sergeev	73
MOLECULAR DYNAMIC OF PODAND 10 AS STUDIED BY NMR AND DIELECTRIC SPECTROSCOPY Bakyt Orozbaev, Monika Makrocka-Rydzik, Stefan Jurga, and Grzegorz Schroeder.....	74
ELECTRIC FIELD GRADIENTS IN MB_{12} (M=Y,ZR AND LU) DODECABORIDES FROM NMR EXPERIMENTS AND AB INITIO CALCULATIONS S. Paluch, O.J. Żogał, B. Jäger, W. Wolf, P. Herzig, N. Shitsevalova, and Y. Paderno.....	75
1H - ^{13}C AND 1H - ^{15}N NMR STUDIES OF THIONIC AND THIOLIC FORMS OF 6-MERCAPTOPYRIMIDINES Leszek Pazderski, Iwona Łakomska, Andrzej Wojtczak, Edward Szłyk, Jerzy Sitkowski, Lech Kozerski, Bohdan Kamiński, Wiktor Koźmiński, Jaromir Tousek, and Radek Marek ...	77
NMR STUDIES OF CATALYTIC ACTIVITY ON THE SURFACE OF RUTHENIUM NANOPARTICLES Tal Pery, Benradeta Walaszek, Susanna Jansat, Jordi Garcia-Anton, Karine Philippot, Bruno Chaudret, Gerd Buntkowsky, and Hans-Heinrich Limbach.....	78
^{13}C CP-MAS NMR STUDIES OF MIANSERIN, A POTENT ANTIDEPRESSANT DRUG Dariusz Maciej Pisklak, Błażej Grodner, Jan Pachecka, and Iwona Wawer	79

USABILITY OF HMRS IN CNS DIAGNOSTICS OF HIV POSITIVE PATIENTS Lilianna Podsiadło, Andrzej Urbanik, Aleksander Garlicki, Justyna Kozub, Barbara Sobiecka, and Tomasz Mach	80
NMR STUDY OF GDFE ₂ H _x HYDRIDES Vit Procházka, Czesław Kapusta, Peter C. Riedi, and Jan Žukrowski	81
NMR RELAXATION IN MAIN CHAINS AND SIDE GROUPS OF CELLULOSE AND ITS DERIVATIVES Adam Rachocki, Jadwiga Tritt-Goc, and Narcyz Piślewski	82
THEORY OF DAMPED QUANTUM ROTATION IN NMR SPECTRA. THE FOUR-FOLD ROTOR T. Ratajczyk and S. Szymanski	83
A ⁵⁵ MN NMR STUDY OF LA _{0.33} ND _{0.33} CA _{0.34} MNO ₃ WITH ¹⁶ O AND ¹⁸ O Damian Rybicki, Czesław Kapusta, Peter C. Riedi, Colin J. Oates, Marcin Sikora, Dariusz Zając, Jose Maria De Teresa, Clara Marquina, and Manuel R. Ibarra	84
APPLICATION OF MOLECULAR MODELING AND DFT CALCULATION OF SPIN-SPIN COUPLING CONSTANTS TO THE CONFORMATIONAL ANALYSIS OF 3,4,5,6-TETRAHYDRO-1H-BENZO[B]AZOCIN-2-ONE Agnieszka Rzepa, Wojciech Migda, and Barbara Rys.....	85
NMR STUDY OF ULTRAFINE POLYTETRAFLUOROETHYLENE Nikolaj Sergeev and Marcin Olszewski	87
¹ H NMR DETECTION OF σ-ADDUCTS IN S _N H REACTIONS OF 3-NITRO-1,5-NAPHTHYRIDINES WITH METHYLAMINE Barbara Szpakiewicz, Maria Grzegózek, and Elżbieta Cholewka	89
MR AND CT IMAGING IN DETERMINATION OF TOOTH CARRIES DECAY Marta M. Tanasiewicz, Władysław P. Węglarz, Tomasz W. Kupka, Cezary Przeorek, and Andrzej Jasiński.....	90
THEORETICAL CALCULATIONS OF ¹⁵ N NMR CHEMICAL SHIFTS OF 6-BENZYLAMINOPURINE DERIVATIVES Jaromír Toušek, and Radek Marek	92
¹ H MAS AND ¹³ C CP/MAS NMR STUDIES OF URINARY STONES Monika Uniczko, Zdzisław Durski, and Waclaw Kolodziejwski	93
ESTIMATION OF SPEECH REGIONS IN BILINGUAL SUBJECTS IN FMRI Andrzej Urbanik, Marek Binder, Barbara Sobiecka, Justyna Kozub, and Amira Bryll	95

FMRI IN ESTIMATION OF INFLUENCE OF DIFFICULTY OF A COGNITIVE TASK ON THE PATTERNS OF BRAIN ACTIVITY Andrzej Urbanik, Marek Binder, Justyna Kozub, and Barbara Sobiecka.....	96
NEURAL CORRELATES OF WORKING MEMORY ACTIVITY DURING PERFORMANCE OF VERBAL AND NONVERBAL TASKS Andrzej Urbanik, Marek Binder, Justyna Kozub, and Barbara Sobiecka.....	97
THE ASSESSMENT OF DEMENTIA CHANGES WITH HMRS METHOD Andrzej Urbanik, Jerzy Walecki, Andrzej Jasiński, Justyna Kozub, Barbara Sobiecka, Maria Orłowiejska, Rafał Motyl, and Andrzej Szczudlik.....	98
APPLICATION OF ¹³ C-NMR TO THE STUDY OF POLYOFIN PYROLIS PRODUCTS Grzegorz Urbanowicz, Jerzy Ossowski, and Marek Matlengiewicz	99
DEUTERIUM ON RU NANOPARTICLES AND IN THE MODEL COMPLEXES: STUDIES OF BINDING AND MOBILITY BY NMR Bernadeta Walaszek, Tal Pery, Karine Philippot, Bruno Chaudret, Hans-Heinrich Limbach, and Gerd Buntkowsky.....	100
DIAGNOSTIC IMPORTANCE OF MAGNETIZATION TRANSFER IN MRI MULTIPLE SCLEROSIS MONITORING Wicher Magdalena, Kluczevska Aneta, Konopka Marek, Kiełtyka Aleksandra, Drzazga Zofia, Pilch-Kowalczyk Marek, Hartel Marcin, and Filippi Massimo	101
¹³ C CP MAS STUDIES OF BAICALEIN AND ITS DERIVATIVES Michał Wolniak, Jan Oszmiański, Sebastian Olejniczak, and Iwona Wawer.....	103
ORDERING EFFECTS IN COMPUTER-SIMULATED BLOCK COPOLYMER MELTS Sebastian Wołoszczuk, Michał Banaszak, and Stefan Jurga	105
³¹ P NMR STUDIES OF HIV-INFECTED HUMAN CELLS Krzysztof Wroblewski, Tomasz Rozmysłowicz, and Glen N. Gaulton.....	106
DETERMINATION OF TETRACYCLIC AMINE DERIVATIVES STRUCTURE USING ¹ H, ¹³ C, 2D NMR Olga W. Yuzlenko and Lilia I.Kasyan	108
NMR STUDY OF MO AND RE MAGNETISM IN DOUBLE PEROVSKITES Dariusz Zając, Czesław Kapusta, Peter C. Riedi, Marcin Sikora, Colin J. Oates, Damian Rybicki, Jose Maria DeTeresa, David Serrate, Clara Marquina, M. Ricardo Ibarra, and Javier Blasco.....	110
IMAGING AND T ₂ RELAXATION MAPPING OF ARTICULAR CARTILAGE USING NUCLEAR MAGNETIC RESONANCE Tomasz Zalewski, Sławomir Kuśmia, Przemysław Lubiatowski, Jacek Kruczyński, and Stefan Jurga	112

THREE-DIMENSIONAL STRUCTURE AND BACKBONE DYNAMICS OF THE MIXED DISULFIDE OF BOVINE APO-S100A1 PROTEIN WITH β -MERCAPTOETHANOL Zhukov I., Ejchart A., and Bierzyński A.....	113
¹³ C CPMAS NMR STUDIES OF NIFEDIPINE AND ITS ANALOGUES Monika Zielińska and Iwona Wawer	114
MRI STUDIES OF TABLETS Monika Zielińska, Bożena Kwiatkowska, and Michał Dera.....	115
POLYMORPHISM OF MORIN (2',3,4',5,7-PENTAHYDROXYFLAVONE) – ¹³ C CPMAS NMR AND GIAO CHF CALCULATIONS Agnieszka Zielińska, Katarzyna Paradowska, Jacek Jakowski, and Iwona Wawer	116

DTI STUDY OF PATIENTS WITH SPONDYLOTIC MYELOPATHY OF THE CERVICAL SPINAL CORD

T. Banasik, M. Hartel¹, A. Kiełtyka¹, M. Konopka¹, T. Skórka, and A. Jasiński

H. Niewodniczański Institute of Nuclear Physics PAN, Kraków, Poland

¹Silesian Diagnostic Imaging Center Helimed, Katowice, Poland

Introduction

Cervical spondylosis is a common degenerative condition of the spine, found in more than 75% of patients after the age of 65. The most serious complication is myelopathy due to cord compression by bulging or herniated disks and osseous spurs, leading to degeneration in the spinal cord tissues [1]. MRI with T₂ weighting has low sensitivity in detecting cervical spondylosis. Recently, interleaved diffusion weighted EPI sequence and DTI in sagittal plane was used successfully to detect this pathology [2]. In this study we applied single-shot EPI – DTI sequence [3] to determine apparent diffusion tensor (ADT) in axial plane to investigate patients with spondylotic myelopathy.

Materials and Methods

A single shot EPI-DTI sequence [3] was applied in 16 patients with symptomatic cervical spondylosis of different severity. Imaging was performed on a GE SIGNA LX Echo-Plus at Helimed in Katowice. DTI was measured applying the diffusion gradients in 6 standard directions. DW images were acquired with a 64 x 64 matrix, FOV = 9 cm, slice thickness = 7 mm, slice separation = 2 mm, number of slices 8, TR = 2 RR, NEX = 8 for b factor of 300, 450, 600 s/mm². Data were analyzed using an IDL based software developed in-house. Values of ADT were determined for different ROI in the white matter and gray matter.

Results

Good quality DW images were recorded in axial plane for diffusion gradient in all directions making possible determination of ADT maps. On most T₂ weighted FSE images regions of higher intensity are not present. However, axial DW images show changes in diffusion values in slices corresponding to narrowing of spinal canal. ADT values in the region of spinal canal narrowing are higher than in the reference group of healthy volunteers. Fractional anisotropy FA determined for selected ROI in the white matter and gray matter show differences when compared to reference values recorded for a group of volunteers.

Conclusion

We have demonstrated the feasibility of EPI-DTI in the axial plane in detection of cervical spinal cord spondylosis.

Acknowledgments

The Committee for Scientific Research of Poland supported this work, under grants No 2P05C 069 26 and 3T11E 012 27.

References:

1. Larocca H. Cervical spondylotic myelopathy: natural history. *Spine* 1988; 13:854–855.
2. Demir A, et al., Diffusion-weighted MR Imaging with Apparent Diffusion Coefficient and Apparent Diffusion Tensor Maps in Cervical Spondylotic Myelopathy. *Radiology* 2003; 229: 37–43
3. Jasinski A., et al., Proc. 11 ISMRM 2003; 2462.

EQUILIBRIUM AND NON-EQUILIBRIUM DIFFUSION MEASUREMENTS IN ZEOLITES BY NMR TECHNIQUES

Krzysztof Banaś¹, Federico Brandani², Douglas M. Ruthven³,
Frank Stallmach², and Jörg Kärger²

¹*Instytut Fizyki Jądrowej im. H. Niewodniczańskiego ul. Radzikowskiego 152 31-342 Kraków, Poland*

²*Fakultät für Physik und Geowissenschaften, Universität Leipzig, Linnestrasse 5, D-04103, Germany*

³*Department of Chemical Engineering, University of Maine, Orono, Maine 04469-5737, USA*

In this paper the Zero Length Column (ZLC) technique extended to the case where the decay of the adsorbed phase concentration is observed directly by NMR is presented. An adsorption-desorption apparatus compatible with a 400 MHz NMR spectrometer was developed. It operates with nitrogen as the inert purge gas. The column of the adsorbent material was placed in the sensitive region of the superconducting magnet and the rf coil of the NMR spectrometer.

The diffusion of propane, n-butane and isobutane in silicalite-1 was investigated by using the novel “ZLC-NMR” technique. This method, together with standard PFG NMR measurements, seems to be a good solution in measuring transport properties of the adsorbed gas in zeolites using macroscopic and microscopic approaches at the same conditions.

The time scales of the adsorption and desorption processes depend on concentration, temperature and crystal shape and were found to be in the range of minutes. From the desorption branch, the non-equilibrium ZLC NMR measurements yield an intracrystalline diffusion coefficients in the range of 10^{-13} to 10^{-11} m²/s for different alkanes in silicalite-1.

It was found that diffusion coefficients for isobutane, n-butane and propane in silicalite-1 measured by the non-equilibrium ZLC-NMR are smaller than the values measured by PFG NMR under equilibrium condition. The differences may indicate transport resistance at the external surface of the silicalite-1 zeolite crystals.

**ONE-BOND CARBON-CARBON COUPLING CONSTANTS ($^1J_{CC}$)
IN DERIVATIVES OF QUINOLIZINE.
AN INFLUENCE OF THE PROTONATION**

**Elżbieta Bednarek^a, Małgorzata Bechcicka^b, Krystyna Kamińska-Trela^b,
and Lidia Kania^b**

a/ National Institute of Public Health, Chełmska 30/34, 00-725 Warszawa,

*b/ Institute of Organic Chemistry, Polish Academy of Sciences, Kasprzaka 44/52,
01-224 Warszawa*

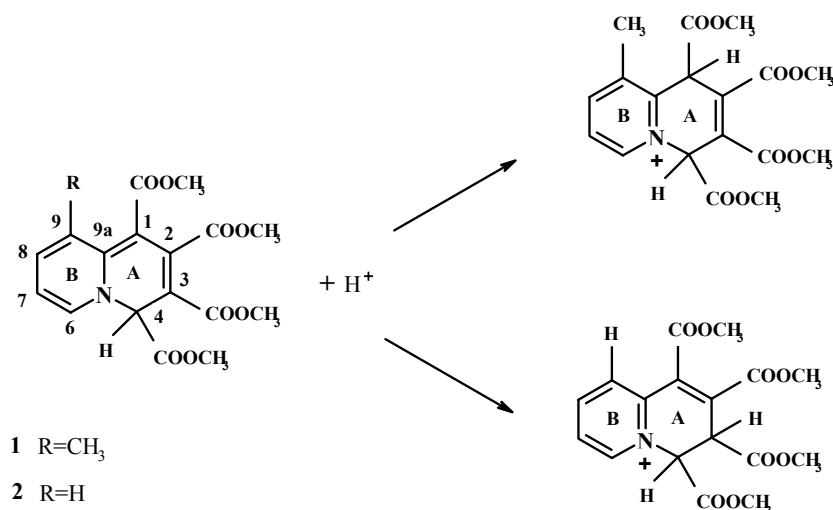
In this communication we present results of our studies on $^1J_{CC}$ couplings in 4*H*-quinolizine-1,2,3,4-tetracarboxylate, its derivatives and the products of their protonation. For comparison also the $^1J_{CC}$ data for 9*H*-tautomer and its derivatives are included.

^{13}C NMR spectra of the parent tetramethyl 9*aH*- and 4*H*-quinolizine-1,2,3,4-tetracarboxylate and their mono- and dimethyl derivatives have been measured in CDCl_3 solution. The protonation studies have been carried out in trifluoroacetic acid.

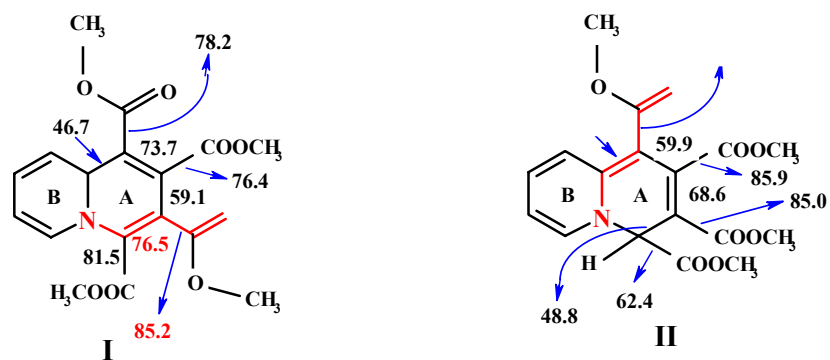
An inspection of the data obtained allowed us conclusion that the protonation of the compounds depends on the position of the methyl substituent in ring B (see scheme 1).

In 9-methyl substituted compounds the protonation occurs at carbon C1 whereas in compounds not bearing this substituent - at carbon C3. This is in agreement with the results published by Acheson et al. [1] who studied UV spectra of the protonated 4*H*-quinolizines.

The most interesting results obtained by us concern the magnitude of the $^1J_{CC}$ couplings in ring A. The largest values are invariably observed for the couplings across those CC bonds which are involved in the N-C=C-C(O) conjugated system (see scheme 2). The couplings in ring B of 9*aH*-quinolizines are typical of the couplings in the conjugated aliphatic system whereas those in the protonated 4*H*-compounds are similar to those in the protonated pyridine.



Scheme 1. Protonation of the parent tetramethyl 4*H*-quinolizine-1,2,3,4-tetracarboxylate and its 9-methyl derivative in trifluoroacetic acid.



Scheme 2. $^1J_{CC}$ coupling constants in parent 9aH- (I) and 4H- (II) quinolizine 1,2,3,4-tetracarboxylate.

Refereces:

1/ R. M. Acheson, G. A. Taylor, *J. Chem. Soc.*, 1960, 1691

R. M. Acheson, R. S. Feinberg, J. M. F. Gagan, *J. Chem. Soc.*, 1965, 948

NMR-BASED METHOD FOR THE LOCATION OF AMINO ACID MOIETIES IN BACTERIAL OLIGOSACCHARIDES

Piotr Bernatowicz¹, Andrzej Ejchart¹, Gabriela Pastuch-Gawolek², Wiesław Szeja³,
Tomasz Lipiński³, and Andrzej Gamian³

¹ *Laboratory of Biological NMR, IBB PAS, Warsaw, Poland*

² *Department of Organic Chemistry, Biochemistry and Biotechnology, Silesian Technical University, Gliwice, Poland*

³ *Ludwik Hirszfeld Institute of Immunology and Experimental Therapy, PAS, Wrocław, Poland*

Structural variations of the core oligosaccharides of several species of Gram-negative bacteria, comprising substitution of amino acid glycine to the molecular backbone, have been recently reported. The genetic control of this process is not yet understood and the rationale behind glycine incorporation into the core oligosaccharides remains unclear, but one could expect that it increases the ability of the bacteria to cause host diseases. Therefore, an analytical method to identify the type of amino acid and to locate the site of its substitution is of importance.

The model monosaccharides, ester-linked with an amino acid, were selected for the elaboration of an NMR-based method: Gly→4GlcOMe, Gly→6GalOMe, and Ala→6GalOMe. ¹H/¹³C chemical shift correlation via long range coupling constant, ³J(C'-O-C-H), was exploited for the detection of the covalent linkage between the amino acid residue and the saccharide moiety. The corresponding cross-peak at ¹³C chemical shift characteristic for ester carbonyl { $\delta(\text{C}') \approx 165\text{-}170$ ppm} appears in a relatively empty spectral region. Its ¹H chemical shift allows one to identify the substitution site providing the spectral assignments of saccharide protons have been performed. At the C' chemical shift one can also observe cross-peak to H_α and H_β protons of the amino acid residue thus identifying its type. It was found that such the HMBC-based NMR method is robust, efficient and reliable.

¹⁹F NMR SPECTRA OF CIPROFLOXACIN

¹Antoni Bijak, ¹Barbara Blicharska, and ²Paola Porcari

¹*Institute of Physics, Jagellonian University, ul. Reymonta 4
30-059 Kraków, Poland*

²*Department of Physics, University of Rome „La Sapienza”
P.le Aldo Moro, 5 00185 Rome, Italy*

Abstract

Ciprofloxacin is synthetic broad spectrum antimicrobial agents for oral administration. It is used to treat infections of the skin, lungs, airways, bones and joints caused by susceptible bacteria. It is also frequently used to treat urinary infections caused by bacteria such as E. Coli.

In our studies we have investigated how the ¹⁹F NMR spectra obtained at 9.3950 T (400 MHZ for protons) changes with concentration and temperature of ciprofloxacin aqueous solution.

T₁ AND T_{1ρ} PROTON RELAXATION TIMES OF STARCH

¹Barbara Blicharska, ¹Magdalena Hyjek, and ²Joanna Szymońska

¹Institute of Physics, Jagellonian University, Kraków, Poland

²Chemistry Department, Agricultural Academy, Kraków, Poland

The change in water mobility and structure of starch during drying or freezing was investigated using ¹H NMR relaxation. Starch was obtained from potato, corn, oat or wheat. Proton NMR spin - lattice and T_{1ρ} relaxation times were recorded. Dipol-dipol interaction was assumed as a main mechanism causing the relaxation process of absorbed water. This model fits well the temperature and frequency dependencies of T₁ and T_{1ρ} and yields the activation energies and correlation times for the system. The changes in these parameters could be correlated with the changes in the structure of starch.

NMR RELAXATION IN BIOPOLYMERS (CELLULOSE AND STARCH)

Barbara Blicharska and Magdalena Hyjek

Institute of Physics, Jagellonian University, Kraków, Poland

The interpretation of the proton NMR relaxation data obtained for cellulose and starch samples are focused on dynamics of various states of “bound water molecules”, which are always absorbed on biopolymers. The water relaxation reflects the response of polymer structure to different treatments such as drying, freezing or chemical processing. Assuming that the dipole-dipole interaction causes mainly the relaxation process, the correlation times and activation energies of the system were calculated. These parameters can be correlated with physical and chemical properties of polymers and from this point of view the NMR relaxation investigation may have a practical aspects.

MAGNETIC ROTATIONAL RESONANCE AND CROSS RELAXATION IN GASES

Jerzy S. Blicharski

M. Smoluchowski Institute of Physics, Jagellonian University, Kraków, Poland

In this paper we present a theory of Magnetic Rotational Resonance (MRR) and cross relaxation in gases. As a special case we consider molecular hydrogen H_2 and D_2 at low temperatures. The theoretical calculations of the cross relaxation rate between the nuclear spins I and molecular angular momentum J are performed in a weak collision approximation [1,2], at the presence of Zeeman interaction, quadrupolar and dipolar interactions and spin-rotational interaction [3,4] as a function of frequency and temperature. Nuclear-rotational Overhauser effect (NROE) and a possibility of detection of the MRR signal is also considered.

References:

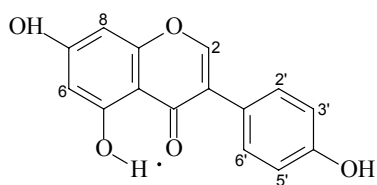
- [1] A.Abragam, The Principles of Nuclear Magnetism, Clarendon Press, Oxford, 1987
- [2] J. S. Blicharski, Acta Phys. Polon. 24, 817 (1963), *ibid.* A41, 223 (1972)
- [3] N.F. Ramsey, Molecular Beams, Clarendon Press, Oxford, 1956
- [4] J.S. Blicharski, A. Gutsze, A. Korzeniowska, Z.T. Lalowicz, Z. Olejniczak, Appl. Magn. Reson. (in press).

INTERACTION OF FLAVONOID TOPOISOMERASES I AND II INHIBITORS WITH DNA OLIGOMERS

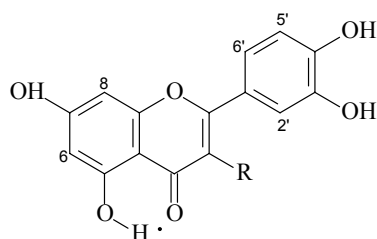
Wojciech Bocian¹, Robert Kawęcki², Elżbieta Bednarek¹, Jerzy Sitkowski^{1,2},
Agnieszka Parcińska¹, and Lech Kozerski^{1,2}

¹ National Institute of Public Health, 00-725 Warsaw, Chełmska 30/34, Poland

² Institute of Organic Chemistry, PAS, 01-224 Warsaw, Kasprzaka 44/52, Poland



1 Genistein



2 R = H Luteolin
3 R = OH Quercetin

We have established a binding affinity of flavonoids (1, 2, 3) to DNA oligomers by means of studying by NMR the diffusion coefficients of these compounds with and without the presence of DNA. The genistein is bound very weakly, $K_a = 1.54 \times 10^2 \text{ M}^{-1}$, as compared to quercetin, with binding affinity, $5.75 \times 10^3 \text{ M}^{-1}$ and luteolin ($2.17 \times 10^4 \text{ M}^{-1}$ as reported in a literature). The chemical shift changes induced on the ligand protons are to lower frequencies, both in luteolin and quercetin, suggesting a stacking the DNA base pair. In the case of genistein a hydrogen bond of the $\text{NH}^{\text{F,B}}$ protons of the cytidine in the edge base pair to genistein hydroxyl is proposed, basing on the shape of the 2D DOSY spectrum.

INTERACTION OF THE CAMPTOTHECIN FAMILY WITH DNA OLIGOMERS

**Wojciech Bocian^a, Elżbieta Bednarek^a, Jerzy Sitkowski^{a,b}, Agnieszka Parcińska^a,
and Lech Kozerski^{a,b}**

^a*National Institute of Public Health, 00-725 Warszawa, Chełmska 30/34, Poland,*

^b*Institute of Organic Chemistry, Polish Academy of Sciences, 01-224 Warszawa, Kasprzaka 44, Poland*

We present the result of our NMR and computational study of interaction of the anticancer drug topotecan (TPT) with DNA oligomers: regular octamer d(GCGATCGC)₂ and nicked DNA decamer¹ of the structure: 3'-TTGCG-5'-PEG6-3'-CGCAACAGCG-5'-PEG6-3'-CGCTG-5' with the nick at T5 - G6 unit, as a model for the DNA/Topoisomerase I/Topotecan complex. The topotecan is a member of camptothecin family drugs and is in clinical use. To the best of our knowledge this report is a non common attempt where the ensemble of conformations in fast exchange defining the drug-biomolecule complex has been treated quantitatively in solution. We believe these results can stimulate the research on a binding mechanism of this family of topo I poisons and a better drug structure development.

The measured by titration and diffusion NMR experiments small binding constants of a range of $2 \div 3 \text{ mM}^{-1}$ indicate that TPT bind weakly to DNA. The weak cross peaks between TPT and DNA and chemical shift changes induced by DNA/TPT interaction are observed. The molecular modeling analysis showed that NMR derived structural parameters can not be fully assigned only to one simple structure of octamer DNA/TPT complex. Therefore we proposed multi-conformational model selected upon unrestrained molecular dynamic simulation in explicit solvent and free energy analysis using the MM-PBSA (molecular mechanics Poisson-Boltzmann surface area) method.

NMR STUDY OF $\text{Sm}_2\text{Co}_{17}\text{H}_x$ HYDRIDES

**Marta Borowiec^a, Czesław Kapusta^a, Małgorzata Jasiurkowska^a, Peter C. Riedi^b,
and Jan Żukrowski^a**

^a *Department of Solid State Physics, Faculty of Physics & Applied Computer Science, AGH University of Science and Technology, Cracow, Poland*

^b *Department of Physics & Astronomy, University of St. Andrews, St. Andrews, KY16 9SS Scotland, UK*

NMR measurements on $\text{Sm}_2\text{Co}_{17}\text{H}_x$ ($x = 0, 1.5, 4.6$) hydrides are reported. The parent $\text{Sm}_2\text{Co}_{17}$ compound belongs to the group of materials for permanent magnets. For x up to 3 hydrogen enters 9e sites and for $x > 3$ it occupies up to 1/3 of 18g sites. In order to determine the influence of hydrogen on the rare earth site properties the ^{147}Sm and ^{149}Sm spin echo spectra have been studied. Powder samples have been measured at zero field and 4.2 K. The spectra consist of quadrupole septets (nuclear spin of ^{147}Sm and ^{149}Sm is 7/2) which are attributed to Sm sites with different numbers of hydrogen nearest neighbours at the 9e and 18g sites. Hydrogen neighbours at 9e sites cause a decrease of Sm hyperfine field which corresponds to an increase of the 6sp and 5d electron polarization that partly cancels the dominant 4f orbital contribution of opposite sign. Also the electric field gradient slightly decreases, which is attributed to an increase of the 6p and 5d electron contribution partly canceling the dominant 4f electron term of opposite sign. Hydrogen neighbours at 18g sites cause an increase of Sm hyperfine field. The results are analysed in terms of electron transfer between hydrogen and samarium sites and the difference of the effect between the 9e and 18g sites is discussed.

ARTIFACTS PRODUCED BY DENTAL MATERIALS IN MR IMAGING

Amira Bryll, Andrzej Urbanik, Anna Jurczak¹, Maria Chomyszyn-Gajewska¹,
Stanisław Sztuk, Małgorzata Szafirski, and Barbara Sobiecka

Department of Radiology, Collegium Medicum, Jagellonian University, Kraków, Poland

*¹Department of Conservative Dentistry, Collegium Medicum, Jagellonian University,
Kraków, Poland*

Purpose:

The aim of the study is estimation of degree of image disturbances caused by dental materials in MR examination, and risk of dislocation of ferromagnetic materials in magnetic field.

Material and method:

25 samples of dental materials containing metals fixed, or present for iatrogenic reasons in oral cavity, were examined in a gel phantom whose signal is close to the signal of soft tissues.

Signa Horizon 1.5T (GEMS) unit was used with spin echo sequences in T1 time with parameters TE: 20ms, TR: 300ms, slice thickness: 3mm, gap: 1.5mm, imaging matrix: 256x256, FOV: 20x20cm.

Results:

Dislocation of examined samples by magnetic field was not noticed. All materials produced artefacts that had different degree of intensity.

Conclusions:

Lack of dislocation of dental materials in gel surrounding indicate that dislocation of those materials fixed permanently in oral cavity of size not exceeding the size of examined samples in 1.5T will not occur.

Materials from precious alloys cause a small degree of image disturbances, but small artefacts may occur some distance away from them. The remaining materials produce image deformations that may alter head MR images

NON-CARTESIAN SAMPLING IN MRI: RADIAL AND SPIRAL SEQUENCES

**Katarzyna Cieřlar, Katarzyna Suchanek, Mateusz Suchanek, Tadeusz Pałasz,
Tomasz Dohnalik, and Zbigniew Olejniczak***

*Institute of Physics, Jagellonian University, Kraków, Poland,
Institute of Nuclear Physics, Kraków, Poland

Data acquisition in the k-space can be accomplished in many different ways. The most commonly used strategy is the 2DFT (spin-wrap) method (Fig 1 a), where the k-space is sampled on a regular cartesian grid. The reconstruction of the image is then performed by the 2D FFT algorithm. Among alternative methods of sampling the k-space there are radial and spiral acquisition schemes. We present two versions of these sequences based on the FID sampling (Fig 1 b and c). The k-space trajectory is given either by a set of radial lines starting from the origin of coordinate system, or by a set of interleaved spirals.

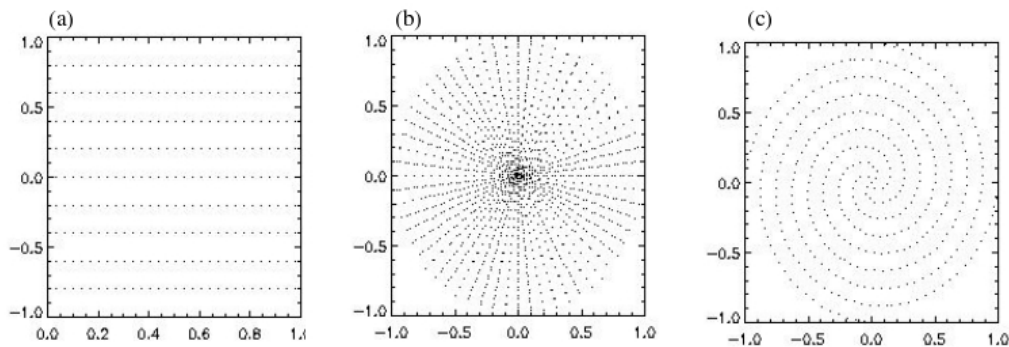


Fig. 1. Data acquisition schemes: (a) spin-wrap, (b) radial, (c) interleaved spiral.

The main disadvantage of non-cartesian imaging is a multistep reconstruction process. The data sets collected along either radial or spiral trajectories need to be regridded onto a cartesian coordinate system. This process has to account for an uneven distribution of the sampled data points by applying a proper density compensation weighting. Following this, the standard 2D FFT is performed to obtain the image.

Due to their inherently high signal-to-noise ratio and short total acquisition time, the non-cartesian sequences offer great advantages for MRI of living objects, especially in the case when the motion artifacts have to be eliminated. The first images obtained by these methods will be presented. Consequently, they will be used in static and dynamic imaging of rat lungs using polarised helium-3 on our 0.08 T MRI system.

References:

- [1]. G.H. Glover, J. M. Pauly, *Magn. Reson. Med.*, 28: 275-289 (1992)
- [2]. C. H. Meyer, B. Hu, D. G. Nishimura, A. Mackovski, *Magn. Reson. Med.*, 28: 202-213 (1992)

“THROUGH SPACE” J-COUPPLINGS OF THE PERI-F ATOM TO THE CH₃ PROTONS IN A TETRAFLUORO DERIVATIVE OF 9-METHYLTRIPTYCENE. STRENGTHENED EVIDENCE OF BLUE-SHIFTING HYDROGEN BOND

I. Czerski^a, K. Kamienska-Trela^a, T. Ratajczyk^a, S. Szymanski^a, and J. Wojcik^a

^a*Institute of Organic Chemistry, Polish Academy of Sciences, Kasprzaka 44/52, 01-224 Warsaw, Poland*

^b*Institute of Biochemistry and Biophysics, Polish Academy of Sciences Pawinskiego 5a, 02-106 Warsaw, Poland*

The 9-methyltriptycene derivatives bearing an electron-donating substituent in the peri position exhibit extremely high potential energy barriers to the methyl group rotation, reaching 40 kJ/mol¹. This allows the methyl group dynamics to be frozen on the timescale of liquid-phase NMR^{1,2}. For a series of such compounds we have recently shown that the standard, classical jump model of the stochastic reorientation of the methyl group is inadequate to the description of the liquid-phase spectra of the methyl protons³. On the other hand, the damped quantum rotor (DQR) model of our own⁴, developed originally to interpret solid state NMR spectra of methyl groups at cryogenic temperatures, has proven perfectly accurate to this purpose. These surprising observations point to a need of a deeper insight in the structural factors that shape up the torsional energy barriers involved.

For 1-X-substituted 9-methyltriptycenes (X = Br, Cl, and F), an extra stabilization of the ground torsional state by the effect dubbed “blue-shifting hydrogen bond”⁵ seems evident⁶. In the compounds discussed, a hallmark of the latter effect, an electron density transfer from the lone pairs on X to the σ^* CH orbital of the methyl proton situated trans to X, could be identified on the basis of the natural bond orbital (NBO) analysis⁶ of the electronic state functions concerned⁷. However, in the existing theories of the blue-shifting H-bond⁵ the role of the protons most proximate to the electron donor, the presence of which is crucial for the whole effect to occur, has not been clarified enough. The present observations of the “through space” J-couplings between the peri-¹⁹F nucleus and the individual methyl protons in the compound mentioned in the title may be helpful for a deepened understanding of the effect. The coupling values that we could determine from the low-temperature NMR spectra of that compound are unusually large; for one of the protons proximate to F the coupling amounts to ca. 8 Hz. The corresponding theoretical values (calculated using Gaussian 2003) are in a reasonable agreement with the observed ones. The above results, evidencing occurrence of an electron density path between F and the methyl protons proximate to F, seem to have no precedence in the literature. Actually, they provide a substantial strengthening of our previous arguments⁷ in favour of the occurrence of the blue-shifting H-bonds to the methyl protons.

References:

¹M. Nakamura *et al.* *Bull. Chem. Soc. Jpn.* **47**, 2415 (1974).

²M. Oki, *Reactivity and Structure Concepts in Organic Chemistry* **30**, 84 (1993).

³P. Bernatowicz and S. Szymanski, *Phys. Rev. Lett.* **89**, 023004 (2002); S. Szymanski and P. Bernatowicz, *Ann. Rep. on NMR Spectr.* **54**, 2 (2004) and references cited therein.

⁴S. Szymanski, *J. Chem. Phys.* **111**, 288 (1999).

⁵K. Mueller-Dethlefs and P. Hobza, *Chem. Rev.* **100**, 143 (2000).

⁶J.P. Foster and F. Weinhold *J. Am. Chem. Soc.* **102**, 7211 (1980); A.E. Reed, L.A. Curtiss, F. Weinhold, *Chem. Rev.* **88**, 899 (1988).

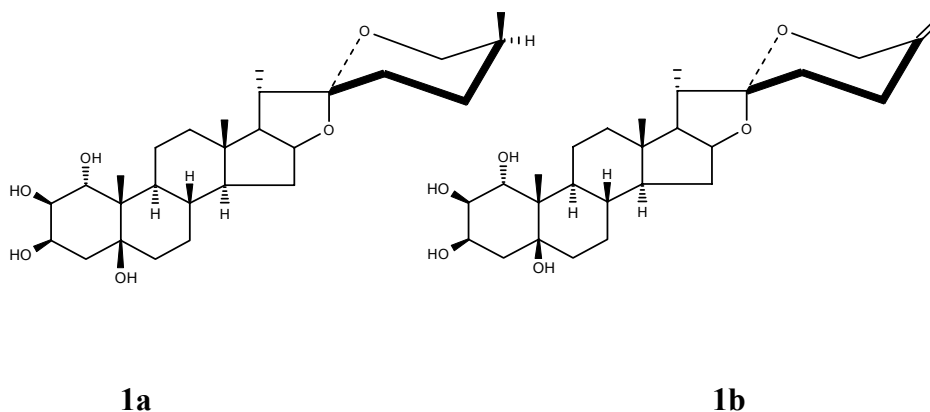
⁷T. Ratajczyk *et al.*, *Angew. Chem.* (submitted).

**NMR STUDIES OF 5 β -SPIROST-25(27)-EN-1 β ,2 β ,3 β -5 β -TETROL
AND ITS 25,27-DIHYDRO DERIVATIVE, NEW SAPOGENINS
FROM *Convallaria majalis* L.**

**Karolina Dąbrowska-Balcerzak^a, Edyta Pindelska^b, Jadwiga Nartowska^c,
and Iwona Wawer^a**

^aDepartment of Physical Chemistry, ^bDepartment of Pharmacognosy, ^cDepartment of Inorganic and Analytical Chemistry, Faculty of Pharmacy,
The Medical University of Warsaw, Banacha 1, 02-097 Warsaw

Two new spirostanol sapogenins were isolated from the roots and rhizomes of *Convallaria majalis* L. The n-butanolic extract contained two compounds: spirostan **1a** and spirosten-type (major) **1b** characterised by identical values of R_f. Since their separation using HPLC was not possible, pure **1a** was obtained by catalytic hydrogenation of **1b**.



In order to get detailed structural information the 1D and 2D NMR spectra (COSY, HETCOR, HMBC, NOESY) were recorded on a BRUKER DRX-500 spectrometer. Besides chemical shifts and coupling constants also long range correlations were important for structure elucidation. The configuration of all hydroxyl groups was determined to be β from the analysis of coupling constants. Characteristic values of ¹³C chemical shifts for C25-C27 (and the negative sign of the specific optical rotation) indicated that the dihydro derivative **1a** is a representative of tetraol of the 25S series.

Solid state ¹³C CPMAS spectra were recorded on a BRUKER DSX-400 WB spectrometer. The ¹³C CPMAS spectrum of solid **1b** exhibited 18 clearly resolved signals for the 27 carbon atoms of the molecule; the signals were assigned by comparison with solution spectra. The signals of methyl carbons and carbons linked to oxygen are separate and can be easily distinguished (especially the signals appearing in the range 55-85 ppm), whereas those of methylene carbons: C2, 4 and 15 give rise to a broad peak at 32-35 ppm. It is interesting that solid state chemical shifts are almost the same as for CDCl₃ solution, the differences are less than 1 ppm. It indicates that the structure and conformation of **1b** is similar in both phases.

Fortunately, we succeed to grow single crystal (**1b**) suitable for X-ray diffraction measurements. Crystallographic results confirmed the β -configuration of hydroxyl groups; the most striking feature of this structure is the pattern of intra- and intermolecular hydrogen bonds, which form “polar head” of this compound.

DETERMINATION OF THE AMPLITUDE OF SPIN MOTIONS BY THE ANALYSIS OF SIDE BANDS IN THE NMR SPECTRUM

Artur Freda and Czesław Lewa

*Institute of Experimental Physics, University of Gdańsk, Wita Stwosza 57, 90-952 Gdańsk, POLAND.
e-mail: dokaf@univ.gda.pl*

The imaging of viscoelastic properties of biological tissues by the employment of magnetic resonance (MR), in particular of MR elastography (MRE) and Elasto-MR spectroscopy (EMRS) has found wide application in medical diagnostics. There are also other methods described in the literature, such as the analysis of a spectrum observed in the presence of an elastic wave in a constant magnetic field, the so-called side bands analysis [1]. In this report, the experimental verification of the principles of this method is demonstrated.

The rotation of a test-tube in the magnetic field gradient results in the occurrence of additional rotational side bands in the NMR spectrum.

When the signal observed is proportional to the squared amplitude of a high frequency (HF) field, the intensity of a single side line is proportional to [1, 2, 3, 4]

$$J_n^2\left(\frac{\gamma B_m}{\Omega}\right) \quad (1)$$

with:

$$\sum_{n=-\infty}^{+\infty} J_n^2 = 1 \quad (2)$$

Three types of measurement were carried out: the first one for a full test-tube [5], the second one for a cut-off layer of the liquid, and in the third one two layers were examined.

The measurements started with the registration of the spectrum at maximum homogeneity of the magnetic field. Next, the magnetic field gradient was generated in the x-axis direction.

The experiments have demonstrated that it is possible to quench completely the side bands of a single thin layer. Figure 1 shows how the surface areas under the principal band change with the magnetic field gradient. The squares of the first type zero-order Bessel functions were fitted to the measurement points.

In the case of the two-layer system, a curve being a superposition of two squares of the Bessel functions was fitted.

Regarding the full test-tube as a set of 0.5 mm thick layers (the thickness the same as in the case of a single layer) the fitting by the use of squared Bessel function proved unsatisfactory. The superposition of five squared Bessel functions allows fitting the curve to the experimental points, thus enabling one of the three quantities occurring in the argument of the Bessel function (1) to be evaluated.

According to the experimental results, if there are no unequivocal reasons to apply the velocity distribution, it is the amplitude of the motion of spins that contributes the most to the properties of the side bands. Given the frequency of rotation and the magnetic field gradient one can determine the amplitude of the motion of spins. It is possible to construct appliances for imaging the motion with the employment of side bands. The full application of the side bands theory is still far off. The use of this method in medical diagnostics requires wide investigations of the properties of side bands and expensive spectrometers or tomographs equipped with ultra fast computers.

At the present stage of investigations it is not possible to decide definitely whether or not the theoretical methods are fully correct. The approach demonstrated may prove insufficient for the examination of biological systems.

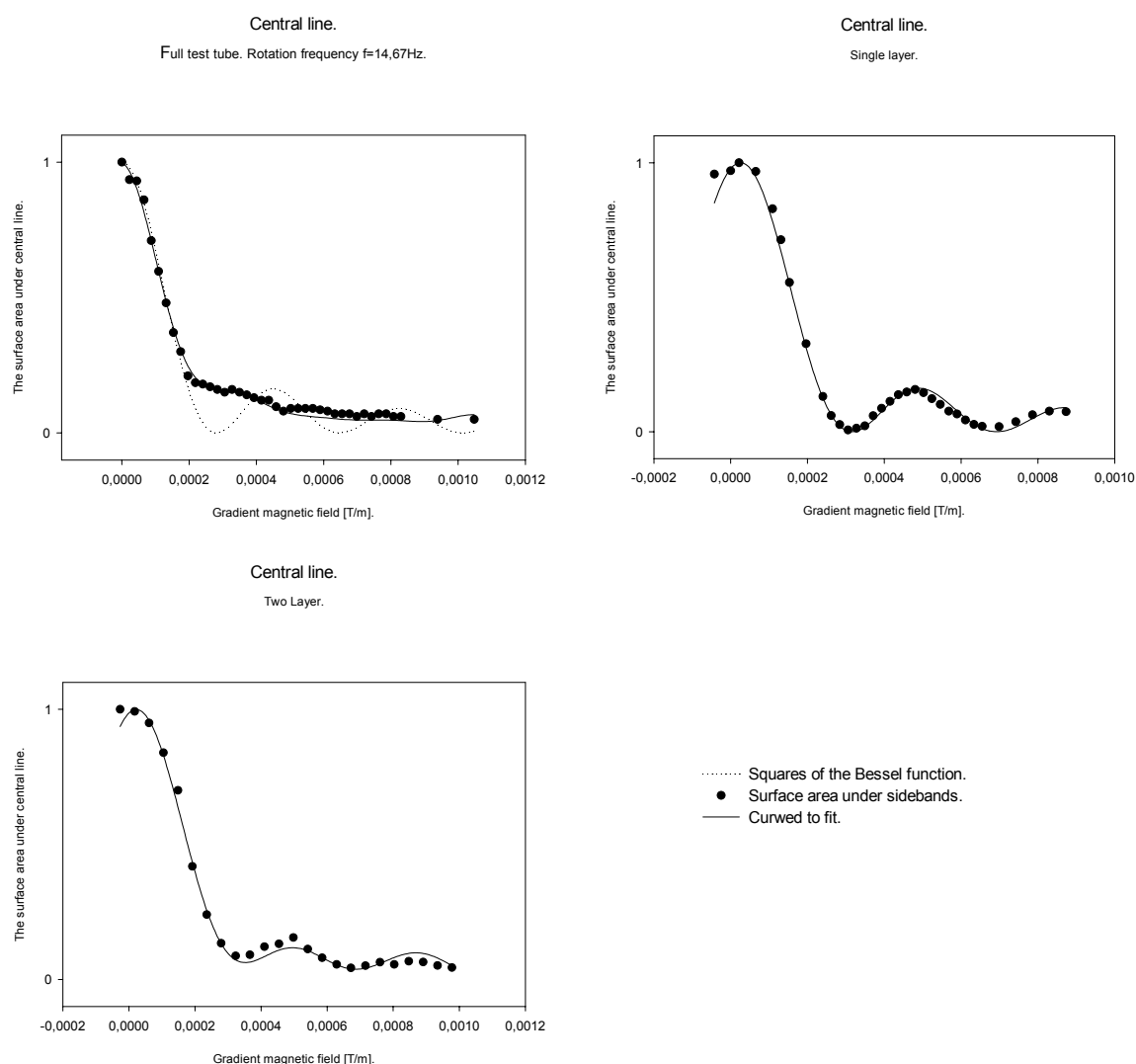


Fig.1. The plots represent surface area under the principal band as a function of the magnetic field homogeneity detuning.

References:

- [1] C.J.Lewa "MRI response in the presence of mechanical waves, NMR frequency modulation, mechanical waves as NMR factor" *Acustica* vol. 77 (1992).
- [2] J.Talpe "Theory of experiments in paramagnetic resonance" Pergamon press. Oxford 1971.
- [3] D.Kruk, B.Blicharska "Analysis of shape of FID signal and NMR spinning sidebands for the Couette flow" *Physica B* 301 (2001).
- [4] B.Blicharska, D.Kruk "Influence of sample rotation on the shape of the free induction decay" *Acta Physica Polonica A* vol.84 (1993).
- [5] J.Klafczyńska "Badanie własności pasm bocznych w widmie NMR w funkcji gradientu pola magnetycznego" Praca magisterska wykonana pod kierunkiem prof. dr hab. C.Lewę w Instytucie Fizyki Doświadczalnej U. G.

NMR DIFFUSION STUDIES USING ULTRAHIGH STATIC MAGNETIC FIELD GRADIENTS

Franz Fajara

Institut für Festkörperphysik TU Darmstadt

Using specially designed superconducting coils we obtain static magnetic field gradients (SFG) of up to about 200 T/m which is far above of what can be achieved by pulsed field gradients (PFG). NMR stimulated echo experiments in such ultrahigh field gradients are well suited for studying small diffusivities, strongly restricted and/or anomalous diffusion. I will start my talk by introducing the special features of such experiments. There is a close analogy to incoherent dynamic neutron scattering and to forced Rayleigh scattering. Most important, the SFG working regime extends down toward diffusion coefficients of below $10^{-15} \text{ m}^2 \text{ s}^{-1}$ and to resolvable root mean square displacements of less than 10 nm. In the latter part I will illustrate these features by a couple of results collected over the last ten years: vacancy diffusion in molecular crystals; decoupling phenomena in supercooled liquids when approaching the glass transition; reptation dynamics in long chain polymer melts; hindered translational diffusion in confining geometries (pores, channels); identification of intracrystalline diffusion of guest molecules in small zeolite crystallites.

¹³C-NMR STUDY OF MICROSTRUCTURE OF BUTYL ACRYLATE-METHYL METHACRYLATE COPOLYMERS

Magdalena Gołabek¹, Piotr Bujak¹, and Marek Matlengiewicz^{1,2}

¹*Department of Environmental Chemistry and Technology, Silesian University, ul. Szkolna 9, 40-006 KATOWICE, Poland*

²*Institute of Coal Chemistry, Polish Academy of Sciences, ul. Sowińskiego 5, 44-121 GLIWICE, Poland*

The microstructure of macromolecular chain of acrylic copolymers can be determined analysing various signals in their ¹³C NMR spectra but the most complete information about the distribution of the configurational-compositional sequences can be obtained from the carbonyl and β-CH₂ carbons, since only these carbons are always present in typical acrylic structural units. The carbonyl signal can provide information on distribution of uneven sequences, usually up to configurational-compositional pentads, while the methylene signal from the main chain is the source of complementary information on even sequences, usually up to tetrads. It was shown recently that for poly(methyl methacrylate-*co*-ethyl acrylate), PMMA/EA, it is possible to obtain full sequence distribution up to pentads by means of detailed analysis of its 100 MHz ¹³C NMR spectrum applying incremental calculation of the position of respective lines and subsequent spectrum simulation. The method developed for PMMA/EA copolymer is quite general and may be applied to a wide range of acrylate-methacrylate copolymers of industrial importance to determine the sequence distribution of these copolymers. This information is necessary to properly relate all the macroscopic properties of the copolymers with their chemical structure.

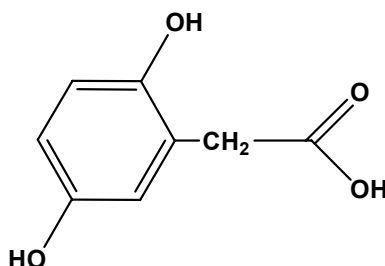
In the present work we apply the same approach to study microstructure of another copolymer, poly(methyl methacrylate-*co*-*n*-butyl acrylate), PMMA/NBA. In the 100 MHz ¹³C NMR spectrum of this copolymer the carbonyl signal at 174-178.5 ppm is clearly split into the lines of configurational-compositional pentads, while the β-methylene signals at 32-55 ppm reveal the lines of individual tetrads.

NMR FINGERPRINT OF 2,5-DIHYDROXYPHENYLACETIC (HOMOGENSIC) ACID

Adam Gryff-Keller and Anna Kraska

*Warsaw University of Technology, Faculty of Chemistry,
Noakowskiego 3, 00-664 Warsaw*

Ochronosis is a rare hereditary disease manifesting itself with the deposition of dark pigment in tissues rich in collagen, which is frequently accompanied by inflammatory arthritis, urinary calculi and other severe symptoms. This disease is caused by an inherited lack of phenylalanine catabolizing enzyme. As a result patients excrete in urine massive amounts of homogentisic acid (alkaptonuria).



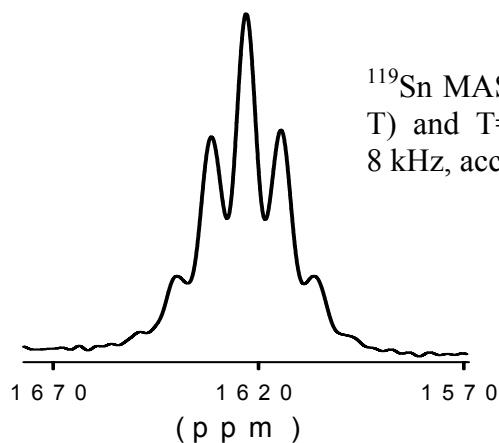
The final medical diagnosis of this disease is based on the determination of the urinary level of this acid, which can be as high as 1 – 3 mole/mole creatinine (as compared to the norm for a healthy subject 0.002 mole/mole creatinine). NMR can potentially be used for such determinations. This study was aimed at collecting all the necessary data for such an analysis. Since, dependently on the acidity, homogentisic acid can exist in water solutions as neutral species, as mono-, di-, or even trianion, its ^1H and ^{13}C NMR spectra are pH-sensitive. In the reported study this dependence has been monitored and interpreted.

INDIRECT NUCLEAR INTERACTIONS IN MPtSn SEMICONDUCTORS (M=Ti, Zr, Hf, Th) : ^{119}Sn AND ^{195}Pt MAS NMR STUDY

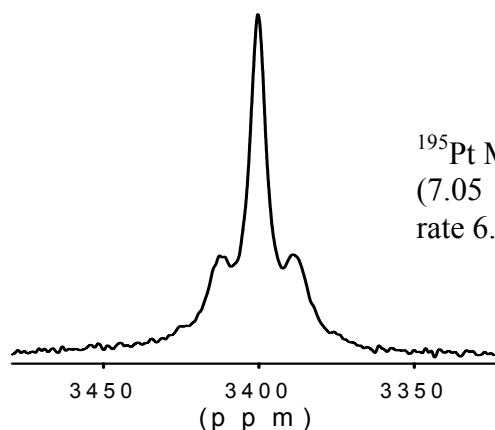
Agnieszka Grykałowska and Bogdan Nowak

*W. Trzebiatowski Institute of Low Temperature and Structure Research,
Polish Academy of Sciences, P.O. Box 1410, 50-950 Wrocław 2, Poland*

The semi-Heusler-type compounds MPtSn (M=Ti,Zr,Hf,Th) crystallize in the cubic MgAgAs-type of structure. This structure may be considered as zinc-blende crystal structure of tin and platinum atoms in which the M atoms occupy the octahedral interstitial sites. Thus each Sn and M atom is tetrahedrally coordinated by Pt atoms, whereas each Pt atom is doubly tetrahedrally coordinated by Sn and M atoms. The tetrahedral geometry implies that the bonding is primarily covalent with sp^3 bonds. Thus the family of MPtSn compounds appears to be an appropriate system to search for electron-coupled interactions. In favorable cases (TiPtSn and ZrPtSn) the ^{119}Sn and ^{195}Pt MAS NMR spectra reveal expected J coupling patterns originating from indirect spin coupling between Pt and Sn nuclei.



^{119}Sn MAS NMR spectrum of TiPtSn at 111.9 MHz (7.05 T) and T=294 K. $J_{\text{iso}}(\text{Sn-Pt}) = 1920$ Hz. Spinning rate 8 kHz, accumulation number 2056.



^{195}Pt MAS NMR spectra of ZrPtSn at 64.4 MHz (7.05 T) and T=294K. $J_{\text{iso}}(\text{Pt-Sn}) = 1550$ Hz. Spinning rate 6.5 kHz, accumulation number 16384.

NMR OF HIGH-TEMPERATURE SUPERCONDUCTORS AND IN PULSED HIGH FIELD MAGNETS

Jürgen Haase

Leibniz-Institut für Festkörper- und Werkstofforschung, Dresden

NMR was one of the most important spectroscopic methods to prove classical superconductivity (BCS theory). It is therefore expected that NMR also holds important clues about the electronic structure of the new, high-temperature superconductors. Important findings from about 15 years of NMR research on high temperature superconductors will be summarized and new NMR evidence will be presented that shows the special physical properties of these materials that still await a satisfying theoretical description. Not only the NMR of superconductors may benefit from very high magnetic fields, and the first results will be reported of carrying NMR in pulsed high field magnets, that allow for magnetic field strengths of 60 T currently, and of up to 100 T in not too distant future.

DESIGN PRINCIPLES OF THE GRAPHICAL USER INTERFACE FOR MRI SYSTEM BASED ON THE MARAN DRX CONSOLE

J.M. Haduch^{1,2}, T. Banasik², A. Jasiński², and T. Skórka²

¹ AGH University of Science and Technology, Faculty of Physics and Applied Computer Science, Kraków, Poland

² The Henryk Niewodniczański Institute of Nuclear Physics PAS Cracow, Department of Magnetic Resonance, Kraków, Poland

Graphical User Interface design is dedicated to Magnetic Resonance Imaging system based on Maran DRX Console operating 4.7 tesla MR system.

GUI has to provide user friendly environment to use imaging sequences already installed and testing the new ones. It should provide easy data processing from phantoms, plants, small animals (*in vivo*) and human limbs. The new interface has to be able to use already existing libraries or object files brought by Maran DRX Console and to overtake almost all functionality offered by the current system [1]. It is designed to operate in MS Windows™ 2000 and XP family operating systems. GUI is being written using Borland Delphi 5.0 Professional environment, object oriented, with VCL and COM technologies and open source libraries, covering multidimensional Fast Fourier Transform (FFT) and Inverted Fast Fourier Transform (IFFT) algorithms, obtained from the FFTW project website and adapted to magnetic resonance imaging purposes. [2][3][4]

The basic aim of designing GUI is to make a very useful and intuitive software allowing user to perform whole experiment without a comprehensive and detailed knowledge of particular procedures and commands already used. It allows to focus on the results and hopefully to save time spared on preparation and setting all the examination parameters including proper slice positioning and selecting field of view.

This software is developed as a MSc. project at AGH University¹.

Literature:

[1] Guihéneuf T.: *RINMR User Manual*, Resonance Instruments Ltd 2002

[2] Paślowski A.: *Programowanie w Delphi 5.0*, Wydawnictwo „Edition 2000”, Kraków 2000

[3] <http://www.fftw.org>

[4] *Borland Delphi 5 for Windows 98, Windows 95, & Windows NT, Object Pascal Language Guide*, Inprise Corporation 1999

EFFECT OF ANTIBIOTICS ON FORMING OF WHEAT THYLAKOIDS AS OBSERVED IN REHYDRATED MEMBRANE LYOPHILIZATES USING PROTON MAGNETIC RELAXATION AND SORPTION ISOTHERM

H. Harańczyk¹, A. Leja¹, and K. Strzałka²

¹*Institute of Physics and* ²*Faculty of Biotechnology, Jagellonian University, Cracow*

The use of antibiotics (chloramphenicol and actidion) strongly influences the photosynthetic membrane structure if applied during the process of thylakoid formation. The subsequent lyophilization procedure preserves the membrane structure, however, the hexagonal phase tubulae are presumably formed.

The rehydration process was performed from the gaseous phase; its kinetics shows single exponential form with the hydration time $t_{\text{hyd}} = (17.1 \pm 3.2)$ h and $t_{\text{hyd}} = (20.2 \pm 7.9)$ h for the membranes modified by the use of chloramphenicol and the use of actidion, respectively, whereas for control sample (only paramagnetic non-functional manganese pool washed out by use of 1mM EDTA) the hydration time equals to $t_{\text{hyd}} = (22.0 \pm 2.8)$ h .

For control and modified membranes the sorption isotherm reveals the sigmoidal form and is successfully fitted using Dent model. The mass of water saturating primary water binding sites, $\Delta M/m_0$, was 0.017, and 0.020, for membranes washed in 1mM EDTA, and chloramphenicol treated, respectively.

Proton magnetic relaxation shows the presence of solid component (described by Gaussian function) and two or three liquid components coming from several water pools appearing in the membrane with increased hydration level. NMR sorption data are well fitted using the parameters obtained from gravimetry. Moreover it revealed the presence of “sealed” water pool, which most likely comes from hexagonal phase tubulae present in photosynthetic membrane lyophilizate.

WATER BOUND IN ANTARCTIC LICHEN *Usnea antarctica* AS OBSERVED BY PROTON RELAXATION AND SORPTION ISOTHERMS.

Harańczyk¹, A. Pietrzyk¹, and ²M.A. Olech

¹*Institute of Physics and* ²*Institute of Botany, Jagellonian University, Cracow*

In search of dehydration limits of living creatures, the attention is focused on species populating habitats experiencing the extremely low hydration and/or decreased temperature. Among them the Antarctic lichens are a good example. In contrast to vascular plants which stop their photosynthetic activity during winter, lichens can be photosynthetically active and productive even if the tissue is frozen.

A fundamental for understanding the molecular mechanism of the metabolic activity recovery during rehydration is knowledge about the number and distribution of water binding sites, sequence and kinetics of their saturation, as well as the formation of tightly and loosely bound water steps at different steps of hydration process.

In our experiment we focused on the hydration processes, the nature of binding sites, and water fractions bonded at subsequent stages of early hydration process for *Usnea antarctica*. Samples were collected in Maritime Antarctic, Antarctic Peninsula, King George Island, Polish Antarctic H. Arctowski Station.

To monitor early hydration processes, the hydration courses from the gaseous phase were performed. For the low target relative humidities the hydration courses are well fitted using single exponential function whereas for higher values of target humidity a second and finally third exponent in hydration function is detected. The observed components respond for: (i) very tightly bound water ($\Delta m/m_0 = 0.030 \pm 0.011$, t_{hyd} short); (ii) tightly bound water ($\Delta m/m_0 = 0.061 \pm 0.028$, $t_{\text{hyd}} = (2.9 \pm 1.0)$ h) and (iii) loosely bound water pool ($t_{\text{hyd}} = (62.2 \pm 21.3)$ h, as averaged over all relative humidities). The sorption isotherm revealed a sigmoidal form and was fitted using Dent model, allowing us to distinguish very tightly bound water pool. The proton relaxation results differentiated tightly and loosely bound water fraction.

A SPECIALIZED PROBEHEAD FOR MR IMAGING OF SMALL OBJECTS *IN VIVO*.

S. Heinze-Paluchowska, T. Skórka, A. Jasiński, P. Borowiec, J. Kiczek, P. Skóra,
and R. Wiertel

H. Niewodniczanski Institute of Nuclear Physics, Polish Academy of Sciences, Krakow

We report the design and construction of a homebuilt probehead to measure small objects (i.e. mouse heart *in vivo*).

Designed probehead contains the homebuilt, unshielded gradient system, high-pass birdcage coil and specialized animal handling system for the 4,7T /310 MRI system with MARAN DRX console.

The gradient system with inner diameter of 60mm produce gradients with a risetime below 100 μ s. The gradient coils are water cooled. Their effectiveness is 0,5 Gs/cm \cdot A. These coils were designed by the Minimum Inductance method. Transversal coils are made of a copper sheet using water jet cutting.

For NMR signal transmission and reception an 8-rung shielded, quadrature birdcage coil with diameter of 40mm was designed and constructed. Dimensions of the coil were optimized for the mouse size in order to obtain best value of the signal to noise ratio.

The probehead has also integrated animal handling system including flanged animal support with positioning pad. It also contains the anesthesia delivery, ECG monitoring and temperature controller. When MRI measurements must be synchronized with cardiac cycle (cardiac triggering), an ECG trigger unit (RAPID Biomedical ECG TRIGGER UNIT HSB) is used for exact ECG triggering. Physiological rates of anesthetized mice can vary due to changes in thermal response. This can invalidate the defined acquisition window, hence introducing motion artefacts. To maintain constant body temperature we use the Variable Temperature Controller (Resonance Instruments) - heating air flown over the mouse.

Acknowledgements:

The Committee for Scientific Research of Poland supported this work, under grants No 3P05A 003 25 and 2P05C 054 26.

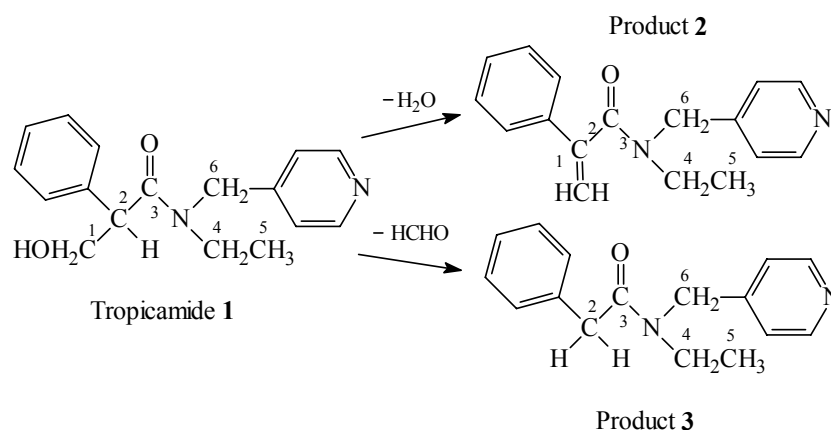
DYNAMIC INVESTIGATIONS ON TROPICAMIDE AND ITS DEGRADATION PRODUCTS

Franciszek Herold¹, Jerzy Kleps¹, Jacek Stefanowicz¹, and Andrzej Zimniak²

¹Department of Drug Technology, ²Department of Physical Chemistry
Faculty of Pharmacy, Medical University of Warsaw, Banacha 1, 02-097 Warsaw

Tropicamide is a drug showing parasympatholytic activity, similarly to atropine. However, due to faster action and less side-effects it displaced to a great extent atropine in the ophthalmic therapeutics. Tropicamide widens the pupil and paralyzes eye accommodation, moreover, it is an antagonist of muscarine receptor M₄.

For several years crystalline tropicamide and its water solutions applied as eye drops have been investigated in terms of their stability. Timm and co-workers [1] observed that two basic decomposition products were formed, **2** and **3**.



Compound **2** is the product of dehydration of tropicamide **1**, and **2** is formed after elimination of formaldehyde. Although tropicamide is satisfactorily stable for medical applications [2], extensive investigations on properties of its degradation products **1** and **2** are important. Results shown below represent one stage of this study.

The dynamic comparative measurements of **1**, **2** and **3** were accomplished. ¹H NMR spectra in d₆-DMSO solutions were recorded starting at 25°C and rising the temperature above the coalescence point. The data are collected in the Table.

Table. Selected data for **1**, **2** and **3** obtained in comparative dynamic ¹H NMR study. Bruker AVANCE DMX 400WB instrument was used, spectra were taken in d₆-DMSO.

Compound	Group of protons investigated	$\Delta = \nu_{\text{Ha}} - \nu_{\text{Hb}}$ [Hz] at 25°C	Coalescence temp. [°C]	τ [s]	ΔG^\ddagger [kJ·mol ⁻¹]
1	N-4CH ₂ -5C	33.4	85	0.0135	85.0
2		57.9	80	0.0078	72.7
3		38.7	75	0.0116	72.8

Rotation around the amide bond CO-N was investigated. The double quartets of protons N-4CH₂-5C were chosen for measurements because they occurred as distinct, non-overlapping multiplets for all three compounds investigated. The frequency difference Δ at 25°C was accepted as reference for stopped rotation.

The free activation enthalpy ΔG^\ddagger was calculated according to Eyring equation:

$$\Delta G^\ddagger [\text{J}\cdot\text{mol}^{-1}] = 8.314T[23.761 + \ln(\tau T)].$$

The average lifetime τ was estimated by use of following approximation:

$$\tau[s] = \frac{\sqrt{2}}{\pi \cdot \Delta \nu}$$

As one can see in the Table, the highest barrier of rotation is observed for tropicamide **1** ($84.96 \text{ kJ}\cdot\text{mol}^{-1}$), whereas the values for both decomposition products **2** and **3** are lower and very similar in magnitude (72.69 and 72.79 , respectively). This result can be explained by the non-bonding attracting interaction between the OH group at the carbon atom 1C and the picolyl ring. Structure of tropicamide **1** was calculated using the AM1 simulation program, and the obtained distance between oxygen atom and the protons at picolyl ring was 2.75 \AA , which makes the interaction possible. Thus, conclusion can be drawn that the tropicamide molecule is more rigid as compared with degradation products **1** and **2**.

References:

- [1] Timm U., Gober B., Dohmet H., Pfeifer S., Pharmazie 1997, 32, 331.
- [2] Pohloudek-Fabini R., Martin E, Gallasch V., Pharmazie 1982, 37, 184.

REORIENTATIONAL MOTIONS OF THE NH₃ LIGANDS IN [Zn(NH₃)₄](BF₄)₂

Łukasz Hetmańczyk^a, Wojciech Medycki^b, Edward Mikuli^a and Anna Migdał-Mikuli^a

^a Jagiellonian University, Faculty of Chemistry, Department of Chemical Physics, 30-060 Kraków, ul. Ingardena 3, Poland

^b Institute of Molecular Physics, Polish Academy of Sciences, 60-179 Poznań, ul. Smoluchowskiego 17, Poland

Tetraaminezinc(II) tetrafluoroborate: [Zn(NH₃)₄](BF₄)₂ is particularly interesting molecular material because of the occurrence of different reorientational motions of the complex cations, NH₃ ligands and BF₄⁻ anions. In [Zn(NH₃)₄]²⁺ cations the Zn²⁺ ion occupies the center of a tetrahedron formed by the NH₃ ligands. The BF₄⁻ anions have also a tetrahedral structure. The crystal structure of the title compound is orthorhombic, space group *Pnma* (No 62) with *a* = 10.523 Å, *b* = 7.892 Å, *c* = 13.354 Å and *Z* = 4 [1]. On heating or on cooling this compound undergoes three solid-solid phase transitions which are attributed to the changes in the molecular groups arrangements as well as the changes of their reorientational dynamics. The DSC measurements [2] performed in the temperature range 90-300 K detected three anomalies of the heat flow connected with three phase transitions. The thermodynamic parameters of these phase transitions are presented in Table. 1.

Table. 1. Thermodynamics parameters of the phase transitions of [Zn(NH₃)₄](BF₄)₂ (on heating)

Compound	<i>T_C</i> [K]	Δ <i>H</i> [kJ·mol ⁻¹]	Δ <i>S</i> [J·mol ⁻¹ ·K ⁻¹]
[Zn(NH ₃) ₄](BF ₄) ₂	179.4	1.37	7.6
	120.6	0.93	7.7
	106.5	0.08	0.7

The measurements of the line width and the second moment of ¹H NMR line were performed in the temperature range of 90-295 K on a 25 MHz laboratory made instrument operating in the double modulation system [1]. The proton ¹H NMR measurements of the spin-lattice relaxation time *T*₁ were performed in the temperature range of 85-295 K on a Bruker SXP 4-100 spectrometer working at the frequency of 84.6 MHz. The temperature of the sample (degassed under a pressure of 10⁻⁵ Torr and sealed under vacuum in glass ampoule) was automatically stabilized by the standard Bruker BS 100/700 liquid nitrogen system with the accuracy ± 1 K. The *T*₁ relaxation times were determined using the π-τ-π/2 sequence of pulses for times shorter than 1 s and saturation method for longer than 1 s.

Fig. 1a shows the temperature dependencies of the slope line width (δ*H*) and the second moment (*M*₂) of ¹H NMR line in the studied compounds. In order to propose a model of internal dynamics, the second moment value was calculated from the van Vleck formula [3]. The onset of the following reorientations was taken into account during the heating of this compound: the reorientation of NH₃ ligands about the M-N axis and the reorientation of tetrahedral cation. It was assumed that the N-H bond distances were of 1.00 Å and all the N-H bonds were tetrahedrally directed with respect to the Zn-N bonds and the distance Zn-N takes the value of 2.01 Å. The *M*₂^{Rigid} obtained the value of 47.3·10⁻⁸ T². The observed value of the second moment of ¹H NMR line for [Zn(NH₃)₄](BF₄)₂ close to 12·10⁻⁸ T² at 90 K can be interpreted as resulting from the NH₃ ligands reorientation. No changes were found in the vicinity of *T*_{C3} and *T*_{C2} phase transition temperatures. On heating at *T*_{C1} the reorientations of tetrahedral [Zn(NH₃)₄]²⁺ cation set on.

The quasielastic neutron scattering (QNS) study [1] in the temperature range of 22–190 K give the evidence of fast (correlation time τ ≈ 10⁻¹¹ – 10⁻¹² s) stochastic reorientational

motions of NH_3 in phases III and II of $[\text{Zn}(\text{NH}_3)_4](\text{BF}_4)_2$. Below T_{C3} the reorientation of NH_3 change drastically (τ becomes shorter than 10^{-10} s).

The results of spin-lattice relaxation time $T_1(^1\text{H})$ versus temperature measurements are presented in Fig 1b. Two components of spin-lattice relaxation time: T_1' and T_1'' were observed because of the cross-relaxation effect between protons and fluorines (compare with [4]) resulting from BF_4^- and NH_3 reorientations with similar τ . Below T_{C3} it can be seen the minimum of T_1 vs. $1000/T$ at ca. 91 K. Evident changes of the T_1 values can be seen at T_{C1} .

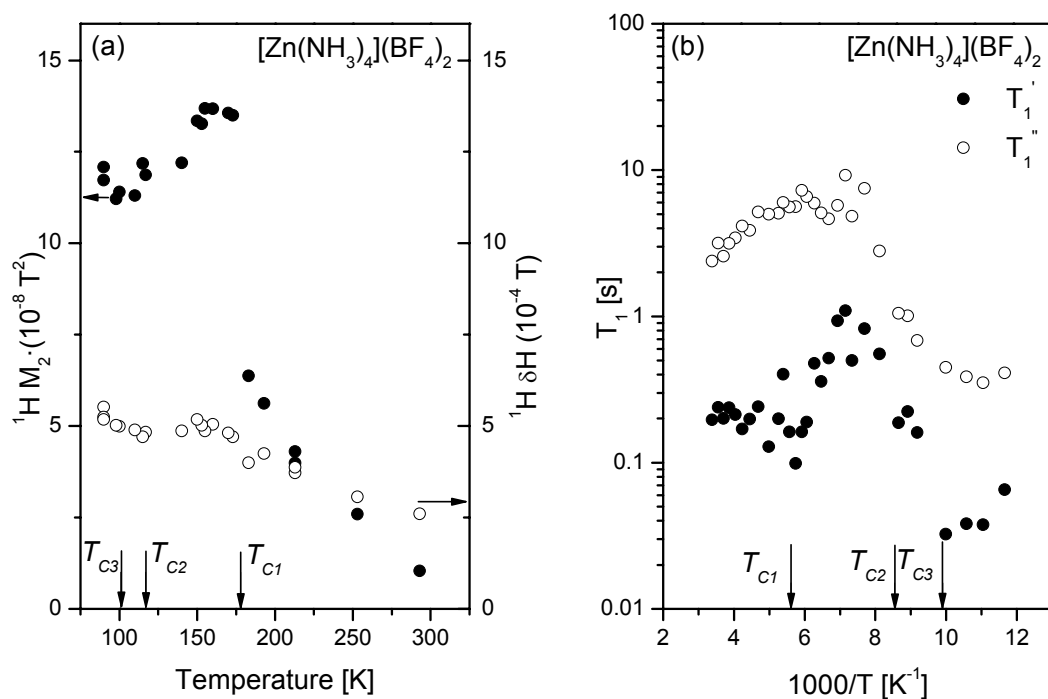


Fig. 1. Temperature dependences: a) of the slope line width (δH) and of the second moment (M_2), b) of the T_1 obtained by ^1H NMR for $[\text{Zn}(\text{NH}_3)_4](\text{BF}_4)_2$

References:

- [1] A. Migdał-Mikuli, E. Mikuli, Ł. Hetmańczyk, I. Natkaniec, K. Hołderna-Natkaniec, W. Łasocha, *J. Solid St. Chem.* **174** (2003) 357.
- [2] A. Migdał-Mikuli, E. Mikuli, Ł. Hetmańczyk, E. Ściesińska, J. Ściesiński, S. Wróbel, N. Górka, *J. Mol. Struct.* **596** (2001) 123.
- [3] J.H. van Vleck, *Phys. Rev.* **74** (1948) 1168.
- [4] E. Mikuli, B. Grad, W. Medycki, K. Hołderna-Natkaniec, *J. Solid St. Chem.* **177** (2004) 3795.

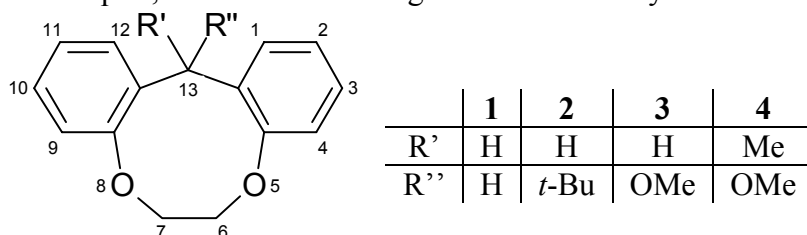
CONFORMATIONAL ANALYSIS OF DIBENZO[E,H][1,4]DIOXONIN DERIVATIVES

Krzysztof Jamroz^a, Edward Szneler^a, **Jacek Grochowski**^b, Paweł Serda^b,
and Barbara Rys^a

^aDepartment of Organic Chemistry, Jagiellonian University, Ingardena 3, 30-060 Kraków

^bRegional Laboratory of Physicochemical Analyses and Structural Research, Jagiellonian University, Ingardena 3, 30-060 Kraków

Conformational analysis of title compounds **1** – **4** was performed by combination of ¹H and ¹³C DNMR techniques, molecular modeling method and X-ray structure determination.



DNMR spectra

In both carbon and proton spectra of compound **1** two spectral processes are observed. In the ¹H NMR spectrum of **1** taken at 300 K two singlets for benzylic and aliphatic CH₂ groups are present. Both signals are gradually broaden with lowering temperature and at 190 K an AX spin system is observed for H-13 and two broad signals of equal intensity for H-6/7. At the same time signal of aromatic protons at H-1/12 undergoes coalescence. At 155 K broad, unequally populated signals in the region of aliphatic proton resonance are observed. In the ¹³C NMR spectra of **1** the first coalescence process does not change the number of signals what corresponds to the racemization of enantiomeric conformations of **1**. At 155 K all signals in ¹³C NMR spectra are broad.

¹H NMR spectra of **2** and **3** are unaffected with temperature lowering at the range of the first coalescence in spectra of **1**. Further lowering of temperature gives two unequally populated signals for methyl and methylene protons in **2** whereas does not cause any changes in spectra of **3**. In carbon spectra of both compounds broadening of signals occurs below 160 K.

The number of signals in the ¹³C NMR spectra of **4** indicates presence of time-averaged plane of symmetry. Signal of carbon C-6/7 is significantly broaden, whereas those corresponding to methyl group and atoms C-12a/13a are absent. Lowering the temperature causes coalescence of all aliphatic signals in the proton spectrum at 250K. Below the first coalescence at 200 K are observed two sets of signals (relative populations 0.84:0.16) for the medium ring and substituents protons. In carbon spectrum at that temperature are present separate signals of methyl, methoxy and methine carbon atoms for major and minor conformer. At 140 K second coalescence is observed in ¹H and ¹³C NMR spectra.

In summary, for compound **1** first observed spectral process corresponds to inversion of chiral conformation and the second one is an interconversion leading to separation of two diastereoconformers. Spectra of compounds **2** and **3** show only one conformer in the range of first coalescence for compounds **1** and **4** suggesting either fast exchange of conformers or the presence of the single symmetrical conformation. Second process separating two diastereoconformers is observed only for compound **2**. In analogy to **1** in spectra of compound **4** two processes can be observed. As a result of the first one two diastereoconformers separate

at 200 K. Slow exchange limit is not reached down to 130 K for the second coalescence process in that compound.

Molecular modeling

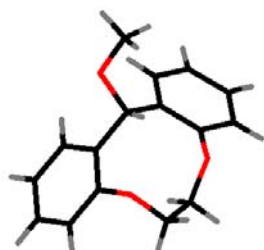
MM+ molecular mechanics and semiempirical AM1 calculations show CB conformation with equatorial substituent at C-13 (see picture 1 representing conformation of **3** in the solid state) as a global minimum for **1** – **3**. The TCB conformation with OMe and *t*-Bu groups in less hindered location, has found to be the second lowest minimum (picture 2). As estimated by AM1 method this conformation is 2.1, 10.0 and 4.4 kJ/mol higher in energy than the global minimum for compounds **1**, **2** and **3**, respectively.

Geometry of the global minimum of compound **4** depends on the method of calculation. Molecular mechanics showed C₂ symmetry TCTB conformation as the lowest energy form. The second higher in energy (9.8 kJ/mol) is the TCB conformation with methyl group in the equatorial orientation. The same conformation of medium ring with axial methyl group is 10.6 kJ/mol above global minimum. Semiempirical AM1 calculations indicate as a global minimum conformation CB with axial methyl group. In the next two conformers medium ring is in the TCB conformation. Their energies are 5.7 kJ/mol and 9.7 kJ/mol higher than the global minimum and correspond to axial and equatorial orientation of methyl group. The twist form (being MM+ global minimum) is 17.20 kJ/mol above CB conformer.

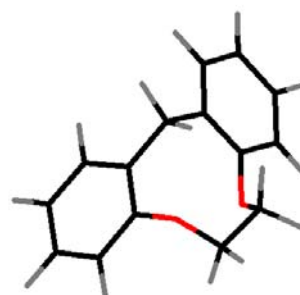
X-ray structure determination

In crystal molecules of **3** adopt CB conformation (picture 1) with methoxy group in equatorial position which is the global minimum in MM+ and AM1 calculations. The most relevant geometric parameters of this conformation are *gauche* orientation in O-C-C-O fragment and H-13...O-5/8 distance of 2.42 to 2.50 Å which is significantly shorter than the sum of the van der Waals radii for H and O atoms (1.2 and 1.5 Å).

Picture 1 Crystal state conformation of **3**.



Picture 2 TCB conformation of **1**.



Conclusions

The ground state conformation of the molecules of compounds **1** – **3** is the chair-boat form. That conformation is stabilized in the solid state by intramolecular hydrogen bond. At high temperature molecules are involved in fast conformational processes. The first coalescence present in the spectra of **1** and **4** is consistent with the slowing down the rate of racemization of enantiomeric ground-state conformers with the barrier ca. 40 kJ/mol.

There is no evidence of slowing down the rate of interconversion of CB conformation in the spectra of **2** and **3**. Inspection of calculated ground-state geometries of these compounds allows us to state that above mentioned conformation process is restricted due to severe steric interaction caused by substituents at axial position. The second conformational process, observed at lower temperature for all compounds might be interpreted as an interconversion of two diastereoisomers. The barrier of ca. 30 kJ/mol separates CB and TCB conformers i.e. two forms of pseudorotation cycle.

PROTON NMR STUDIES OF MOLECULAR DYNAMICS IN POLYDIMETHYLSILOXANE

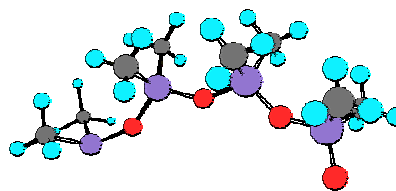
Mariusz Jancelewicz, Hieronim Maciejewski*, and Stefan Jurga.

*Institute of Physics, Adam Mickiewicz University, Umultowska 85,
PL- 61614 Poznan, Poland.*

**Poznan Science and Technology Park, Rubiez 46, PL-61612 Poznan, Poland.*

Polydimethylsiloxane (PDMS) belongs to a group of polymers containing a silicon – oxygen skeleton with methyl groups on the silicon atom (see molecular structure). Major application for PDMS is as lubricant oils and as plasticiser in silicon jointing compounds in the construction industry.

In this paper we present results of measurements of the magnetic relaxation time T_1 in the frequency domain, results of DSC and rheology measurements. T_1 ^1H NMR relaxation dispersion of the PDMS has been measured by Fast Field Cycling technique in the Larmor frequency range from 10 kHz up to 12 MHz. Results of dispersion measurements indicate the T_1 dependence according to Rouse model [1,2].



Molecular structure of PDMS
(red – oxygen; violet – silicon;
black – carbon; blue - hydrogen).

References:

- [1] N. Fatkullin, R. Kimmich, E. Fischer, C. Mattea, U. Beginn, M. Kroutieva;
The confined-to-bulk dynamics transition of polymer melts in nanoscopic pores of solid matrices with varying pore diameter; *New Journal of Physics* 6 (2004) 46.
- [2] R. Kimmich, N. Fatkullin, E. Fischer, C. Mattea, U. Beginn;
Reptation in Artificial Tibes and the Corset Effect of Confined Polymer Dynamics;
Mat. Res. Soc. Symp. Proc. Vol. 790.

APPLICATION OF NMR SPECTROSCOPY FOR INVESTIGATION OF COMPLEXES OF RHODIUM SALTS WITH NITROGENOUS BASES

Jarosław Jaźwiński

Instytut Chemii Organicznej Polskiej Akademii Nauk, 01-224 Warszawa. ul. Kasprzaka 44/52
e-mail: jarjazw@icho.edu.pl

Dimeric rhodium(II) tetracarboxylates, like $\text{Rh}_2(\text{CF}_3\text{COO})_4$ and $\text{Rh}_2(\text{CH}_3\text{COO})_4$, can potentially form, with organic ligands, adducts with various stoichiometry and structure (Fig. 1). A ligand and dirhodium salt in the solution yields usually an equilibrium mixture of adducts and uncomplexed ligand.

Various nitrogenous bases, like amines, pyridine and azoles, were used as the model ligands. The NMR spectroscopy (^1H , ^{13}C i ^{15}N NMR) was applied for investigation a binding process in the CDCl_3 solution. Identification of adducts existing in the solution, and influence of binding on spectral parameters of nitrogenous ligand, were the main aim of the work.

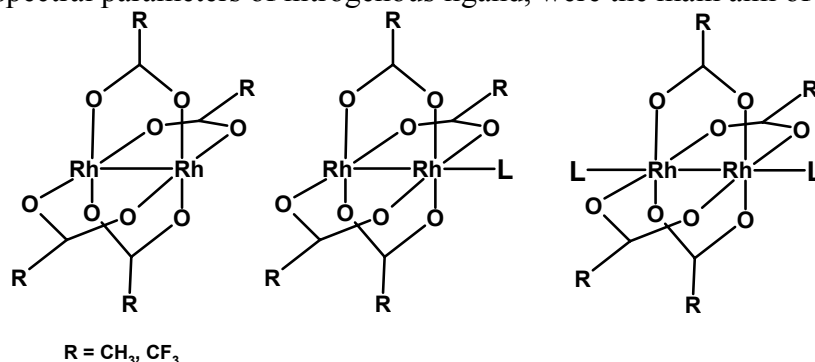


Figure 1. Rhodium(II) tetracarboxylate dimers and two kinds of adducts with organic ligands L, 1 : 1 and 1 : 2.

At room temperature, due to fast exchange of the ligand, usually one set of signals is observed in the NMR spectrum. Only shift of NMR signals reveals ligand interaction with dirhodium salt. However, at low temperature (below 253 K) ligand exchange rate decreases and allows, in certain cases, to observe the NMR signals of all individual species existing in the solution. The NMR investigations lead to the following conclusions: (i) Two kinds of adducts, 1 : 1 and 1 : 2, are successively formed in the solution, depending on ligand-to-rhodium salt ratio; (ii) Binding of dirhodium salt results the high field shift of ^{15}N signal; the adduct formation shift defined as $\Delta\delta = \delta_{\text{adduct}} - \delta_{\text{free base}}$ is in the range from -9 to -30 ppm for amines and from -70 to -150 ppm for aromatic nitrogenous base (pyridine, azoles). (iii) The magnitude of $\Delta\delta(^{15}\text{N})$ is larger for 1 : 1 adduct than for 1 : 2 adduct; of *ca.* 10 ppm.

Foregoing findings can be applied for structure investigation of dirhodium(II) complexes, and for determination of binding site for ligands containing a few heteroatoms.

The work was supported by the State Committee for Scientific Research under Grant No 4 T09A 060 25

PROTON NMR STUDIES OF HARD DENTAL TISSUES UNDER FAST MAS

Joanna Kolmas¹, Zofia Paszkiewicz², Anna Slosarczyk², and Wacław Kołodziej¹

¹*Department of Inorganic and Analytical Chemistry, Medical University of Warsaw, ul. Banacha 1, 02-097 Warszawa, Poland.*

²*Stanisław Staszic Univ., Min. And Mat. Faculty of Materials Science and Ceramics, Al. Mickiewicza 30, Kraków 30-059, Poland.*

Enamel, dentin and dental cementum were studied by proton solid-state NMR with magic-angle spinning (MAS). The experiments were done at 400 MHz using the Bloch decay pulse sequence and the MAS rate at 30 kHz. Collagen type I, carbonate apatite and hydroxyapatites calcined at various temperatures were used as principal organic and inorganic standards for mineralized tissues. The proton lines were assigned and their shapes and intensities were analysed. The signal of structural hydroxyl groups from enamel appeared at ca. 0.0 ppm, as expected from the study of the mineral standards. However, this signal from dentin and cementum was not clearly detectable. It was found possible to assess the water content of apatites from proton spectra recorded with fast MAS.

MOBILITY OF CD₄ MOLECULES IN NANOSCALE CAGES OF ZEOLITES AS STUDIED BY DEUTERON NMR RELAXATION

Agnieszka M. Korzeniowska, Zdzisław T. Lalowicz, and Aleksander Gutsze¹

H. Niewodniczański Institute of Nuclear Physics, Kraków,

¹*Biophysics Department, Medical Academy, Bydgoszcz*

Deuteron spin-lattice relaxation was applied to study mobility of CD₄ molecules trapped in the cages of zeolite NaY. There are two, interconnected sets of cages: α -cages and β -cages with 1.16nm and 0.74nm diameter, respectively. The relaxation temperature dependence, measured between 4K and 300K, can be divided into four ranges with characteristic motional parameters. At higher temperatures exchange between cages dominates. Increasing rate of translational motion leads to significant reduction of the relaxation rate. Features typical for quantum rotors were observed at low temperatures. Molecules in the α -cages exhibit reorientational freedom, while motion of those in β -cages is significantly restricted. Increasing abundance of molecules in β -cages indicates slow diffusion down to low temperatures.

DETERMINATION OF ROTATIONAL DIFFUSION TENSOR FROM RELAXATION DATA. CREATININE IN WATER SOLUTION Dmytro

Kotsyubynskyy and Adam Gryff-Keller

Faculty of Chemistry, Warsaw University of Technology, Noakowskiego 3, Warsaw (Pl)

Although the rotational diffusion theory of asymmetrical top was developed many years ago, its applications to interpretation of relaxation data in the case of molecules of low symmetry are very rare. It seems that it is because the appropriate formulas accessible in the literature are complex and it happens that they involve some errors not always easy to localize. Even after breaking through these obstacles the simultaneous determination of rotational diffusion coefficients and directions of principal diffusion axes from the experimental relaxation data is in practice rather difficult. In such a situation we have decided to develop a possibly general computer program (using the FORTRAN language) enabling solution of the above task and based on the Canet's presentation of relaxation formulas. In addition to the available experimental relaxation data, the input for our program includes the data defining the molecular geometry, electric field gradient tensors and magnetic shielding tensors for appropriate nuclei. These data are composed of fragments of Gaussian 98 output. The present version of our program is amenable to analyze only the longitudinal relaxation data due to dipolar, quadrupole and CSA relaxation mechanisms, but it is to be generalized. In the course of the optimization procedure the least-squares sum of deviations between the experimental and calculated relaxation times weighted by their error estimates is used as the criterion. For a given orientation of the diffusion axes the diffusion coefficients are optimized. The directions of one or all three axes can be found using the molecular symmetry (or pseudosymmetry), selected to be parallel to the inertia axes, or optimized by an automatic search.

The effectiveness of the program has been tested through its application in the study of the reorientation of creatinine molecules in water solution. The creatinine molecules are rigid and almost planar, which fixes the direction of one of reorientation axes. As the input data the dipolar ^1H - ^1H , ^1H - ^{13}C , and quadrupole ^2H and ^{14}N T_1 relaxation times have been used. The molecular geometry and EFG tensors have been calculated using Gaussian 98 program adopting DFT B3LYP/6-311G(2d,p) level of the theory.

Reference:

[1] Canet D., Concepts in Magn. Reson., 10(5), 291-297 (1998).

NMR STUDY ON DIASTEREOMERIC DERIVATIVES OF 5-SUBSTITUTED CREATININES

Hanna Krawczyk, Agnieszka Pietras, and Anna Kraska

Faculty of Chemistry, Warsaw University of Technology, Noakowskiego 3, 00-664 Warsaw, Poland,

e-mail: hkraw@ch.pw.edu.pl

2-amino-1-methyl-2-imidazolin-4-one derivatives are natural compounds important in medicine and biology [1-4]. A novel creatinine metabolite, creatol (5-hydroxycreatinine) has been recently isolated from urine of patients with chronic renal failure by Nakamura and Ienaga [5]. Also 2-amino-imidazole derivatives isolated from broiled food were shown to be very potent mutagenes [6]. Moreover, 5- substituted creatinines are supposed to be present in urine of patients with cancer tumours [7]. The molecules of 5-substituted creatinines are chiral and they may occur in urine in one or two enantiomeric forms, which may be important for medical diagnostics.

In the present study 5-substituted creatinines were converted into their diastereomeric derivatives and their NMR ^1H and ^{13}C spectra were recorded. Then the proton and carbon chemical shifts for selected molecules were calculated using GIAO - DFT method by the Gaussian 03W program. Presently, the attempts at determination of configuration of diastereomers are being made.

References:

- [1] S. Narayanan, H. D. Appleton *Clin. Chem.* 1980, **26**, 8, 119-1126.
- [2] M. Pischetsrieder *J. Agric. Food Chem.* 1996, **44**, 2081-2085.
- [3] G. Guella, I. Marcini, H. Zbirowius, F. Pietra *Helv. Chim. Acta* 1988, **71**, 773-782.
- [4] S. Grivas, P. Schuisky *Heterocycles* 1998, **48**, 1575-1580.
- [5] K. Nakamura and K. Ienaga *Experientia* 1990, **46**, 470-472.
- [6] T. Matsushima in *Molecular Interrelations of Nutrition and Cancer*, Raven Press, New York (1982).
- [7] A.V. Arakali, J. McCloskey, R. Parthasarathy, J. L. Alderfer, G. B. Chheda, T. Srikrishnan *Nucleosides & Nucleotides* 1997, **16**(12), 2193-2218.

DIPOLAR RELAXATION PROCESSES IN THE PRESENCE OF NEIGHBORING QUADRUPOLE SPINS. LaF_3 CRYSTALS AS AN EXAMPLE

Danuta Kruk*, Oliver Lips, Alexei Privalov, and Franz Fajara

*Institute of Solid State Physics, Technical University Darmstadt, Hochschulstr.6,
64289 Darmstadt, Germany*

**also: Institute of Physics, Jagellonian University, Reymonta 4, 30059 Krakow, Poland*

In multispin systems containing both quadrupolar ($S \geq 1$) and dipolar ($I = 1/2$) nuclei connected by mutual dipole-dipole interactions, transitions of the dipolar spins leading to their longitudinal relaxation are accompanied by the quadrupole spin transitions between energy levels determined by static quadrupole interactions together with Zeeman couplings. Only in the high field limit, when the Zeeman coupling of the quadrupole spin is much stronger than its quadrupole interaction the high spin is quantized in the laboratory frame. Thus, the 'classical' Solomon-Blombergen-Morgan (SBM) approach to dipolar relaxation, developed under the assumption of a Zeeman energy structure for both interacting spins, cannot be treated as a proper description of frequency dependent relaxation processes of the dipolar spins. In addition, the high spin nucleus usually provides through its own relaxation mechanism an additional source of relaxation for the dipolar nuclei. From the perspective of the spin $1/2$ the relaxation processes of the quadrupole spin contribute to time fluctuations of the mutual dipole-dipole coupling in a manner similar to other stochastic processes like for example jump diffusion. However, the quadrupole high-spin exhibit complex, multiexponential relaxation. Under certain motional conditions, a well defined relaxation rate can be assigned to each coherence associated with a quadrupole spin transition. Since the dipolar spin senses the various quadrupole relaxation rates corresponding to particular quadrupole spin modes and coherences, fluctuations of the mutual dipole-dipole coupling cannot be described by one characteristic time constant. It should be emphasized that the field dependent quadrupole relaxation rates are also affected by the static quadrupole coupling through its contribution to the energy level structure of the quadrupole spin.

We present a general description of spin - lattice relaxation of a dipolar spin $1/2$ induced by its coupling to an ensemble of quadrupole spins, valid for an arbitrary magnetic field and arbitrary quadrupole spin quantum number. Our approach includes the effects of the quadrupole spins being quantized in a frame determined by a superposition of the quadrupole and Zeeman interactions, as well as the multiexponential quadrupole relaxation. We provide in this way a general tool appropriate for interpretation of field-dependent relaxation studies for a wide class of solid state systems containing dipolar as well as quadrupole spins with mutual dipole-dipole couplings. We prove also, that the general approach converges to the SBM expression in the high field limit, if the lattice motion is significantly faster than the quadrupole relaxation.

We apply the general approach to interpret frequency dependent fluorine relaxation studies for LaF_3 crystals, and discuss its remarkable agreement with the experimental data.

¹H NMR STUDIES OF POLY(ε-CAPROLACTONE) – SODIUM MONTMORILLONITE NANOCOMPOSITES

Justyna Krzaczkowska and Stefan Jurga

*Department of Macromolecular Physics, Adam Mickiewicz University,
Umultowska 85, 61-614 Poznań, Poland*

The poly(ε-caprolactone) – sodium montmorillonite nanocomposite belongs to the new class of polymer-layered silicate composites consisting of organic-synthetic polymer matrix and inorganic filler-layered structure clay minerals. In recent years these kinds of materials have become of great interest for practical applications because they exhibit a much more advantageous properties than conventional composites [1].

Sodium montmorillonite is built of two tetrahedral silicate layers separated by an octahedral (metallohydroxyl) layer. These layers form stacks separated by van der Waals gap (interlayer space or gallery). The isomorphic ions substitution within the tetrahedral and octahedral layers generates a negative charge on the basal planes which is compensated by sodium ions adsorption into interlayer space [2]. Sodium ions are exchanged with surfactant molecules in an ion-exchange reaction leading to increased ability of the clay to adsorb polymer chains. The in situ intercalative polymerisation of ε-caprolactone catalysed by surfactant (hexadecyltrimethylammonium bromide-HTAB) leads to the intercalation of polymer into montmorillonite structure [3].

In this work the ¹H NMR techniques were used to gain insight into molecular dynamics of the intercalated poly(ε-caprolactone) chains. The second moment M_2 of protons was measured to reveal intra-molecular motions of polymer molecules and phase transitions in nanocomposites. The experiment was performed for pure sodium montmorillonite and for nanocomposites with different amount of polymer. The second moment of NMR line decreasing with the increasing of temperature as for polymers are observed. Fast Field Cycling ¹H relaxometry was applied for samples with different concentration of poly(ε-caprolactone) and at various temperatures to describe polymer chains motions. Previously we have reported on molecular dynamics and structure of octahedral and tetrahedral ²⁷Al ions coordinated sodium montmorillonite nanocomposites [4]. In our studies we have noticed the correlation between interlayer distance in clay structure and molecular dynamics of intercalated polymer. The higher concentration of the clay resulted in the shorter interlayer space as evidenced by SAXS [4].

References:

- [1] S.S. Ray and M. Okamoto, *Progress in Polymer Science*, **28** (2003) 1539.
- [2] M. Alexandre, P. Dubois, *Materials Science and Engineering*, **28** (2000) 1.
- [3] A. Kiersnowski, M. Kozak, S. Jurga, J. Pięłowski, *Polymers and Polymer Composites*, **12** (2004) in press.
- [4] J. Krzaczkowska, Z. Fojud, M. Kozak, S. Jurga, *Journal of Molecular Structure*, in press.

Acknowledgements:

We are grateful to A. Kiersnowski, J. Pięłowski and M. Kozak for sample preparation and J.K acknowledges Adam Mickiewicz University (Collegium Polonicum, Słubice) and the European University Viadrina (Frankfurt/ Oder) for the Europa Fellows Grant.

THE ANALYSIS OF ^{31}P MR SPECTRA OF PHOSPHOLIPIDS' EXTRACTS' OF BONE MARROW BLASTS' CELLS FROM PATIENTS WITH ACUTE LEUKEMIA (AL)

Małgorzata Kuliszkiewicz-Janus¹, Mariusz Tuz², Marek Kielbiński¹, and Stanisław Baczyński³

¹Dept. of Hematology, Wrocław Medical University, ²Institute of Experimental Physics, University of Wrocław, ³Dept. of Chemistry, University of Wrocław, Poland, EU

I. Introduction

Phospholipids are major components of cells' membranes. ^{31}P NMR spectroscopy is convenient and precise analytical tool for the phospholipids analysis of extracts from biological samples [1]. Thanks to acquiring spectra from the substance consisting of ^{31}P , the ^{31}P MRS allows for non-invasive studies of neoplasm metabolism. This method was used for analysis of phospholipids' changes in neoplastic cells of breast, colon and esophageal [2,3,4]. The aim of this investigation were: to examine whether ^{31}P NMR spectra of phospholipids' extracts from mononuclear bone marrow's cells could be used to: (1) the analysis of phospholipids' metabolism of blast cells from bone marrow from patients with AL; (2) differentiate between patients responding and non responding to the therapy.

II. Material and Methods

^{31}P MRS spectra originated from 29 patients with acute leukemia (14 females and 15 males), aged from 22 to 76, median 57 years. Patients were divided into two groups: R–responding ones (13 patients: 7 females, 6 males), aged from 22 to 66 (median 42 years), and NR–resistant to therapy (16 patients: 7 females, 9 males), aged from 23 to 76 (median 63 years). All spectra came from phospholipids extracts prepared from 60×10^6 cells/ml. Cellular lipids were isolated from marrow mononuclear cells by Ficoll buffy coat centrifugation and next underwent methanol-chloroform extraction. AMX 300 BRUKER spectrometer 7,05 T was applied. Chemical shifts were compared to 85% orthophosphoric acid at 0 ppm. MDPA was used as external reference substance (16,726 ppm related to 85% orthophosphoric acid). Calculations of phospholipids' concentrations based on integral intensities of peaks (Table 1).

III. Results

^{31}P MRS spectra of phospholipids' extracts from blast cells from bone marrow consists of 8 peaks due to phospholipids: PC-phosphatidylcholine, CPLAS-phosphatidylcholine's plasmalogen, LPC-lysophosphatidylcholine, SM-sphingomyelin, PE-phosphatidylethanolamine, PI-phosphatidylinositol, PS-phosphatidylserine, CL-cardiolipin and one due to MDPA-external reference substance. The assignment of signals was accomplished by addition of synthetic phospholipids (from SIGMA). Observations indicated that ^{31}P MRS spectra from patients responding to therapy (group R) differed from these obtained from non-responders (group NR). A decrease of integral intensities due to SM and PS was observed in NR group in reference to R group (Fig. 1). Additionally, in case of 5 patients of R group peak due to CL was confirmed. In NR group there was no resonant peak due to CL in ^{31}P MRS.

Table 1. Phospholipids' concentrations (10^{-6} mole/l) of blast cells from bone marrow of patients with AL

Phospholipids Group	PC	CPLAS	SM	PI+PE	PS	CL
R	486±324	44±29	127±106	289±204	102±65	18±24
NR	286±139	63±071	38±41	241±161	20±33	0±0
p	NS	NS	p<0,01	NS	p<0,01	p<0,01

NR–non-responding, R–responding to therapy

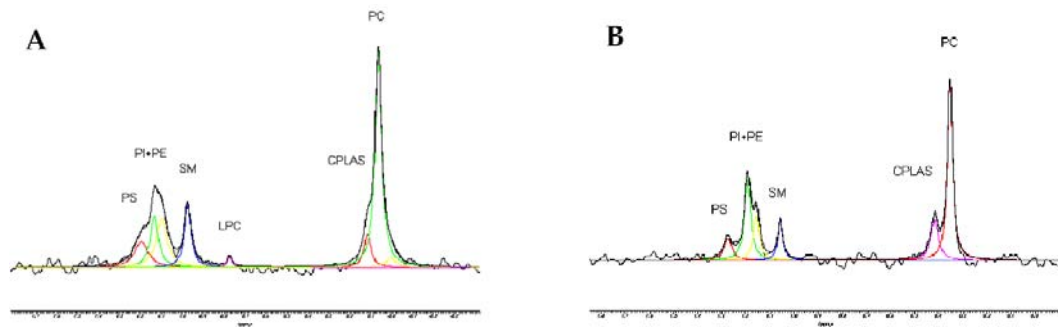


Fig. 1. ^{31}P MRS spectrum of patient: responding to the therapy (a), non-responding (b).

Concentrations of SM, PS, and CL (level $p=0,01$) for NR group are significantly diminished in reference to R group. There are no significant differences between NR and R group due to concentrations of PC, CPLAS, and PI+PE.

IV. Discussion

Concentrations of SM, PS, and CL from marrow's mononuclear cells of patients, who are resistant to therapy, are significantly diminished in reference to patients, who are responding to the treatment. It's very likely that observed reduction in SM level in blast cells' extraction is due to activation of SMnase by TNF. SMnase cleaves SM, generating choline phosphate and ceramide. The latter mediates apoptosis, induces differentiation and inhibits growth of the leukemic cells. Discoveries related to the metabolism of ceramide suggest that this agent may have important influence on the effectiveness of various cancers' therapies. The cytostatic effect of chemotherapy reduces with the inhibition of ceramide's degradation [5]. In the early phase of apoptosis, PS is translocated from the inner side of the plasma membrane to the outer layer, which allows phagocytes to recognize and engulf the apoptotic cells [6]. Reasons of reduction SM, PS, and CL in the extracts of marrow's mononuclear blasts require further investigation. Our data shows that ^{31}P MRS spectra differ from group R and NR.

V. References:

- Schiller J, Arnold K: Application of high resolution ^{31}P NMR spectroscopy to the characterization of the phospholipids composition of tissues and body fluids-a methodological review.; *Med Sci Monit.* 2002 Nov; 8(11):MT205-22.
- Merchant T. E., Meneses P., Gierke L. W., Den Otter W., Glonek T.: ^{31}P magnetic resonance phospholipid profiles of neoplastic human breast tissues. *Br J Cancer* 1991;63:693-698.
- Merchant T. E., Kasimos J. N., de Graaf P. W., Minsky B. D., Gierke L. W., Glonek T.: Phospholipid profiles of human colon cancer using ^{31}P magnetic resonance spectroscopy. *Int J Colorect Dis.* 1991;6:121-126.

4. Merchant T. E., de Graaf P. W., Minsky B. D., Obertop H., Glonek T.: Esophageal Cancer Phospholipid Characterization by ^{31}P NMR.; NMR Biomed. Vol.6.187-193 (1993).
5. Senchenkov A., Litwak D. A., Cabot M. C. J. Natl. Cancer Inst 2001, 93, 347-57.
6. Arroyo A, Modriansky M, Serinkan FB, Bello RI, Matsura T, Jiang J, Tyurin VA, Tyurina YY, Fadeel B, Kagan VE.: NADPH oxidase-dependent oxidation and externalization of phosphatidylserine during apoptosis in Me₂SO-differentiated HL-60 cells. Role in phagocytic clearance. J Biol Chem. 2002 Dec 20;277(51):49965-75.
7. Kuliszkievicz-Janus M., Baczyński S. Magnetic Resonance in Colloid and Interface Science 2002, 347-354 Kluwer Academic Publishers. J. Fraissard and O. Lapina (eds).

BINARY MIXTURE OF HARD SPHERES AS A MODEL COLLOIDAL SYSTEM INVESTIGATED BY MOLECULAR COMPUTER SIMULATION

Bartosz Kuroczycki, Michał Banaszak, and Stefan Jurga

Department of Macromolecular Physics, Adam Mickiewicz University, Poznan, Poland

Computer simulation is a very important tool in the investigating physical properties of colloidal suspensions, melts and other mixtures.

In this work, we use Molecular Dynamics simulation (Hard Spheres algorithm) for binary hard sphere mixtures. The model is a system consisting of many small spheres which surround few large spheres. There is only hard potential between spheres.

Hydrodynamic interactions between components (large sphere \rightarrow small sphere \rightarrow large sphere) originate from the microscopic structure. We do not use any approximation such as Onsen's tensor etc.. Static and dynamics properties of colloidal suspensions are similar to those of the simple fluids. Especially phase transitions in the simple fluid can be compared to the phase transitions in our binary mixtures (fluid \rightarrow glass \rightarrow crystal). However, diffusivity, and relaxation times for fluid molecules are about 10^9 larger than relaxation times of molecules in suspensions. Therefore, lifetime of the metastable phase of suspension observed before crystallization, can be long enough (from minute to hours) to allow experimental studies. This long time gives possibility to accurately measure physical properties in this state [1]. Colloidal suspension can be studied by many experimental methods such as: rheological experiments (viscosity and elastic properties), light scattering (structural properties and diffusion coefficients) and NMR (memory coefficients and structure relaxation). For example cores of polymethylmetacrylate (PMMA) stabilized by thin layers of poly-12-hydroxystearic acid and suspended in cis-decalin can be used [2]. In our simulation we calculated radial distribution function (RDF) and the compressibility factor (Z). The results are compared to Monte Carlo (MC) simulations [3] and theoretical results [3].

References:

1. "Observation of Glass Transition in Suspension of Spherical Colloidal Particles", P.N.Pusey and W.van Meegen, Phys. Rev. Lett. Vol 59, Nr 18, p. 2083-2086, November 1987.
2. "Viscosity and Structural Relaxation in Suspensions of Hard-Sphere Colloids", P.N. Segre, S.P. Meeker, P.N. Pusey, and W.C. Poon, Phys. Rev. Lett. Vol.75, nr 5, p. 958- 961, July 1995.
3. "Monte Carlo data of dilute solutions of large spheres in binary hard sphere mixtures", Dapeng Cao, Kwong-Yu Chan, Douglas Henderson, Wenchuan Wang, Molec. Phys. 2000, Vol.98, No 9, p. 619-624.
4. „COMPUTER SIMULATION OF LIQUIDS”, M.P. Allen and D.J. Tildesley.

APPLICATIONS OF ^{19}F MR SPECTROSCOPY TO DIAGNOSTIC AND THERAPY MONITORING OF BRAIN TUMOR ON A RAT MODEL *IN VIVO*

M. Labak, Z. Sulek, K. Majcher, P. Grieb¹, T. Kryczka¹, and A. Jasiński

H. Niewodniczański Institute of Nuclear Physics PAS, Kraków

¹*M. Mossakowski Medical Research Centre PAS, Warszawa*

Purpose: The aim of this work is to apply ^{19}F MR Spectroscopy (MRS) in biomedical research in diagnosis and monitoring of brain tumor therapy. Local dosage of cytotoxic drug 5-fluorouracil (5-FU) via a biopolymer matrix releasing the 5-FU was studied *in vivo* using ^{19}F MRS. Regions of the rat brain where the anesthetic (*halothane*) is accumulated were studied *in vivo* with ^{19}F MRS.

Materials and Methods: The experiment was conducted on 3 *Wistar* rats weighing 280 – 300 g. The biopolymer matrix saturated with 5-FU was implanted into rat cerebral cortex. All *in vivo* MRS measurements were performed at 4.7T system with a Maran DRX console from Resonance Instruments, using FID and Fast Spin Echo (FSE) sequences. A surface coil tunable to ^1H and ^{19}F was used for proton imaging and fluorine spectroscopy. The proton images were acquired with a 256×256 matrix, FOV = 40 mm, slice thickness = 2 mm. The ^{19}F whole brain spectra were collected by FID, whereas 1D projections with a slice thickness = 2 mm were recorded with 256 points and FOV = 80,5 mm. The same sequence was used for proton imaging and ^{19}F MRS to detect the *halothane* (CF_3CHBrCl) signal in the brain during anesthesia. Rats were maintained at 37°C using water-circulating heating pad. All experiments were ECG and breath monitored.

Results and discussion: Good quality coronal, sagittal and horizontal ^1H MR images were obtained from rat brain (Fig. a). 3 weeks after operation of grafting the biopolymer, fluorine signal from 5-FU (Fig. b) was found in the brain. Narrow line suggests that ^{19}F signal comes from mobile molecules. We can suppose that 5-FU is able to join with molecules of large mass having freedom of motion. Unfortunately, low SNR of 5-FU signal didn't allow us to measure the spatial distribution of released cytotoxic drug.

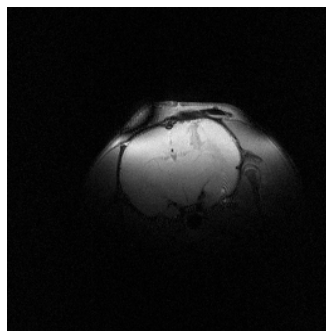
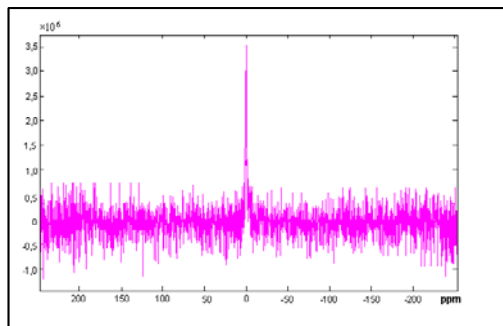


Fig. a



Fig. b



In another experiment fluorine signal from *halothane* was detected 60 minutes after anesthetic delivery was stopped. Result of these studies show that the anesthetic decomposes evenly in the brain and the largest its concentration was found in the meninges and cerebra spinal fluid (CSF), what suggests that the signal comes from unbound ^{19}F .

Conclusions: Our results shows that ^{19}F MRS opens access to artificially induced fluorocompounds such as 5-fluorouracil and its metabolites, what finds use in the tumors therapy and monitoring their response to this cytostatic.

NMR STUDY OF Nd₂Fe₁₄BD_x HYDRIDES

**Andrzej Lemański^a, Małgorzata Jasiurkowska^a, Czesław Kapusta^a, Peter C. Riedi^b,
Olivier Isnard^c, and Daniel Fruchart^c**

^a *Department of Solid State Physics, Faculty of Physics & Applied Computer Science, AGH University of Science and Technology, Cracow, Poland*

^b *Department of Physics & Astronomy, University of St. Andrews, St. Andrews, KY16 9SS Scotland, UK*

^c *Laboratoire de Cristallographie, CNRS, 38042 Grenoble, Cedex 9, France*

NMR measurements on Nd₂Fe₁₄BD_x (x = 0, 1, 2, 4) hydrides are reported. The parent Nd₂Fe₁₄B compound is a material for novel permanent magnets. In order to determine the influence of hydrogen on the rare earth site properties the ¹⁴³Nd and ¹⁴⁵Nd spin echo spectra and spin echo decays were measured at zero field and 4.2 K. The spectra consist of poorly resolved quadrupole septets (nuclear spin of ¹⁴³Nd and ¹⁴⁵Nd is 7/2) which are attributed to Nd 4g and 4f sites. For both lines an overall decrease of the hyperfine fields and an increase of electric field gradients is observed. The decrease of Nd hyperfine field corresponds to an increase of the 6s and 5d electron polarization that partly cancels the dominant 4f orbital contribution of the opposite sign. An increase of the electric field gradient is attributed to a decrease of the 6p and 5d electron contribution (lattice EFG) which partly cancels the dominant 4f electron term of opposite sign. A decrease of the lattice EFG, which has been observed in our previous ¹³⁹La NMR study of La₂Fe₁₄BD_x reflects a decrease of the crystalline electric field coefficient A₂⁰ and corresponds to a decrease of the magnetocrystalline anisotropy with hydrogen introduction. The results are analysed in terms of hydrogen site occupation and the electron transfer between hydrogen and neodymium sites.

INVESTIGATION OF TEMPERATURE CHANGES IN THE PROPERTIES OF RINGER'S SOLUTIONS BY ¹H NMR AND DENSITOVISCOMETRY

D. Lewandowska, T. Klinkosz, and T. Podoski*

Institute of Experimental Physics, University of Gdańsk, ul. Wita Stwosza 57, 80-952 Gdańsk

** Maritime Academy, ul. Morska 83, 81-225 Gdynia*

Blood is a liquid tissue consisting of cellular elements and a liquid medium called plasma. Plasma contains both organic and inorganic components. Among the inorganic ones, sodium, potassium, chloride and hydrocarbon ions are predominant. Proper composition of plasma ensures normal function of cells, in particular neurons and muscle fibres. The organism has developed certain mechanisms protecting against water and electrolyte depletion. These mechanisms are sometimes insufficient to keep proper water and electrolyte level. To supplement such depletions, electrolyte solutions are used in infusions, such as multicomponent Ringer's solution, administered directly to the blood stream and used as a solvent for intravenous drugs during surgery and in postoperative treatment. The knowledge of the changes in physical properties of infusion solutions is helpful in their administration.

Four Ringer's solutions with different compositions proposed in biomedical literature (9–15 g/l) and different expiry dates were examined. Two of them, solutions RRI and RRII, were prepared in the laboratory to conform to the requirements established for infusion solutions. The next were physiologic salines, SFI and SFII, produced by Biomed and used in medical practice. They had the same composition, but SFII was already withdrawn from the medical use after the expiration date.

¹H NMR spectra were recorded by means of a Brüker type AF spectrometer with a frequency of 200 MHz. The viscosity of solutions was measured with an HVA 6 capillary viscosimeter, and the density with a DMA 602 densitometer, both from Anton Paar GmbH. All the measurements were carried out in the temperature range 293–333 K.

The results were analysed in accordance with the model of ionic hydrates. It was found that the values of chemical shifts of protons decreased linearly with temperature, equally for all solutions irrespective of the differences in composition. The direction of temperature changes did not affect the results either. This was confirmed by the lack of irreversible, temperature-dependent changes in the short-range order of the solutions examined.

In the NMR investigations, no significant differences were observed in the behaviour of solutions RRI and RRI compared with SFI and SFII. The results obtained for samples of SFI and SFII did not differ, thus indicating that macroscopic properties did not essentially change in time (up to one year from the expiry date).

The activation energy determined from the temperature measurements of viscosity amounted to 16.7 ± 0.2 kJ/mol for Ringer's solution, and 20.6 ± 0.9 kJ/mol for physiologic saline. This, compared to the respective value (15.4 ± 0.3 kJ/mol) for pure water, indicates greater translational mobility of the molecules of pure water compared to water molecules in solution and confirms the formation of associated molecules.

The density measurements imply that density grows with the increasing content of electrolytes. Both density itself and coefficient of temperature density changes are the highest for the solution of physiologic saline with the highest concentration of ions. Different hydration capacities of individual ions determine the degree of the ordered state of water molecules in the solution.

Baczyński's relation (inverse viscosity versus inverse density) is nonlinear, indicating the existence of strong intermolecular interactions between water molecules and ions, which leads to the formation of ionic hydrates.

The coefficient of dynamic viscosity of the solutions investigated strongly and nonlinearly decreases with growing temperature. This phenomenon is caused by the cleavage of hydrogen bonds, resulting in the disintegration of big and poorly mobile groups of water molecules.

Greater differences in density between solution RRI and solutions SFI and SFII may be accounted for by different concentrations of individual ions in these solutions. This is related with different degrees of the ordered state of water molecules and different hydration capacity of ions.

^1H , ^{13}C AND ^{19}F NMR STUDIES OF GASEOUS AND LIQUID SEVOFLURANE

Edyta Maciaga, Włodzimierz Makulski, Karol Jackowski, and Barbara Blicharska*

Department of Chemistry, Warsaw University, Pasteura 1, 02-093 Warsaw

**Institute of Physics, Jagellonian University, Reymonta 4, 30-059 Krakow*

Sevoflurane (2,2,2-trifluoro-1-(trifluoromethyl) ethyl ether), also called fluoromethyl, is a new and efficient agent used for induction and general anesthesia maintenance. It is often used as volatile drug for inhalation, at various concentrations together with nitrous oxide and oxygen. The increasing application of sevoflurane as anaesthetic causes the need of better understanding of its physico-chemical quantities, including NMR parameters.

The present work has been designed to investigate selected NMR spectral parameters for sevoflurane in the gas phase. ^1H and ^{19}F chemical shieldings have been monitored as function of added buffer gases density, i.e. CO_2 and Xe , in the density range 0.2 to 1.5 mol/L. The addition of these inert gases of ca. 5 -35 atm was important to obtain the well resolved spectra with narrow lines. We have found linear density dependences of ^1H and ^{19}F chemical shifts (nuclear magnetic shieldings) in the gas phase; their extrapolation to the zero-density limit delivered the σ_0 parameters for nuclei in sevoflurane molecule. The $^2\text{J}(\text{HF})$ spin-spin coupling constant was investigated from both ^1H and ^{19}F NMR spectra. The detailed examination of our results revealed almost no density dependence of this coupling constant.

The extrapolation of parameters mentioned above to the zero-density limit allowed to determinate values free from intermolecular interactions. These new results can be very useful in the verification of appropriate chemical shielding and indirect spin-spin coupling values obtained from modern ab initio calculations.

Additionally, high-resolution ^1H , ^{13}C and ^{19}F NMR spectra of pure liquid sevoflurane were recorded. We have made the precise measurements of ^1H - ^{13}C and ^{19}F - ^{13}C spin-spin coupling constants in liquids. All the spectra (liquid and gas) were measured on Varian Unity-Plus NMR spectrometer operating at proton frequency 500.609 MHz, using C_6D_6 as a secondary reference.

The work described here presents only the beginning in the route for obtaining all other NMR parameters from gaseous measurements. We hope to carry out further experimental studies in the near future.

Acknowledgements:

This work was supported by the Polish State Committee for Scientific Research as the research grant number A T09A 03523 available in years 2003-2005.

References:

- [1] B.W. Urban, M. Bleckwenn, Br.J. Anaesth., 89 (2002) 156.
- [2] P. Tang, J. Zubryzcki, Y. Xu, J. Comput. Chem., 22 (2001) 436.
- [3] A. Foris, Magn. Reson. Chem., 39 (2001) 386.
- [4] C. Sandorfy, J. Mol. Struct. 708 (2004) 3.

FUNCTIONAL MAGNETIC RESONANCE IMAGING OF THE RAT SPINAL CORD

K. Majcher¹, B. Tomanek^{2,3}, A. Jasinski¹, T. Foniok², U. I. Tuor^{2,3}, and G. Hess⁴

¹*Institute of Nuclear Physics, Polish Academy of Sciences, Krakow, Poland,* ²*National Research Council of Canada, Institute for Biodiagnostics, Calgary, Alberta, Canada,* ³*Department of Neurosciences, Experimental Imaging Centre, University of Calgary, Alberta, Canada,* ⁴*Institute of Pharmacology, Polish Academy of Sciences and Jagellonian University, Krakow, Poland*

Synopsis

Spinal functional Magnetic Resonance Imaging (fMRI) was used to study neuronal activation within the brain in response to electrical stimulation of the forepaw. Fast spin echo (FSE) images were used for spinal cord at 9.4T using a volume transmit/receive rf coil. Consistent activation was observed within the dorsal horn of the rat spinal cord. We anticipate that spinal cord fMRI will be able to provide important new information concerning the integrative responses of central nervous system (CNS).

Introduction

Spinal fMRI was introduced for human studies in 2001 [2] and more recently for the study of animals [3]. Spinal fMRI is a non-invasive technique for the study of neuronal activity of the interconnected regions within spinal cord *in vivo*. Therefore it could be used as a non-invasive technique allowing observation of the spinal neuronal activity elicited by stimulus, both for clinical assessment and for research of CNS function.

Materials and Methods

Animal preparation: Five Wistar rats were used. The animals were anesthetized with isoflurane. The rectal temperature was monitored and maintained at $37 \pm 0.5^\circ\text{C}$. Animals were intubated and ventilated (ventilation volume 3-4 ml; BP: PO₂ 100-120 mm Hg, PCO₂ 35-45 mm Hg). Bupivacaine was administered into the cannulation wound site before closure. Anesthesia was gradually switched from isoflurane to α -chloralose (30 mg/ml, 80 mg/kg) administered intravenously over approximately 20 min at the initial dose of 80 mg/kg and maintained at 20mg/kg, administered every 45 min. Following the completion of the imaging experiment, rats were immediately euthanased with pentobarbital (120mg/kg, i.v.).
Experimental Setup: A 9.4T/21cm horizontal bore magnet (Magnex, UK) with Avance console (Bruker, Germany) was used. Data were analyzed using custom made software. The animals were placed supine in the $5 \times 7\text{cm}$ volume rf coil with the brain and cervical lower spine within the homogenous B₁ field of the rf coil allowing slice positioning in the areas of expected neuronal activation. **Experiment design:** Functional images were acquired from the spinal cord. Five axial slices were acquired within the spinal cord. A multislice, single-shot FSE sequence was used (TE = 3ms, TE_{eff} = 43.7ms, TR=7sec, FOV=2×2 cm, matrix size 64×64, 4 averages, slice thickness 2 mm, 0.5 mm gap). Data acquisition was gated with the respiratory cycle. Anatomical T₂-weighted FSE images of the spinal cord were also acquired. **Stimulation paradigm:** The stimulation paradigm consisted of 31 time points with continuous 5 rest and stimulation periods (5 off – 6 on – 7 off - 7on – 6 off). Five stimulation experiments were performed with each animal with 5 min break period, allowing comparison of the results between animals and between single stimulation experiments within the same animal. For electrical stimulation (6 mA, 0.3 ms pulse length, 3 Hz) two small needle electrodes were placed subcutaneously and taped.

Results and Discussion

Functional images of appropriate quality were obtained from four animals. The amplitude of changes in image intensity was approximately 3% and followed the stimulation paradigm ($p \leq 0.001$). Electrical stimulation of the forepaw resulted in the activation within gray matter of the spinal cord. The sites of activity were localized mainly in the dorsal horn of the spinal cord. An example of spinal fMRI obtained from one animal is shown (Fig. 1A-E) at the level of C8-C6, where transduced signal reaches gray matter neurons and then crosses the cord to the opposite side within the ventral horn. The fMR images of the spinal cord were superimposed on anatomical images at five different levels of the cervical spinal cord corresponding to T2/T1, T1/C8, C7, C6 and C5 cervical levels (Fig. 1 A-E) respectively.. The intensity changes of the activated voxels within spinal cord follow the stimulation paradigm ($p \leq 0.001$) for each animal. These results demonstrate that the technique developed is able to assess functional activation in the spinal cord of the rat. This technique could be a valuable tool to understand the interaction of functional pathways in normal conditions and the effects of injury and treatment.

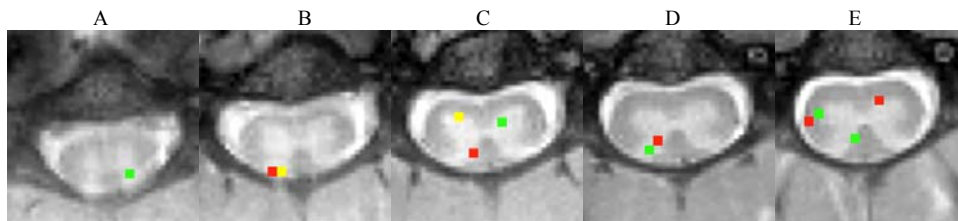


FIG. 1. Neuronal activity in the rat spinal cord (A-E) and brain (F) obtained simultaneously. The spinal images are superimposed on anatomical images at five different levels of the cervical spinal cord: T2/T1, T1/C8, C7, C6 and C5 cervical levels from left to right (A-E) respectively. The ventral surface is at the top, dorsal surface at the bottom. The color used to indicate the active voxels corresponds to the level of the correlation to the paradigm: red corresponds to the highest, yellow -medium and green the lowest correlation coefficient respectively.

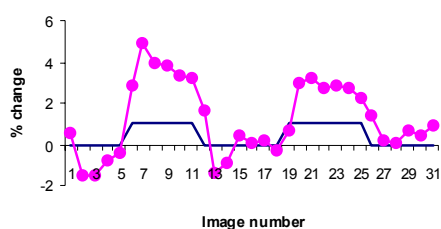


Fig.2. Time course of the intensity changes in voxels of activation shown in Fig 1: the dotted line indicates the stimulation paradigm, and the solid line indicates the actual time courses for active pixels within the spinal cord.

Reference:

1. Bandettini P.A. et al, NMR Biomed 7, 12-20, 1994.
2. Stroman P.W. et al Concepts in Magnetic Resonance Part A, **16A(1)**: 28-34, 2003.
3. Lawrence J, et al NeuroImage 22, 1802-1807, 2004.

Acknowledgment:

This work was supported by NATO Collaborative Linkage Grant No 979848.

MOLECULAR MOTION IN ETHYLENE/NORBORNENE COPOLYMERS

Monika Makrocka-Rydzik, Bakyt Orozbaev, Stanisław Głowinkowski,
and Stefan Jurga

Department of Macromolecular Physics, Adam Mickiewicz University, Umultowska 85,
61-614 Poznań, Poland

The TOPAS copolymers (Thermoplastic Olefin Polymers of Amorphous Structure) are materials of interest because of their outstanding features such as optical clarity, biocompatibility and strong resistance to temperature. High moisture barrier effect, high strength and low density make these polymers useful for packaging of medical and food products [1]. TOPAS copolymers are obtained by means of metallocene catalyzed ethylene/norbornene copolymerization [2]. Norbornene, incorporated randomly in the main chain, prevents crystallization, as well as stiffens and strengthens the polymer. The relatively high glass transition temperatures of these copolymers cover the range from 80 to 180°C proportionally to norbornene comonomer content.

In this report NMR and Broadband Dielectric Spectroscopies were employed to study molecular dynamics and structure of TOPAS copolymers with varied proportions of ethylene and norbornene comonomers. The NMR spin-lattice relaxation times below room temperature [Fig.1] are governed by local motions of ethylene units involving trans-gauche isomerization as it was observed in polyethylene [3]. The same motion manifests as \square relaxation in our dielectric relaxation studies [Fig.2], which is supported by similar activation parameters obtained from both experiments [Fig.1 and 3].

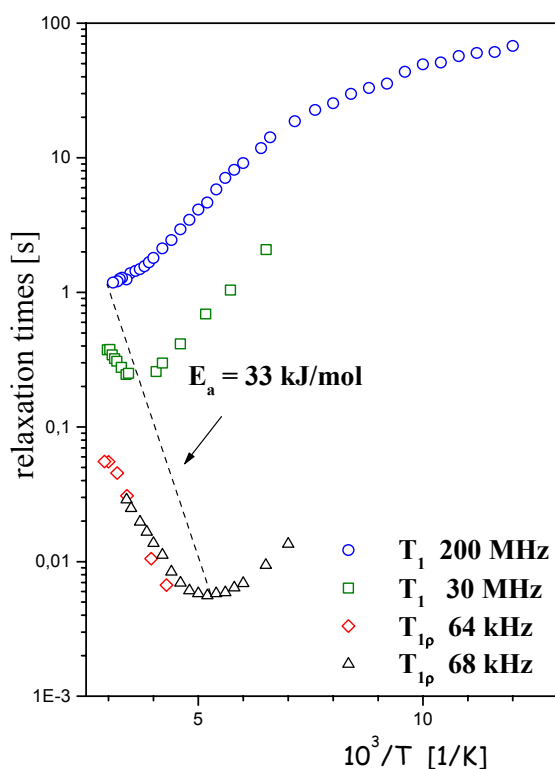


Fig.1 Temperature dependences of the ^1H spin-lattice relaxation times T_1 and $T_{1\rho}$ of Topas 8007

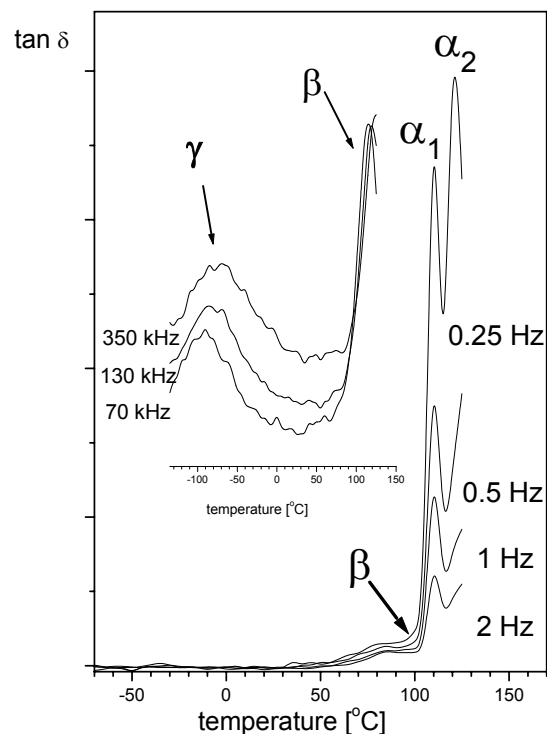


Fig.2 Temperature dependence of $\tan \delta$ for Topas 8007 at selected frequencies

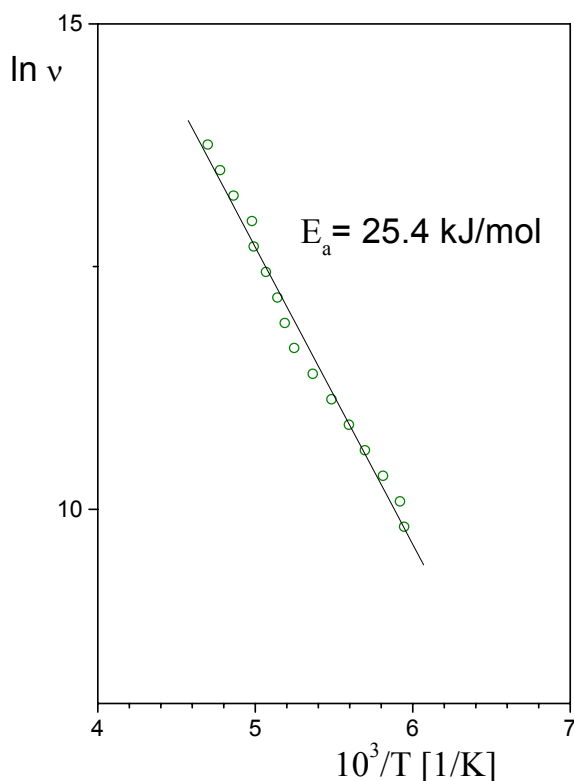


Fig.3 Frequency–temperature location of the loss maxima for γ absorption in Topas 8007

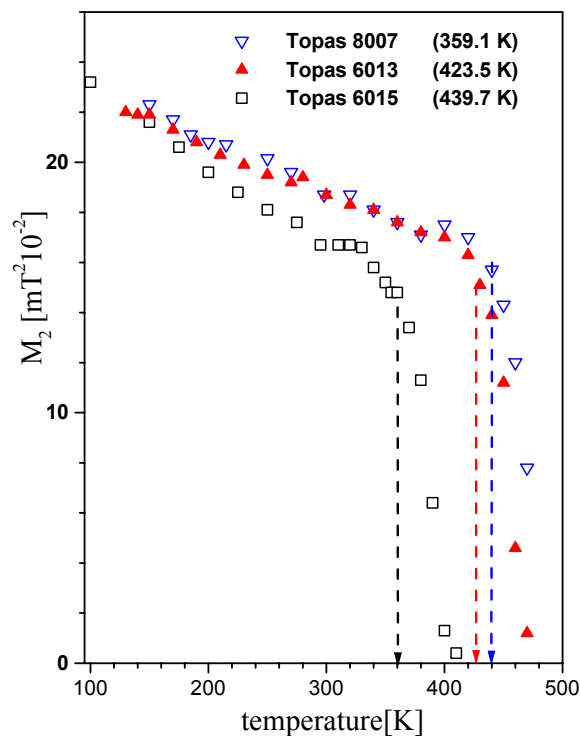


Fig.4 Temperature dependences the second moment of ^1H NMR. Glass transition temperatures are given in brackets and denoted by dash lines

Analysis of the second moment of NMR line temperature behavior [Fig.4] and dielectric relaxation data [Fig.4], covering temperatures below as well as above glass transition, indicate existence of another motional processes, which are discussed in terms of three relaxation processes: (i) β -relaxation assigned to short range segmental motion involving norbornene units [4,5] while (ii) α_1 -relaxation and (iii) α_2 -relaxation are associated with the dynamic glass transition.

References:

- [1] Lamonte R.R.; McNally D. *Advanced materials & processes* 2001, 159, 33
- [2] Mülhaupt R., *Macromol. Chem. Phys.* 2003, 204, 289
- [3] Glowinkowski S; Makrocka-Rydzik M; Wanke S; Jurga S, *Europ. Polym. J.* 2002, 38, 961
- [4] Ekizoglou N.; Thorshaug K.; Cerrada M. L.; Benavente R.; Pérez E.; Pereña J. M., *J. Appl. Polym. Sci.* 2003, 89, 3358
- [5] Chu, P. P.; Cheng, M.-H.; Huang, W.-J.; Chang, F.-C.; *Macromolecules*; 2000, 33; 9360

TAUTOMERISM AND HYDROGEN BONDING OF PURINE ANALOGUES

Radek Marek^a, Jaromír Toušek^b, Jiří Brus^c, Kateřina Maliňáková^a, Zdeněk Trávníček^d,
and Michal Hocek^e

^a National Centre for Biomolecular Research, Faculty of Science, Masaryk University
Kotlářská 2, CZ-611 37 Brno, Czech Republic

^b Department of Theoretical and Physical Chemistry, Faculty of Science, Masaryk University
Kotlářská 2, CZ-611 37 Brno, Czech Republic

^c Institute of Macromolecular Chemistry, Academy of Sciences of the Czech Republic
Heyrovského nám. 2, CZ-16206 Prague, Czech Republic

^d Laboratory of Growth Regulators & Institute of Experimental Botany AS, Palacký
University Šlechtitelů 11, CZ-78371 Olomouc, Czech Republic

^e Institute of Organic Chemistry and Biochemistry, Academy of Sciences of the Czech
Republic Flemingovo nám. 2, CZ-16610 Prague, Czech Republic

Biogenetic purine bases play central roles in most biological processes. Structural modifications of the purine bases, nucleosides, and nucleotides have resulted in the discovery of thousands of biologically active compounds, including many clinically used drugs.

The proper characterization of the tautomeric equilibria and protonation sites of the variously substituted purine derivatives under diverse conditions is of great importance and significance. Processes involving the change of the proton position play a direct role in the selectivity of recognition at the active sites of enzymes and alkylation reactions. These equilibria are governed by the electron distribution within the molecule and by the intermolecular effects such as solvation or crystal packing. ¹⁵N NMR spectroscopy is a very sensitive probe for studying the electron distribution, tautomeric equilibria, and protonation processes [1-3].

The variously substituted purine derivatives were investigated by using inverse-detected ¹⁵N NMR spectroscopy in the solution at a range of temperatures [4]. Slow-spinning ¹⁵N CP/MAS data of selected compounds were recorded in order to study intermolecular interactions in the solid-state and principal values of the ¹⁵N chemical shift tensors [5,6]. DFT calculations of nitrogen chemical shifts were used for determining the solvation effects in the solution and bonding patterns in the solid state, assigning the nitrogen resonances observed in the solid-state spectra, and determining the orientation of the principal components of the chemical shift tensors. Structural arrangements have been correlated with the geometry obtained from single-crystal X-ray diffraction analysis.

Benefits of studying the structure by all these approaches will be discussed [7].

References:

1. M. Witanowski, L. Stefaniak, G. A. Webb, *Annu. Rep. NMR Spectrosc.*, **1993**, 25, 1.
2. R. Marek, A. Lyčka, *Curr. Org. Chem.*, **2002**, 6, 35.
3. R. Marek, V. Sklenář, *Annu. Rep. NMR Spectrosc.*, **2005**, 54, 203.
4. P. Sečkářová, R. Marek, K. Maliňáková, E. Kolehmainen, D. Hocková, M. Hocek, V. Sklenář, *Tetrahedron Lett.*, **2004**, 45, 6259.
5. D. Stueber, D.M. Grant, *J. Am. Chem. Soc.*, **2002**, 124, 10539.
6. R. Marek, J. Brus, J. Toušek, L. Kovács, D. Hocková, *Magn. Reson. Chem.*, **2002**, 40, 353.
7. R. Marek, et al., unpublished results.

DO ZPV CORRECTIONS TO NMR SHIELDINGS CHANGE WITH THE CONFORMATION?

The Dimethoxymethane Study

Wojciech Migda

Department of Chemistry, Jagellonian University, Ingardena 3, 30-060 Kraków, Poland

Zero-Point Vibrational (ZPV) corrections to NMR shieldings have been calculated since 1996, when the paper by Fukui et al. was first published [1]. Since then, the level of sophistication of applied computational methods and the size of studied molecules have grown enormously reaching the mark set recently by Gauss et al., who calculated ZPV corrections for molecules as large as acetone at the coupled clusters level [2]. Till now however, all undertaken efforts have focused only on studying single conformers, preventing any possibility of exploring conformational dependence of ZPV corrections to NMR shieldings.

In this work we present results of calculations of ZPV corrections to ^1H , ^{13}C and ^{17}O NMR shielding constants in different conformers of dimethoxymethane (DMM). We extended the study to methyl-propyl ether (MPE) as well to further explain observed findings.



These two molecules are known to attain several analogous conformations. In this work the gauche-gauche (*gg*), gauche-anti (*ga*) and anti-anti (*aa*) conformers were investigated for the former compound, whereas gauche-gauche (*gg*), gauche-anti (*ga*), anti-gauche (*ag*) and anti-anti (*aa*) forms were considered for the latter.

The employed methodology was very similar to that recently used by Bühl, who studied ZPV corrections to shieldings in inorganic complexes [3]. In this method, based on the approach developed by Ruud et al. [4], firstly, the effective geometry of the molecule is established based on the evaluation of the cubic force field, followed by calculation of corrections, which require computation of second derivatives of the properties. The B3LYP density functional was used for calculation of the geometries and the cubic force field, whereas the MPW1PW91 functional was used in the shieldings calculations. The TZVP++ basis set was used throughout. The DFT calculations were performed using the GAUSSIAN03 program and its results were processed with a modified code of the DALTON program to yield the final data. For the cubic force field determination using numerical differentiation of gradients along normal coordinates the step of 0.0075 Å was used; for the calculation of the second derivatives of the nuclear shieldings the step of 0.05 Å was used.

In the molecule of DMM we observed significant changes of ZPV corrections with conformation only for the ^1H and ^{13}C nuclei of the terminal methyl groups, and only these nuclei in this fragment of the compound will be discussed below. When the ^{13}C nucleus is considered, the ZPV corrections are equal to -1.93 ppm in the *gg* form. For the two respective methyl groups in the *ga* conformation they change to -2.33 ppm (CH_3 gauche) and -3.00 ppm (CH_3 anti). Finally, in the *aa* form the corrections reach the value of -3.48 ppm.

For the three ^1H nuclei in the methyl groups the changes are even more dramatic. The analogous values decrease from $-0.25\div-0.22$ ppm (*gg*), through $-0.33\div-0.30$ ppm (*ga*, CH_3 *gauche*) and $-0.58\div-0.46$ ppm (*ga*, CH_3 *anti*) to $-0.57\div-0.52$ ppm (*aa*) – in this case the ZPV corrections more than double going from *gg* to *aa* conformer!

Regardless of the nucleus under consideration we observe changes of the ZPV correction with the conformation. In this trend corrections for the methyl groups in the *gauche* arrangement are smaller than respective values for the group in the *anti* alignment. Moreover, the results are influenced by the orientation of the group at the other end of the investigated molecule. But what is responsible for that progression? Is it a purely structural effect, relying mainly on the changes of the torsional angles, or it could be the result of the presence of stereoelectronic interactions in the molecule – *the anomeric effect*?

To answer this question we investigated the molecule of MPE, which is similar to the DMM in the C-O-C fragment, though its structural features disable any possibility of stereoelectronic interactions. Considering only the C-O-C moiety, alike the results for the DMM, the major changes to ZPV corrections were observed only for the terminal methyl group. For its ^{13}C nucleus the correction to the shielding in the *gg* form is equal -2.86 ppm, a value almost 1 ppm larger than in the analogous DMM conformer. In the *ga* conformation, in which the C-O-C moiety has the same arrangement, the value of the correction increases to -3.02 ppm – compare it with -2.33 ppm in DMM. But as we turn our attention to the *anti* alignment of the methyl group in the *ag* and *aa* forms of MPE the values are almost identical to the results in DMM: -3.04 and -3.51 ppm.

In the case of the ^1H nuclei in the methyl group ZPV corrections vary from $-0.40\div-0.38$ ppm and $-0.43\div-0.40$ for the *gauche* oriented methyl in the *gg* and *ga* forms to $-0.52\div-0.44$ ppm and $-0.59\div-0.52$ ppm for the methyl in the *anti* arrangement in *ag* and *aa* conformations. Here, just like for the ^{13}C nucleus, the values for the CH_3 group in the *anti* orientation are closer to the results for DMM than those for the methyl in the *gauche* arrangement.

From the above results one can see, that, firstly, in MPE the ZPV corrections do change too. Secondly, values calculated for the methyl group in the *anti* orientation are almost the same as those in the DMM. But when the *gauche* orientation is considered the discrepancy is evident. The only difference between the two is the fact that the *gauche* orientation in DMM means presence of the anomeric effect. Thus if in the case of the MPE the changes of ZPV corrections can be explained only as a result of changes of the conformation, for the DMM stereoelectronic interactions – *the anomeric effect* – must be accounted for the much more distinct changes of the corrections.

References:

1. H. Fukui, T. Baba, J. Narumi, H. Inomata, K. Miura, H. Matsuda, J. Chem. Phys. 105 (1996) 4662.
2. A.A. Auer, J. Gauss, J.F. Stanton, J. Chem. Phys. 118 (2003) 10407.
3. M. Bühl, P. Imhof, M. Repisky, ChemPhysChem 5 (2004) 410.
4. Ruud, P.-O. Åstrand, P.R. Taylor, J. Chem. Phys. 112 (2000) 2668.

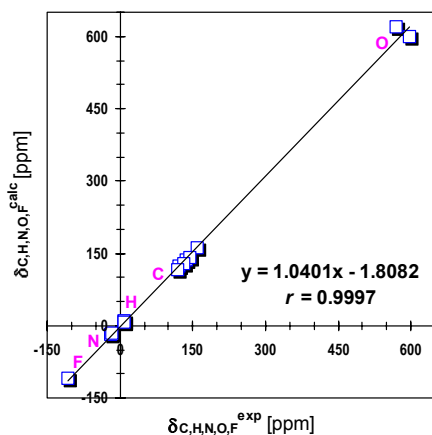
MULTINUCLEAR CORRELATION $\delta_{C,H,\dots}^{\text{EXP}}$ VS. $\delta_{C,H,\dots}^{\text{GIAO}}$ AS A TOOL IN STEREOCHEMICAL ANALYSIS AND NMR SIGNAL ASSIGNMENT

Ryszard B. Nazarski

Department of Organic Chemistry, Institute of Chemistry, University of Łódź,
90-950 Łódź 1, P.O. Box 376, Poland. E-mail: rynaz@chemul.uni.lodz.pl

It is well established that statistical processing of the relation between experimental isotropic δ_X^{EXP} data (where X is the NMR-active nucleus) and corresponding nuclear magnetic shieldings σ_X^{GIAO} (or recalculated values δ_X^{GIAO}), predicted usually for different molecular models by the GIAO methodology at the HF or DFT level, afforded the most verificative criterion of goodness of various structural choices that are taken for molecular objects studied by NMR spectroscopy in solution.

For example, time-averaged forms of two conformationally flexible medium-sized molecules were elucidated very recently, based on best fitting of the measured data δ_C and δ_H to those computed by the GIAO method at the *ab initio* HF/6-31G* level [1]. Excellent statistical results obtained were regarded as the best proof of correctness of the proposed overall solution conformations. Indeed, very strong ($r > 0.999$) *two-nuclear* linear correlations of type δ_X^{GIAO} vs. δ_{Xn}^{EXP} ($n = 2$) were achieved, which merit some comment. Double sets of values δ_C and δ_H , calculated and measured, are usually considered as *two independent* series of the NMR parameters that must be correlated independently. Frequently, such separate mathematical operations involve several structurally close systems [2]. However, there is no reason against performing mutual multinuclear linear regression analyses, *i.e.* involving different δ_X s for the same molecule, provided that appropriate standards of δ_X s are applied. An approach of this type was used only occasionally before [1,3].



In this communicate, an expansion of the foregoing idea will be presented, for $n > 2$. A large variety of different heteroatom(s)-containing organic molecules were used as test systems. Also different levels of modeling and/or NMR calculations were applied. Especially interesting is the case of 2,4-dinitrofluorobenzene, for which a five-nuclear correlation $\delta_{Xn}^{\text{GIAO}} = f(\delta_{Xn}^{\text{EXP}})$ was examined at the B3LYP/6-31+G** level (Figure, δ_{Xn}^{EXP} from [4]). In certain cases, the achieved results strongly suggest the necessity of reassignment of some NMR signals reported in the literature.

References:

1. Michalik, E; Nazarski, R. B. *Tetrahedron*, **2004**, *60*, 9213-9222.
2. See *e.g.* (a) Forsyth, D.A.; Sebag, A. B. *J. Am. Chem. Soc.* **1997**, *119*, 9483-9494. (b) Tähtinen, P.; Bagno, A.; Klika, K. D.; Pihlaja, K. *J. Am. Chem. Soc.* **2003**, *125*, 4609-4618. (c) Kupka, T.; Pasterna, G.; Jaworska, M.; Karali, A.; Dais, P. *Magn. Reson. Chem.* **2000**, *38*, 149-155.
3. (a) Alkorta, I.; Elguero, J. *New. J. Chem.* **1998**, *22*, 381-385. (b) Perczel, A.; Császár, A. G. *Eur. Phys. J. D* **2002**, *20*, 513-530, and previous papers in the series.
4. Ariza-Castolo, A.; Guerrero-Alvarez, J. A.; Peralta-Cruz J. *Magn. Reson. Chem.* **2003**, *41*, 49-52.

**UNIQUE INFORMATION ABOUT MOLECULAR DYNAMICS AND TIMESCALE
OF MOLECULAR MOTIONS IN BIOPOLYMER OF LACTIDE
AND ϵ -CAPROLACTONE USING SOLID-STATE NMR SPECTROSCOPY**

Alovidin Nazirov¹, Farhod Nozirov², Stefan Jurga¹

¹ *Department of Macromolecular Physics, Adam Mickiewicz University, Umultowska 85, 61-614 Poznań, Poland.*

² *Center for Interdisciplinary Magnetic Resonance, National High Magnetic Field Laboratory, 1800 East Paul Dirac Drive, Tallahassee, FL 32310, USA*

Solid-state NMR is a powerful technique for the understanding of molecular dynamics, timescale of molecular motions and the chemical structure. Combining classical and advanced high resolution solid-state NMR as well as Fast Field Cycling NMR for measurements of a second moment and the relaxation times gives significant information about the local and segmental chain motions of polymers, which are very important parameters for solid-state physics of macromolecules.

We studied the ¹H and ¹³C NMR relaxation times and spectra of biopolymers, which are derived from L-lactide and ϵ -Caprolactone. Analysis of the experimental data shows that the average environment of chain in the Lac/Cap binary mixture strongly depends on the concentration of lactide monomer. The low concentration of caprolactone monomers in a chain architecture causes the copolymer to be more rigid and the shift glass phase temperature T_g to be higher. When increasing the concentration of caprolactone, the activation energy of the molecular motion increases from 7.7 to 25 kJ/mol. This indicates that the chains of copolymer with a architecture of 0.3Lac/0.7Cap are more flexible than those of 0.7Lac/0.3Cap. In order to understand fully the physical-chemical properties of these new kinds of biomaterials further experiments are required.

INTERACTION BETWEEN POLY(ACRYLIC ACID) AND A NONIONIC SURFACTANT. A RHEOLOGY AND SELF-DIFFUSION NMR INVESTIGATION

Grzegorz Nowaczyk, Dimitris Vlassopoulos*, and Stefan Jurga

Institute of Physics, Adam Mickiewicz University, Umultowska 85, PL-61614 Poznań, Poland

** Institute of Electronic Structure and Laser, Foundation for Research and Technology - Hellas, P.O. Box 1527, GR-711 10 Heraklion, Greece*

The interaction between polymers and surfactants is of importance in many colloidal systems. Here we report studies of poly(acrylic acid) microgels (carbopol[®]971) and nonionic surfactant (Brij 58) by means of rheological and NMR diffusion methods. Viscoelastic properties and polymer NMR self-diffusion were studied as a function of surfactant concentration.

Carbopol[®]971 was provided by Noveon, Inc. The polymer powder was dispersed in distilled water or D₂O with or without surfactants. Rheological measurements were made in the temperature range from 10 to 50°C at the frequency from 0,1 up to 100 rad/s. Using Bruker DMX 400 spektrometer the self-diffusion experiments were performed.

It was found that the addition of surfactant leads to a shrinkage of microgel particles. Above 3% concentration of Brij 58 much smaller particles bound together trough the surfactant.

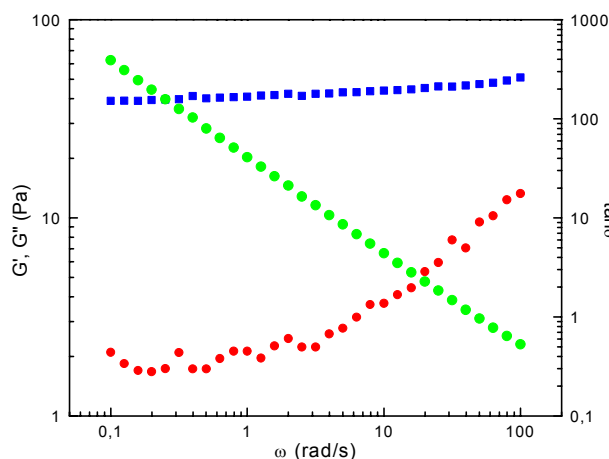


Fig. 1. G' , G'' and $\tan\delta$ for Carbopol 1% at 20°C.

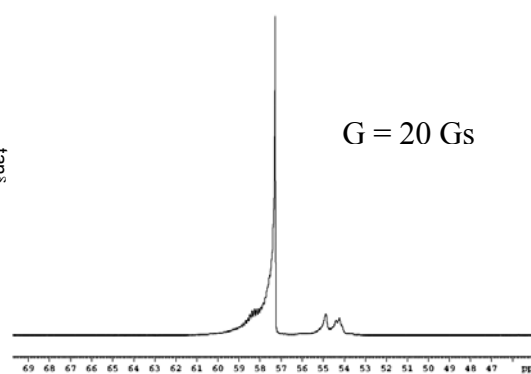


Fig. 2. NMR spectrum of Carbopol dispersed in D₂O at magnetic gradient field 20 Gs.

References:

- [1] S. Matsukawa, H. Yasunaga, C. Zhao, S. Kuroki, H. Kurosu, I. Ando, Diffusion processes in polymer gels as studied by pulsed field-gradient spin echo NMR spectroscopy, *Prog. Polym., Sci.*, 24 (1999) 995-1044.
- [2] R. Barreiro-Iglesias, C. Alvarez-Lorenzo, A. Concheiro, Poly(acrylic acid) microgels (carbopol[®]934) / surfactant interactions in aqueous media Part I: Nonionic surfactants, *Int. J. Pharm.*, 258 (2003) 165-177.

NMR STUDY OF CMR EFFECT IN MANGANITES

Colin J.Oates¹, Czesław Kapusta¹, Marcin Sikora¹, Dariusz Zając¹, Peter C.Riedi²,
Christine Martin³, Cedric Yaicle³, Antoine Maignan⁴, Jose Maria DeTeresa⁴,
and M. Ricardo Ibarra⁴

¹ *Department of Solid State Physics, Faculty of Physics & Applied Computer Science, AGH University of Science and Technology, 30-059, Kraków, Poland*

² *School of Physics and Astronomy, University of St. Andrews, North Haugh, St. Andrews, KY16 9SS, Scotland, UK*

³ *Laboratoire CRISMAT – UMR 6508, ISMRA et Université de Caen, 6 Boulevard du Marechal JUIN, 14050 Caen Cedex, France*

⁴ *Magnetismo de Sólidos, Instituto de Ciencia de Materiales de Aragon, CSIC-Universidad de Zaragoza, Facultad de Ciencias, 50009 Zaragoza, Spain*

This presentation concerns the NMR study of the colossal magnetoresistance (CMR) effect in the mixed valence manganites. The compounds exhibit a decrease of electrical resistivity in the applied magnetic field by several orders of magnitude. The effect is related to the interplay of spin and lattice systems and the resulting intrinsic magnetic and electronic phase separation into e.g. antiferromagnetic insulating (AFI) and ferromagnetic metallic (FMM) as well as paramagnetic insulating (PMI) and ferromagnetic metallic (FMM) phases. Two groups of systems are presented: $\text{Sm}_{0.55}\text{Sr}_{0.45}\text{MnO}_3$ which exhibit a huge CMR effect around magnetic ordering temperature, T_C and $(\text{Pr,Ca})(\text{Mn,Ga})\text{O}_3$ system which shows a magnetic field induced insulator-to-metal (I-M) transition at low temperatures. The former exhibits a FMM-PMI separation and the latter shows the AFI-FMM phase separation.

The ^{55}Mn spin echo spectra were measured at zero field and in the applied magnetic field with automated, frequency swept spectrometer. Polycrystalline samples of $\text{Sm}_{0.55}\text{Sr}_{0.45}\text{MnO}_3$, $\text{Pr}_{0.5}\text{Ca}_{0.5}\text{Mn}_{1-x}\text{Ga}_x\text{O}_3$ ($x=0$ and 0.03) and $\text{Pr}_{0.67}\text{Ca}_{0.33}\text{MnO}_3$ were measured. In the spectra the resonance related to the “motionally narrowed”, double exchange controlled FMM phase was distinguished and its intensity was related to the amount of the FMM phase. Such an NMR magnetometry on $\text{Pr}_{0.5}\text{Ca}_{0.5}\text{Mn}_{1-x}\text{Ga}_x\text{O}_3$ ($x=0.03$) at 3 K shows a step-like increase in the DE line intensity in the applied magnetic field, Fig.1, which corresponds to an increase of the amount of the FMM phase. This coincides well with a step-like feature in the bulk magnetization measurements. The low temperature I-M transition for $\text{Pr}_{0.67}\text{Ca}_{0.33}\text{MnO}_3$ at ambient pressure occurs at fields greater than 5T; however at 1.1GPa, the DE line corresponding to the ferromagnetic metallic phase is already present at zero field.

Temperature dependent ^{55}Mn NMR study of $\text{Sm}_{0.55}\text{Sr}_{0.45}\text{MnO}_3$ at zero field shows a single DE signal up to 139K, which corresponds to T_C determined from bulk magnetisation measurements. The hyperfine field at this temperature, which corresponds to the local Mn magnetisation, $\langle S_z \rangle$, is only slightly lower from its low temperature value, whereas the intensity of the DE line mimics the temperature dependent magnetisation curve, measured at a small field, 0.01 Tesla. Applying a magnetic field up to 2 Tesla at T_C gives rise to an increase of the DE signal intensity and the corresponding increase of the amount of the FMM phase coincides well with that derived from the magnetisation measurements at the respective fields.

The results show the same microscopic nature of the magnetic field induced low temperature I-M transition and the genuine CMR effect at the magnetic ordering temperature. It relies in an increase of the amount of the FMM phase in the applied magnetic field, which can eventually lead to its percolation. This results in a dramatic decrease of the electrical resistivity of these materials in the applied field, which is generally termed as CMR.

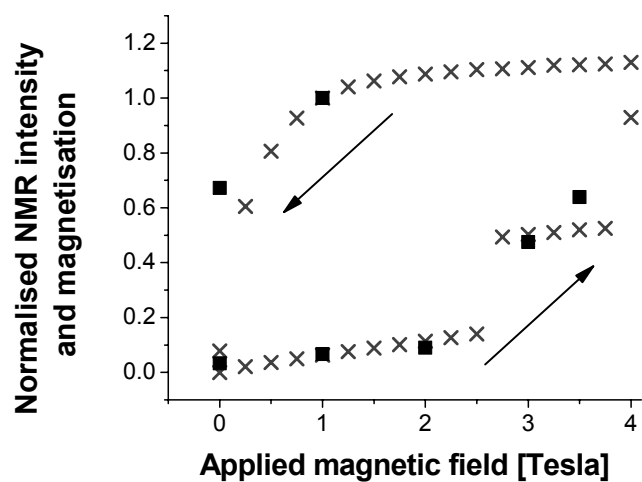


Fig. 1. A plot of the absolute intensity of the ^{55}Mn DE line at different fields (filled squares), combined with magnetization measurements (crosses). Both plots are normalized to their corresponding values at 1 Tesla (magnetized at 6 Tesla).

NON-MARKOVIAN PROCESSES OF MOLECULAR MOTIONS IN SOLIDS

Marcin Olszewski and Nikolaj Sergeev

*Institute of Physics, University of Szczecin, ul. Wielkopolska 15, 70-451 Szczecin, Poland,
e-mail: marcin.olszewski@wp.pl*

Motions of molecules or molecular groups in solids are considered as a stochastic process in majority of theories analyzing influence of the molecular dynamics on the NMR [1]. In condensed matter only the components in a configuration space are usually taken into account [1,2]. However it is not always reasonable. Reorientations or diffusion of molecular groups are often connected with the large structural fluctuations in solid dynamics. This leads

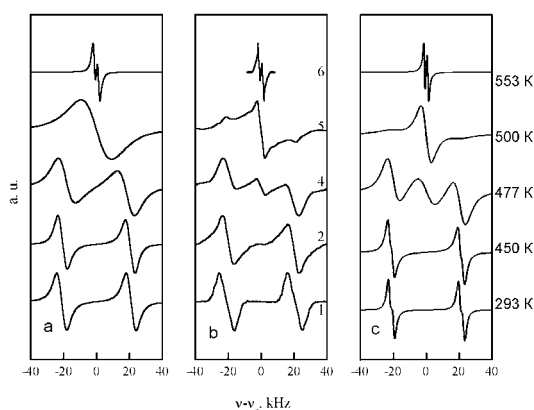


Fig.: The temperature dependence of the ^1H NMR spectrum of natrolite for the case when vector B_0 lies in $[110]$ direction: (a) theoretical NMR spectra obtained for the model of homogeneous diffusion of water molecules with the activation energy $E_a=73$ kJ/mole; (b) experimental NMR spectra; (c) theoretical NMR spectra obtained for the non-Markov model of water molecular motions with fluctuations driven by dichotomic noise ($E_a=73$ kJ/mole and $\sigma=4,2$ kJ/mole).

with temperature.

The numerical methods have been used to analyze temperature dependencies of NMR line when the fluctuations have a more complicated and real character. The Orstein-Uhlenbeck process (diffusion, stationary, Gaussian, Markov process) has been used to describe changing of activation energy with time.

References:

- [1] A. Abragam, *The Principles of Nuclear Magnetism*, Clarendon Press, Oxford, 1961.
- [2] N.G. van Kampen, *Stochastic Processes in Physics and Chemistry*, North-Holland, Amsterdam, 1981.
- [3] H. Sillescu, *J. Chem. Phys.*, 104, 4877 (1996).
- [4] M. Olszewski, N.A. Sergeev, A.V. Sapiga, *Z. Naturforsch.*, 59a, 501-504 (2004).

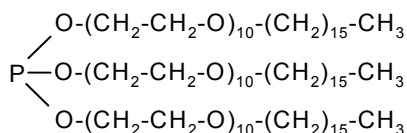
to the creation of additional “non-observable” states. In that case the non-Markovian models can be useful. It has been made use of the procedure of the creation of non-Markovian process, connected with the projection from a higher-dimensional Markov process by integrating over all “non-observable” variables [3].

In case of non-Markovian molecular motions we assume that the activation energy fluctuates and causes the transformation of transition probability matrix into the stochastic matrix. Then master equation changes into the stochastic equation. It has been shown in [4] that the simple fluctuations driven by a bitable process of telegraphic type, called dichotomic noise (DN) may very well explain the observed temperature dependence of NMR spectra in the mineral natrolite. Markov model of the water molecules diffusion with single correlation time can not correctly describe behavior of these spectra

MOLECULAR DYNAMIC OF PODAND 10 AS STUDIED BY NMR AND DIELECTRIC SPECTROSCOPY

Bakyt Orozbaev, Monika Makrocka-Rydzik, Stefan Jurga, and Grzegorz Schroeder

Institute of Physics, A. Mickiewicz University, Umultowska 85, 61-614 Poznan, POLAND
Institute of Chemics, A. Mickiewicz University, Grunwaldzka 6, 60-780 Poznan, POLAND



The structural and dynamical properties of Podand 10 were studied by the second moment technique (M_2), the Differential Scanning Calorimetry (DSC) and Dielectric Spectroscopy.

The thermal properties of the sample in temperature range $-60\text{ }^\circ\text{C}$ to $120\text{ }^\circ\text{C}$ were examined using a Netzsch Differential Scanning Calorimeter (DSC-204), (Fig. 1). The sample weight was about 5 mg and the heating rate was $10\text{ }^\circ\text{C}/\text{min}$.

Dielectric relaxation spectra (Fig. 2) were collected using a Novocontrol BDS-80 broadband dielectric spectrometer. Experiments were performed in the frequency domain ($0.01\text{ Hz} - 1.8\text{ GHz}$), between $-60\text{ }^\circ\text{C}$ and $80\text{ }^\circ\text{C}$ with $5\text{ }^\circ\text{C}$ increments. Sample was cooled and heated in the presence of N_2 during the dielectric measurements.

The broad-line ^1H NMR spectra were recorded on a spectrometer driven by a marginal oscillator operating at 28 MHz. The second moment of proton spectra was computed for experimental data and compared with theoretical one.

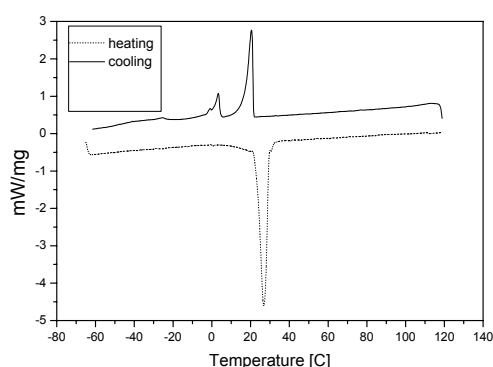


Fig. 1. DSC thermogram of Podand 10

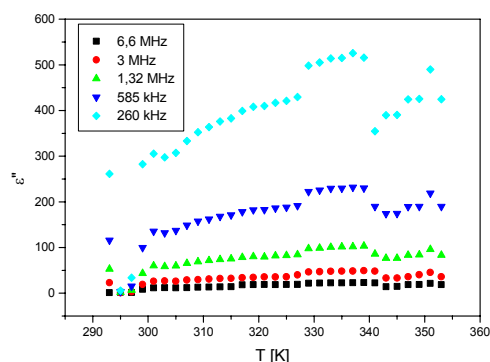


Fig. 2. ϵ'' of Podand 10 vs. temperature

ELECTRIC FIELD GRADIENTS IN MB_{12} ($M=Y,Zr$ and Lu) DODECABORIDES FROM NMR EXPERIMENTS AND *ab initio* CALCULATIONS

S. Paluch¹, O.J. Żogał¹, B. Jäger², W. Wolf³, P. Herzig², N. Shitsevalova⁴,
and Y. Paderno⁴

¹ *W Trzebiatowski Institute for Low Temperature and Structure Research, Polish Academy of Sciences, P.O.Box 1410, 50-950 Wrocław, Poland;* ² *Institut für Physikalische Chemie, Universität Wien, Währingerstr. 42, 1090 Vienna, Austria;* ³ *Materials Design s.a.r.l., 44,av.F.-A. Bartholdi, 72000 Les Mans, France;* ⁴ *Institute for Problems of Materials Science, Academy of Sciences of Ukraine, 3 Krzhizhanovsky str., 03680 Kiev, Ukraine*

Three compounds, YB_{12} , ZrB_{12} and LuB_{12} have been investigated by electric –field gradient (EFG) at the boron sites using the ^{11}B nuclear magnetic resonance (NMR) technique and by performing first –principles calculations.

The crystal structure of cubic MB_{12} (space group $Fm-3m$, no.225) consists of a face-centered-cubic lattice with the cubo-octahedral B_{12} grouping. Such B_{12} cluster together with crystal lattice for ZrB_{12} is shown on Fig.1.

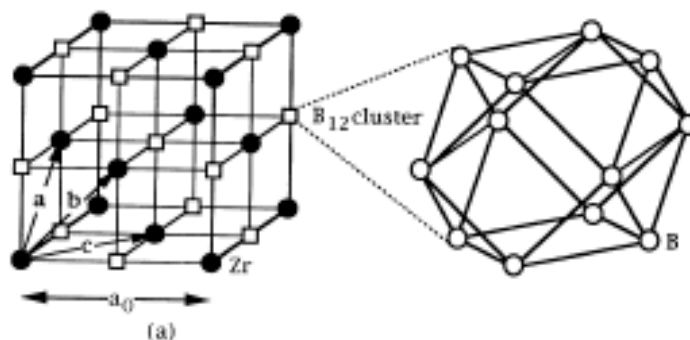


Fig.1

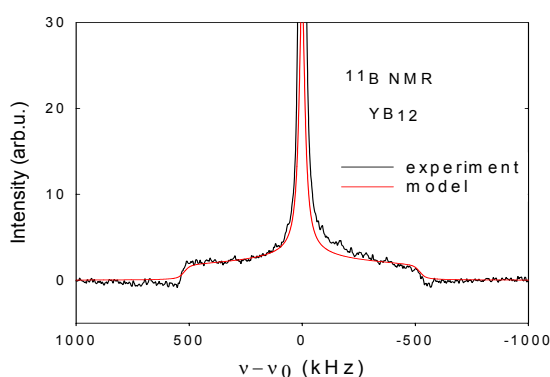


Fig. 2

Boron site point symmetry permits a non –axial symmetry of EFG tensor [1]. In this case both the V_{zz} and η parameters characterizing the tensor are expected to possess a non-zero values. The metallic conductivity of the MB_{12} compounds imposes an use of powder sample for the NMR experiments and typical spectrum for such a case is shown in Fig.2.

In the Fig.2 a solid line (red) represents simulated spectrum for specific values of the V_{zz} and η whereas the other line (black) is the experimental spectrum of the ^{11}B NMR. The simulation was made using Massiot et al. [2] program. Numerical values of the V_{zz} and η resulted from the simulated spectra for the MB_{12} are given in Table 1.

Table 1. Experimental (2nd and 3rd columns) and calculated boron EFGs (in 10^{20} V/m²) assuming an ^{11}B nuclear quadrupole moment of $0.04 \text{ e|x}10^{-28} \text{ m}^2$.

	$ V_{zz} $	η	V_{xx}	V_{yy}	V_{zz}	η
YB_{12}	11.0 ± 0.6	0.93	-0.49	-12.29	12.78	0.92
ZrB_{12}	11.2 ± 0.6	0.94	0.12	12.3	-12.4	0.98
LuB_{12}	11.6 ± 0.6	0.98	-0.20	-12.58	12.78	0.97

For the theoretical calculations structure optimizations were performed as a first step. For obtained structural parameters the EFGs were computed within the local-density approximation [3]. Agreement between experimental and theoretical values of the $|V_{zz}|$ and η is quite satisfactory and could be even better if one uses the ^{11}B nuclear quadrupolar moment of $0.0355 \text{ e|x}10^{-28} \text{ m}^2$ reported by Nöth et al [4].

Acknowledgement:

The work was supported in part by 03-51-3036 INTAS Project.

References:

1. The properties of the EFG tensor one can find in : B.C.Gerstein, C.R.Dybowski, Transient techniques in NMR of Solids, Academic Press, (1985)
2. D.Massiot, F.Fayon, M.Capron, I.King, S.Le.Calve, B.Alonso, J.-O.Durand, B.Bujoli, Z.Gan, G.Hoatson, Magn.Reson.Chem. 40, 70 (2002)
3. Some details on the theoretical calculations of the EFG one can find , for example, at P.Herzig, W.Wolf, O.J. Żogał, Phys.Rev.B62, 7098 (2000).
4. H. Nöth, B.Wrackmeyer in: P.Diehl, E.Fluck, R.Kosfeld, (Eds.) , NMR basic Principles and Progress, vol.14, Springer, (1978) p.1

^1H - ^{13}C AND ^1H - ^{15}N NMR STUDIES OF THIONIC AND THIOLIC FORMS OF 6-MERCAPTOPURINES

Leszek Pazderski¹, Iwona Łakomska¹, Andrzej Wojtczak¹, Edward Szłyk¹,
Jerzy Sitkowski^{2,3}, Lech Kozerski², Bohdan Kamieński³, Wiktor Koźmiński⁴,
Jaromir Tousek⁵, and Radek Marek⁵

¹Faculty of Chemistry, Nicholas Copernicus University, Gagarina 7, Toruń (PL)

²National Institute of Public Health, Chełmska 30/34, Warsaw (PL)

³Institute of Organic Chemistry, Polish Academy of Sciences, Kasprzaka 44/52, Warsaw (PL)

⁴Faculty of Chemistry, Warsaw University, Pasteura 1, Warsaw (PL)

⁵Department of Chemistry, Faculty of Science, Masaryk University, Kotlářská 2, Brno (CZ)

6-Mercaptopurine (6mpH), 2,6-dimercaptopurine (2,6dmp) and 6-mercaptopurine-9-ribose (6mp-9rb) were studied with ^1H - ^{13}C HMBC and ^1H - ^{15}N HMBC in $\text{dms}\text{-}d_6$ solution. The ^{15}N NMR signals were unambiguously assigned and the distribution of the mobile protons was proposed on the basis of chemical shifts and J_{HC} , J_{HN} coupling constants (the latter determined with HECADÉ). All discussed heterocycles were proved to be thionic species with the predominance of the following tautomers: N(1)H, N(7)H for 6mpH, N(1)H, N(3)H, N(7)H for 2,6dmp, N(1)H for 6mp-9rb. For 6mpH the ratio of N(1)H, N(7)H : N(1)H, N(9)H tautomers was evaluated to be ca. 75:25 by using quantum-chemical calculations. The ^{15}N NMR studies of the $\text{dms}\text{-}d_6/\text{HCl}$ solution, containing dissolved 6-mercaptopurinium chloride (6mpH₂Cl), exhibited the presence of unexpected, thiolic forms of neutral 6mpH, probably formed by the hydrolysis process. They were slowly converted into the stable, thionic 6mpH₂⁺ cation. The latter individual revealed an unusual, among the whole class of purines, protonation pattern of N(1)H, N(3)H, N(7)H, entirely different from that known for 6mpH₂⁺ within the solid phase. An unstable species of probably 6mpH·H₃O⁺ type was also detected and fully characterized by ^{13}C and ^{15}N NMR. The ^{13}C and ^{15}N CP/MAS spectra were obtained for solid 6mpH·H₂O, anhydrous 6mpH, 2,6dmp and 6mpH₂Cl, the signals assignments being proposed in relation to the re-determined X-ray structures.

This work was supported by the grant of the Polish Committee for Scientific Research (4T09A 11623) and of the Ministry of Education of the Czech Republic (Cz-Pl 13/2004/Cz).

NMR STUDIES OF CATALYTIC ACTIVITY ON THE SURFACE OF RUTHENIUM NANOPARTICLES

**Tal Pery,[§] Benradeta Walaszek,[§] Susanna Jansat,[†] Jordi Garcia-Anton,[†]
Karine Philippot,[†] Bruno Chaudret,[†] Gerd Buntkowsky[§], and Hans-Heinrich Limbach[§]**

[§]*Institut für Chemie, Freie Universität Berlin, Takustr. 3, 14195 Berlin, Germany and*
[†]*Laboratoire de Chimie de Coordination du CNRS, 205, Route de Narbonne, 31077 Toulouse*
Cedex 04, France.

email: pery@chemie.fu-berlin.de

Metal Nanoparticles are known for their interesting catalytical properties. However they have been considered a long time as ill defined Objects. Heretogenous catalysis takes place on the surface of the catalyst, preferentially on defects, steps and edges. Through their small size Nanoparticles have a very huge amount of surface atoms; they also reveal a large amount of edge atoms on their surface which explains their big catalytic activity. For a better understanding of the catalytical properties, the particles' surface has to be well characterized. NMR, especially the combination of different solid state, liquid and gas phase NMR techniques is a powerful tool to investigate the dynamics of molecules on the particles surface and to study their reactivity.

Ruthenium Nanoparticles were obtained by decomposition of an organometallic precursor Ru(COD)(COT) (COD = 1,5-cyclooctadiene; COT = cyclooctatriene) in mild conditions (room temperature, 3 bar H₂) in THF and in the presence of stabilizing ligands.

We performed our studies using gas phase and liquid NMR as well as static ²H solid state NMR. In this presentation, reactivity studies of different reactions catalyzed by Ruthenium Nanoparticles are shown. They include the H/D exchange of the aliphatic chains of the protecting ligand, the oxidation of carbon monoxide, oxidation of dihydrogen as well as hydrogenation reactions.

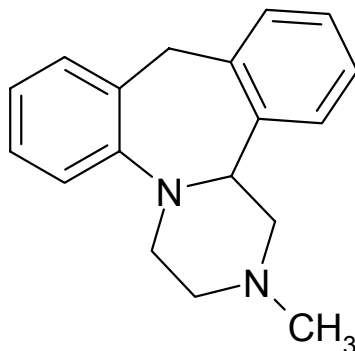
¹³C CP-MAS NMR STUDIES OF MIANSERIN, A POTENT ANTIDEPRESSANT DRUG

Dariusz Maciej Pisklak^a, Błażej Grodner^b, Jan Pachecka^b, and Iwona Wawer^a

^aDepartment of Physical Chemistry

^bDepartment of Biochemistry and Clinical Chemistry
Faculty of Pharmacy Medical University of Warsaw

Mianserin is a tetracyclic antidepressant with potent serotonergic properties being 5-HT₁, 5-HT₂ and 5-HT₃ receptor agonist. It has noradrenergic activity due to the presynaptic α_2 blockage and strong antihistamine effects. Crystal structure of mianserin has been determined in 1996 [1]. Molecular structure and conformations of mianserin are of interest since it determined specific affinities for receptorial subtypes.



¹³C NMR spectra for solution and solid state were recorded on a BRUKER AVANCE DSX-400 spectrometer. The powder sample was packed into a ZrO₂ rotor and spun at 10 kHz.

The ¹³C resonances in the solid state spectrum were assigned on the basis of liquid-state chemical shifts. Dipolar dephasing pulse sequence was used to observe selectively the quaternary carbons. In order to gain a better insight into the solid-state interactions of mianserin, the cross-polarization variable contact time experiments were performed.

An attempt has been made to reproduce and interpret the changes in shieldings from the *ab-initio* theoretical methods. NMR shielding constants were calculated using GIAO-DFT approach.

Reference:

1. A. Dalpiaz, V. Ferreti, P. Gilli, V. Bertolasi, Stereochemistry of serotonin receptor ligands from crystallographic data, *Acta Cryst. B*52 (1996) 509-518

USABILITY OF HMRS IN CNS DIAGNOSTICS OF HIV POSITIVE PATIENTS

Lilianna Podsiadło, Andrzej Urbanik, Aleksander Garlicki¹, Justyna Kozub,
Barbara Sobiecka, and Tomasz Mach¹

Department of Radiology, Collegium Medicum of Jagellonian University, Kraków, Poland,

¹Department of Infection Diseases, Collegium Medicum of Jagellonian University, Kraków, Poland

Purpose:

The aim of the study is presentation of brain metabolic changes of HIV – positive patients in different stages of disease involvement using HMRS. HIV- positive patients with the clinical symptoms of brain injury were compared with the neuroasymptomatic patients.

Material and Method:

MRI and HMRS were performed in 19 patients (4 women, 15 men), 23 to 49 years old using 1,5 T Signa Horizon (GEMS) unit. Saggital and axial T1 weighted and axial T2-weighted images were performed. The spectral processing was performed using PRESS technique. MR pictures and spectrum from the periventricular, frontal and parieto- occipital regions were evaluated.

In 4 patients AIDS dementia complex was clinically stated; slowly progressive dementing illness (group 1), while the remaining patients had no clinical changes concerning CNS (group 2). Hemi or tetraplegia, bradypsychia and hypokinesia were observed in the all patients of the group 1. The patient with tetraplegia suffered from the toxoplasmatic encephalitis and meningitis in the past.

One patient with hemiplegia was suffered from the right facial nerve paralysis and motor aphasia.

Results:

MRI:

group 1 - brain atrophy and focal hyperintense lesion in T2- weighted MR images and hypointense lesion in T1 weighted MR images in the centrum semiovale and in the periventricular white matter, caused by gliosis, were dominating signs. In 1 patient the area of extravasated blood in stage of MHB, after vasculitis was observed.

group 2 – in 10 cases no CNS changes were observed, in 5 remaining cases moderate degree of brain atrophy was observed.

HMRS:

group 1 –significant decrease in NAA/Cr and increase in Cho/Cr, moderate increase ml/Cr and Lac/Cr ratios was observed.

group 2 – different intensity significant decrease of NAA/Cr ratios, moderate increase in Ch/Cr and significant increase ml/Cr ratios was observed.

Conclusions:

1. HMRS is non-invasi, neurochemical method, based on the magnetic resonance phenomenon, that allows the evaluation of the brain metabolism and detection of neuronal markers and in this way expands CNS diagnostic possibilities in HIV – positive patients.

2. Stage of involvement of the process and imaging of metabolite changes in cases without morphological manifestation is allowed by HMRS.

NMR STUDY OF GdFe_2H_x HYDRIDES

Vit Procházka^a, Czesław Kapusta^a, Peter C. Riedi^b, and Jan Żukrowski^a

^a *Department of Solid State Physics, Faculty of Physics & Applied Computer Science, AGH University of Science and Technology, Cracow, Poland*

^b *Department of Physics & Astronomy, University of St. Andrews, St. Andrews, KY16 9SS Scotland, UK*

NMR measurements on GdFe_2H_x ($x = 0, 1.05, 1.7, 2.45, 2.85$) hydrides are reported. Spin echo spectra at zero field and the relaxation times T_2 have been measured on powder samples at 4.2 K. The values of x have been chosen at characteristic points of phase diagram and correspond to single phase compounds [1]. The spectra for $x=0$ and 1.05 exhibit two narrow lines at 58 MHz and 75 MHz identified as ^{155}Gd and ^{157}Gd resonances corresponding to Gd site with no hydrogen as nearest neighbour. The Gd hyperfine field derived from the resonant frequencies amounts to 43.7 T and T_2 is of 1 ms. Broad spectra in the 40-110 MHz range and an order of magnitude shorter T_2 are obtained for the compounds with $x>1.05$ and attributed to hydrogen resonances. The spectrum for the compound with $x=1.7$ consists of four overlapping peaks and they collapse into an unresolved broad line with increasing x . The Gd resonances for $x>1.05$ are smeared out due to a distribution of hyperfine fields [2] and electric field gradients caused by hydrogen neighbours. The hyperfine field on hydrogen determined from the central frequency amounts to 2.1 T. The results are analysed in terms of hydrogen occupation of A2B2 sites and the change of the easy magnetisation direction with x . A comparison of hydrogen hyperfine field with dipolar fields at H sites evaluated from lattice sums is made and a conclusion on the hydrogen occupation is drawn.

NMR RELAXATION IN MAIN CHAINS AND SIDE GROUPS OF CELLULOSE AND ITS DERIVATIVES

Adam Rachocki, Jadwiga Tritt-Goc, and Narcyz Piślewski

*Institute of Molecular Physics, Polish Academy of Sciences,
M. Smoluchowskiego 17, 60-179 Poznań, Poland*

Cellulose and the other polysaccharides: methyl cellulose – MC, hydroxypropyl cellulose – HPC and hydroxypropyl methyl cellulose – HPMC were the subject of our study by ^1H NMR method. The polymers under study consist of repeated glucose units carrying two side groups (-OR) and one group (-CH₂-OR). For cellulose R=H and we have two hydroxyl groups (-OH) and one methylol group (-CH₂-OH) attached to the glucose ring, for MC R=H or CH₃ whereas for HPC R=H or propylene group. It follows that the studied polysaccharides are characterised by the same repeating glucose units, but with different side groups. The side groups differ in lengths and molecular weight. The main goal of our study was to determine the molecular origin of the relaxation and the influence of the different side groups of glucose unit on the relaxation.

The proton spin – lattice relaxation times and the proton NMR second moments were studied as a function of temperature for MC, HPC and HPMC at 90 MHz. The two T_1 minima are clearly visible in the temperature range from about 100 K to 400 K in studied polymers – fig.1.

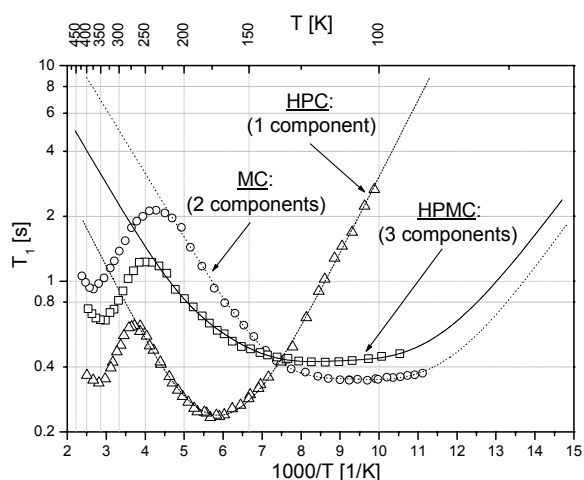


Fig.1. ^1H NMR relaxation times T_1 vs. inverse temperature in MC, HPC and HPMC

The low temperature T_1 minimum corresponds to the rotation of the CH₃ groups and the high temperature one assigned to the local motion of the segment of the polymer chain. The Field-Cycling NMR Relaxometry also researched the high-temperature minima where the frequency dependencies of spin-lattice relaxation times T_1 were observed in the range between 20 kHz and 40 MHz for nine different temperatures. The chosen temperatures were above the glass transition temperatures T_g determined for studied polymers by DSC method.

THEORY OF DAMPED QUANTUM ROTATION IN NMR SPECTRA. THE FOUR-FOLD ROTOR

T. Ratajczyk and S. Szymanski

*Institute of Organic Chemistry, Polish Academy of Sciences, Kasprzaka 44/52,
01-224 Warsaw, Poland*

The methyl group and its analogs $-XY_3$ are known as quantum rotors. In NMR spectra measured at sufficiently low temperatures, the tunneling splittings of the torsional sublevels of such rotors are, by virtue of the Pauli principle, converted into apparent spin couplings between the Y nuclei¹. With temperature increase, the spectra broaden, the individual lines coalesce and, ultimately, a motionally averaged pattern showing no fine structure due to the spin couplings is attained. This is generally regarded as a transition from the (coherent) quantum to the (stochastic) classical regime in the dynamic behavior of the rotor. However, in a series of theoretical^{2,3} and experimental studies⁴⁻⁷, the latter view has recently been challenged. The stochastic dynamics were shown to be still influenced by the Pauli principle; in consequence, they are controlled by two quantum (i.e., coherence-damping) rate constants instead of the single classical constant in the familiar jump model. Such quantum stochastic behavior could be observed not only at cryogenic temperatures in the solid state⁴ but, for strongly hindered methyl groups, in liquids at ambient temperatures as well⁵⁻⁷. The theoretical model affording a perfect reproduction of the observed spectra was once dubbed damped quantum rotation (DQR) model^{2,3}.

In the present contribution, the DQR theory is extended to four-fold quantum rotors XY_4 . The pertinent molecular models can be found, for example, among organic complexes of tetrahydrides of molybdenum and tungsten. According to the standard approach, the stochastic dynamics of such four-fold rotors are controlled by at most two classical rate constants. One of them measures random clockwise and anti-clockwise jumps between neighboring wells of the pertinent four-fold torsional potential and the other the possible direct jumps between every second well. In the DQR model, in place of the two classical constants, there occur three quantum rate constants describing damping processes of three different quantum coherences between the tunneling-split sublevels of the XY_4 rotor. Like in the case of the three-fold rotor, the classical jump model can be arrived at when the magnitudes of these three quantum constants happen to show some simple relationships. Perspectives of further extension of the DQR model, up to five- and six-fold rotors (such as the cyclopentadienyl and benzene rings), are also discussed.

References:

1. F. Apaydin and S. Clough, *J. Phys. C Ser. 2* **1**, 932 (1968).
2. S. Szymanski, *J. Chem. Phys.* **111**, 288 (1999).
3. P. Bernatowicz and S. Szymanski, *J. Magn. Reson.* **164**, 60 (2003).
4. S. Szymanski et al., *J. Magn. Reson.* **148**, 277 (2001).
5. P. Bernatowicz and S. Szymanski, *Phys. Rev. Lett.* **89**, 023004 (2002).
6. I. Czerski et al., *J. Chem. Phys.* **118**, 7157 (2003).
7. P. Bernatowicz et al., *J. Magn. Reson.* **169**, 284 (2004).

A ^{55}Mn NMR STUDY OF $\text{La}_{0.33}\text{Nd}_{0.33}\text{Ca}_{0.34}\text{MnO}_3$ WITH ^{16}O AND ^{18}O

**Damian Rybicki^a, Czesław Kapusta^a, Peter C. Riedi^b, Colin J. Oates^a, Marcin Sikora^a,
Dariusz Zajac^a, Jose Maria De Teresa^c, Clara Marquina^c, and Manuel R. Ibarra^c**

^a *Department of Solid State Physics, Faculty of Physics & Applied Computer Science, AGH University of Science and Technology, Cracow, Poland*

^b *Department of Physics & Astronomy, University of St. Andrews, St. Andrews, KY16 9SS Scotland, UK*

^c *Instituto de Ciencia de Materiales de Aragón, Universidad de Zaragoza-CSIC, 50009 Zaragoza, Spain*

This report presents a ^{55}Mn NMR study of ^{16}O and ^{18}O containing $\text{La}_{0.33}\text{Nd}_{0.33}\text{Ca}_{0.34}\text{MnO}_3$. Previous bulk measurements reported in the literature reveal that at low temperatures $\text{La}_{0.33}\text{Nd}_{0.33}\text{Ca}_{0.34}\text{Mn}^{16}\text{O}_3$ shows charge ordered (CO) and ferromagnetic (FM) insulating phases, whereas $\text{La}_{0.33}\text{Nd}_{0.33}\text{Ca}_{0.34}\text{Mn}^{18}\text{O}_3$ exhibits a charge ordered insulating behaviour. Application of a magnetic field can change the low temperature insulating state to a metallic one in both compounds and the field required for that is two times higher for $\text{La}_{0.33}\text{Nd}_{0.33}\text{Ca}_{0.34}\text{Mn}^{18}\text{O}_3$. The ^{55}Mn spin echo spectra have been measured at 4.2 K. They contain a single line centred at the frequency corresponding to the double exchange (DE) state of manganese in both compounds. This is attributed to a presence of ferromagnetic metallic (FMM) regions. The intensity of the resonant line is more than an order of magnitude lower for $\text{La}_{0.33}\text{Nd}_{0.33}\text{Ca}_{0.34}\text{Mn}^{18}\text{O}_3$, which indicates an order of magnitude lower content of the FMM phase in this compound. The Mn resonances of the CO or FM insulating phases are not observed possibly due to a fast nuclear relaxation. The measurements of the spectra for large pulse spacing show a pronounced minimum at the center of the DE line. This is related to a minimum of the spin-spin relaxation time at the line center caused by the Suhl-Nakamura interaction between nuclear spins. This interaction is effective in the large regions of uniform magnetisation and the effect shows that the FMM regions are at least tens of nanometers in size for both compounds. The results are discussed in terms of phase segregation in the compounds and the influence of oxygen isotopic substitution on it.

APPLICATION OF MOLECULAR MODELING AND DFT CALCULATION OF SPIN-SPIN COUPLING CONSTANTS TO THE CONFORMATIONAL ANALYSIS OF 3,4,5,6-TETRAHYDRO-1H-BENZO[B]AZOCIN-2-ONE

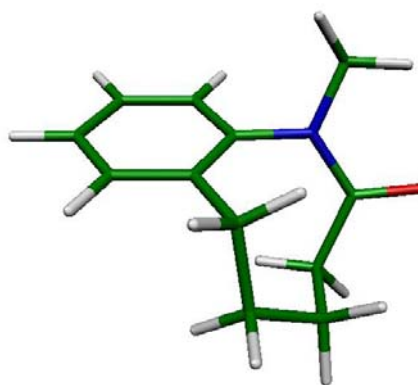
Agnieszka Rzepa, Wojciech Migda, and Barbara Rys

Department of Organic Chemistry, Jagellonian University, Ingardena 3, 30-060 Kraków

The well known relation between the torsion angle and homo- and heteronuclear vicinal coupling constants is the most useful tool for determination of the conformation of the molecule. However, calculation of the torsion angle from the experimental coupling constants requires usage of the empirical corrections reflecting the electronic and steric influence of the substituents in the vicinity of the coupled nuclei. Another possibility to solve the question of the relation between conformation and coupling constants is to calculate J constants for assumed conformation and compare them with experimental ones. Recent development of the DFT methods [1] gives an opportunity to realize this approach. But still there is a question of the reliability of obtained values.

We have decided to check this approach on the example of conformationally homogenic example, namely the 8-membered ring lactam. In the ^1H NMR spectrum of this compound separate signals for all eight aliphatic protons are observed. That means that the molecules are frozen in the chiral conformation causing the diastereotopic relation between all geminal protons. All of them, but *pro-R-3* and *pro-R-5*, represent the well resolved first-order pattern and doubtlessly permitted extraction of coupling constants.

The experimental values were compared with those calculated by DFT methods. The potential energy surface of the molecule was searched by molecular mechanics methods. The minima found were subjected to AM1 calculations. It allowed us to locate three different conformations. The global energy minimum is separated from the next one by 16 kJ/mol. The lowest energy structure was then optimized at the B3LYP/6-31G** level. The obtained geometry is presented below.

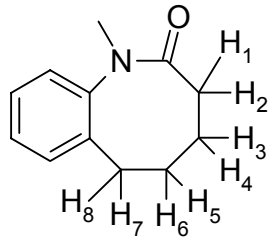


Shielding constants and nuclear coupling constants for eight-membered ring protons were calculated using the B3LYP/cc-pVTZ method and procedure described by Pihlaja involving scaling of the FC contribution into J . [2] All DFT calculations were performed with the Gaussian 03 Rev. C.02 program.

Results of the calculations and the experimentally estimated coupling constants are summarized in the Table. From their comparison a very good agreement is clearly seen which allowed us to state that the applied methodology might be successful in addressing the question about the conformation of the molecule. Moreover, calculated proton shielding constants well reproduce the difference in the chemical shifts observed in the spectrum.

Table. Comparison of experimental and calculated geminal and vicinal coupling constants

	1	2	3	4	5	6	7	
1	calcd.							
	exp.							
2	calcd.	12.1						
	exp.	12.2						
3	calcd.	1.2	8.5					
	exp.	1.4	8.2					
4	calcd.	12.6	1.4	14.8				
	exp.	12.2	1.4	14.4				
5	calcd.	0.3	0.2	2.0	6.1			
	exp.	-	-	-	5.6			
6	calcd.	0.2	0.4	6.0	13.7	14.3		
	exp.	-	-	5.8	12.7	14.0		
7	calcd.	0.0	0.0	0.2	0.3	1.1	12.5	
	exp.	-	-	-	-	1.2	12.6/12.2	
8	calcd.	0.0	0.2	0.5	0.4	7.7	1.3	13.8
	exp.	-	-	-	-	7.4	1.4	13.6

**References:**

1. T. Helgaker, M. Jaszuński, K. Ruud *Chem. Rev.* **1999**, *99*, 293. H. Fukui, T. Baba *Nucl. Magn. Reson.* **2002**, *31*, 122.
2. P. Tähtinen, A. Bagno, K. D. Klika, K. Pihlaja *J. Am. Chem. Soc.* **2003**, *123*, 4609.

NMR STUDY OF ULTRAFINE POLYTETRAFLUOROETHYLENE

Nikolaj Sergeev and Marcin Olszewski

*Institute of Physics, University of Szczecin, ul. Wielkopolska 15, 70-451 Szczecin, Poland,
e-mail: sergeev@wmf.univ.szczecin.pl*

Introduction:

Polytetrafluoroethylene (PTFE) – $(CF_2)_n$ –, obtained by thermal gas dynamic method [1], has a number of unique properties due to which it has found wide application in many areas (see [2] and references therein). The physical essence of this method is the preparation of an aerosol mixture of monomers and oligomers; in definite thermodynamic conditions, the mixture polymerizes into ultrafine powder (UPTFE) possessing improved adhesion to metal surfaces while retaining its protective and friction characteristics. In spite of broad practical application of UPTFE powder, the mechanism of its destruction, the microscopic and supramolecular structure, the internal mobility remain unknown. In the present work we report our interpretation of ^{19}F NMR data obtained in [2,3].

Experimental Results and Discussion

The experimental temperature dependence of the second moment of ^{19}F NMR spectrum and of the spin-lattice relaxation time (T_1) obtained in [2,3], are shown in Figs.1 and 2.

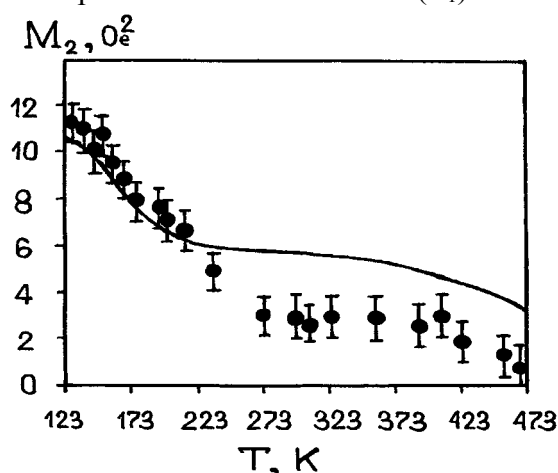


Fig. 1. Temperature dependence of the second moment M_2 (Oe^2) of ^{19}F NMR spectrum of UPTFE. (•) – experimental data and the solid line is the theoretical curve.

PTFE is a partially crystalline polymer, which has been extensively studied by different physical methods. The IR and NMR spectroscopic investigations of UPTFE demonstrated that thermal gas dynamic dispersing changes the structure of polytetrafluoroethylene macromolecules and leads to the formation of oligomers with terminal $-CF_3$ and $-C=CF_2$ groups [2]. From these investigations it follows also that the crystallinity and the formation of macromolecular packing possessing in UPTFE are higher compared to PTFE samples.

The temperature dependence of the second moment (Fig.1) clearly shows that in the temperature range 270-400K, it is observed one more plateau, which may be ascribed to reorientations of both individual CF_2 groups and macromolecules. The experimental value of the second moment on this plateau ($3 Oe^2$) is close to the theoretical value of $2.67 Oe^2$, obtained for the macromolecule reorienting along the longitudinal axis [2,3]. From

In the low-temperature region ($T < 140K$), the second moment of UPTFE is independent on temperature and close to the theoretical value ($M_2 = 9.89 Oe^2$ [2]). This fact indicates that the fluoride subsystem is rigid in this temperature range. At elevated temperatures (150-400K), the resonance signal is narrowed. The transformation is the result of the motion of fluorine atoms with a frequency higher than the width of the NMR spectral line.

In the low-temperature region ($T < 293K$), the shape of the experimental temperature dependence of T_1 is similar to \cup curve with minimal value equals to 425 ms. At $T > 295K$ the shape of the experimental temperature dependence of T_1 is similar to \cap curve with maximal value equals to 1 s.

comparison of the NMR spectra narrowing of PTFE and UPTFE it follows that the motions of fluorine atoms in UPTFE start at lower temperatures than in PTFE [2,3]. This agrees with the assumption concerning the low-molecular composition of UPTFE. Above 400K, the NMR spectrum of UPTFE is narrowed into a narrow line. This transformation of NMR spectrum in this temperature range is result of the diffusion of macromolecule or its segments with a frequency higher than the width of the NMR spectral line.

In order to interpret the experimental results, obtained in [2,3] we have used the theory developed in [4]. The calculated theoretical dependences of $M_2(T)$ and $T_1(T)$ are shown in Figs. 1 and 2. It is well known, that the specific of majority of polymer is its dynamic inhomogeneous. The dynamical inhomogeneous leads to the distribution of the activation energy and the correlation time of molecular motion. So we assumed that the dynamic processes are described by the normal distributions of the activation energies

$$p(E_{ai}) = \frac{1}{\sqrt{2\pi\sigma_{Ei}}} \exp\left\{-\frac{E_{ai} - \bar{E}_{ai}}{2\sigma_{Ei}^2}\right\}. \quad (1)$$

For the first dynamical process (the reorientations of molecular segments about the longitudinal axis of the macromolecule) we used the following parameters in Eq.(1):

$\sigma_{E_1} = 5,6$ kJ/mol and $\bar{E}_{a1} = 25$ kJ/mol. For the second dynamical process (the diffusion of the molecular segments) we used the following parameters in Eq.(1): $\sigma_{E_2} = 16.6$ kJ/mol and $\bar{E}_{a2} = 83$ kJ/mol.

From Figs.1 and 2 we see that developed in [4] theory describes rather well the observed temperature dependences of the second moment $M_2(T)$ and spin-lattice relaxation rate ($T_1^{-1}(T)$) of ^{19}F nuclei in UPTFE. This confirms also that the proposed model of two independent type of molecular motions (reorientation and diffusion) may be considered as a preferable model for molecular mobility of fluorine nuclei in UPTFE.

References:

1. A.K. Tsvetnikov and A.A. Uminskii, "Method for Processing Polytetrafluoroethylene," Russian Federation Patent No 1775419.
2. L.N. Ignatieva, A.K. Tsvetnikov, A.N. Livshits, V.I. Saldin, and V.M. Buznik. "Spectroscopic Study of Modified Polytetrafluoroethylene". Journal of Structural Chemistry, Vol. 43, No 1, pp. 64-68, 2002.
3. V.M. Buznik, A.K. Tsvetnikov, Yu.G. Kriger, A.R. Semenov, N.A. Sergeev. "NMR - Relaxation Study of Molecular Motions in Modified Polytetrafluoroethylene". Journal of Structural Chemistry, 2004 (in press).
4. P. Bilski, M. Olszewski, N.A. Sergeev and J. Wąsicki. "Calculation of dipolar correlation function in solids with internal mobility". Solid State Nuclear Magnetic Resonance, Vol.25, pp. 15-20, 2004.

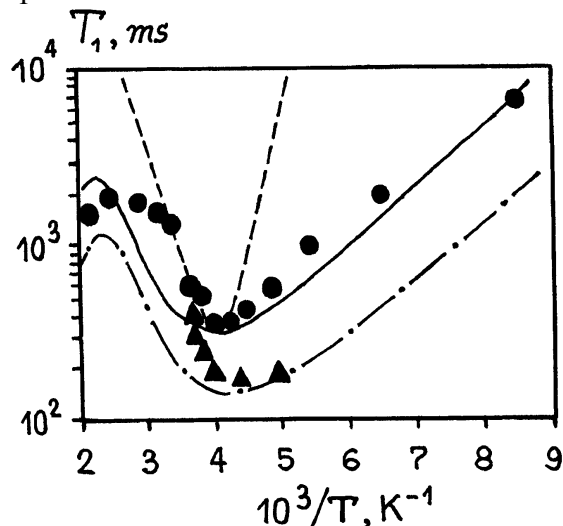
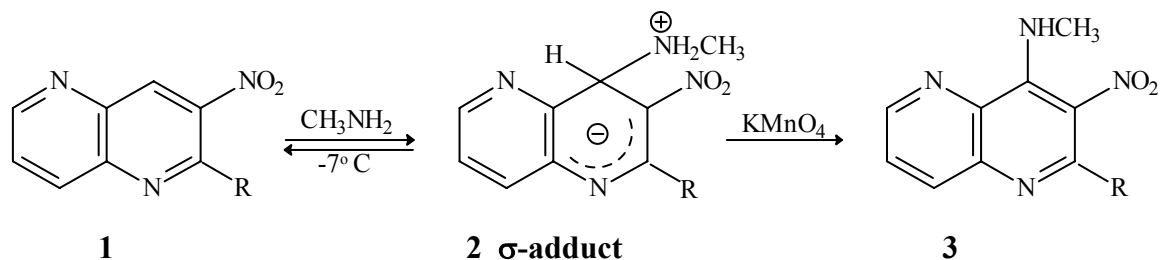


Fig. 2. Temperature dependence of the spin-lattice relaxation time T_1 of ^{19}F in UPTFE. (●) – experimental data and (—) - theoretical curve obtained for $\nu_0 = \omega_0 / 2\pi = 38$ MHz; (▲) – experimental data and (- · - · -) - theoretical curve obtained for $\nu_0 = \omega_0 / 2\pi = 15$ MHz; (---) – theoretical curve calculated using classical BPP theory. This curve was obtained with correlation time $\tau_c = (3,4 \pm 0,6) \cdot 10^{-14} \exp(28,8 \pm 0,4 \text{ kJ/mol/kT})$ s.

¹H NMR DETECTION OF σ -ADDUCTS IN S_NH REACTIONS OF 3-NITRO-1,5-NAPHTHYRIDINES WITH METHYLAMINE

Barbara Szpakiewicz, Maria Grzeżożek, and Elżbieta Cholewka

*Institute of Organic Chemistry and Technology, Cracow University of Technology,
PL 31155 Kraków, Poland*



R = D, H, Cl, OC₂H₅, NH₂, NHCH₃, OH

Some 2-R-3-nitro-1,5-naphthyridines **1** undergo dehydromethylation in the solution of potassium permanganate in liquid methylamine. The S_NH reaction proceeds via the intermediary methylamino σ -adducts **2** which are subsequently oxidized by KMnO₄ to the corresponding methylamino nitro compounds **3**. In all cases mentioned reactions the intermediary σ -adducts **2**, could be detected by ¹H NMR spectroscopy. Addition of methylamine to the sp² carbon atom of 3-nitro-1,5-naphthyridines induces the change of its hybridization from sp² to sp³ (tetrahedral centre of σ -adduct) which is reflected in a considerable upfield shift signal of the hydrogen atom attached to the C-4 carbon atom. This rehybridization sp² to sp³ is due to the 4-methylamino σ -adduct formation. The upfield shift, $\Delta\delta$, of the signals of the C-4 hydrogen atom at the tetrahedral centre of the methylamino σ -adducts lie between 3.38 - 3.87 ppm and are in the same range as those found for the amino σ -adducts of some 3-nitro-1,5-naphthyridines, $\Delta\delta$ 2.55 - 3.81 [1]. In the case of 3-nitro-1,5-naphthyridine, additional evidence that addition has taken place at C-4 and not at C-2 was provided by ¹H NMR spectrum of 2-deuterio-3-nitro-1,5-naphthyridine in liquid methylamine. The spectrum showed the signal of the C-4 hydrogen at 5.32 ppm and its upfield shift $\Delta\delta$ 3.84 ppm. These values are identical to the 4-H of 3-nitro-1,5-naphthyridine.

¹H NMR spectroscopy is a very good method to detection of intermediary covalent σ -adducts, like **2** and the determination of their structures plays an important role in the interpretation of the mechanism of S_NH reaction.

Reference:

[1]. M. Woźniak, H.C. van der Plas, M. Tomula and A. Van Veldhuizen, Recl. Trav. Chim. Pays-Bas, **102**, 511 (1983).

MR AND CT IMAGING IN DETERMINATION OF TOOTH CARIES DECAY

Marta M. Tanasiewicz¹, Władysław P. Węglarz², Tomasz W. Kupka¹,
Cezary Przeorek³, and Andrzej Jasiński²

¹ Department of Preclinical Dentistry, Medical University of Silesia, Zabrze

² Department of Magnetic Resonance, H. Niewodniczański Institute of Nuclear Physics Polish Academy of Sciences, Kraków, Poland

³ Comprehensive Cancer Centre, Maria Skłodowska-Curie Memorial Institute, Branch Gliwice

X-ray based visualisation techniques were for many years the only way to assess structure and state of the human teeth. MRI has been used in the research of the healthy and decayed teeth during last decade [1-7]. Several papers were presented showing usefulness of spin echo and gradient echo imaging, Single Point Imaging, SPRITE and STRAFI techniques for visualization of the dental surface geometry as well as for distinction between soft tissue (pulp) and mineralized tissue (enamel, dentine and root cement) in the extracted teeth. Recently, MRI was used for estimation of the facial bone structure, in preparation to implantation, localisation of the tumor in the facial bone tissue, and in detection of the osteoporosis.

The aim of this work was to investigate potential of MRI for detection and estimation of the caries, and compare it with CT, on the level of laboratory pre-clinical tests. This work was done within the project to develop original, MRI based diagnostic technique for dentistry needs.

MRI and CT experiments were performed on the same decayed extracted human tooth (impossible conservative therapy), obtained at Dept. of Dental Surgery MUS. After extraction tooth was stored in saline. MRI measurements were done in MR Tomography Lab INP. Prior to the experiment, tooth was degassed to minimize magnetic susceptibility artifacts. A 3D spin echo pulse sequence on the 4.7 T research MRI system, equipped with Maran DRX console, and dedicated home-built probehead, was used to obtain three dimensional (256x128x128) images of the teeth. Corresponding resolution was 60x120x160 μm^3 . High intensity signal from water penetrated into the porous decayed regions of tooth, contrasted with lack of signal from mineralized tooth tissue, allow for visualisation of the presence and extent of caries. CT measurements were done as OrbiSinus Topogram 1.0 T20s, with in plane resolution 512x512 (FOV 165x165 mm) for 281/0.1mm slices.

Presented results show possibility of both CT and MR imaging of the caries in teeth. The challenges in transferring MR technique into *in vivo* conditions in present stage are: slow data collection and lack of dedicated hardware.

Acknowledgments: Supported by Grant no: 2 P05C 054 26 from Ministry of Science and Informatisation of Poland.

References:

- [1] Lloyd C.H., *et. al.* Quintessence Int. **28**, 349-355 (1997).
- [2] M. Tanasiewicz, W.P. Węglarz, T. Kupka, Z. Sułek, M. Gibas, A. Jasiński, *Stomatologia Współczesna*, V, 2002.
- [3] W.P. Węglarz, T. Kupka, M. Tanasiewicz, T. Banasik, Z. Sułek, M. Gibas, A. Jasiński, *Valetudinaria, Postępy Medycyny Klinicznej i Wojskowej*. IV Zjazd Polskiego Medycznego Towarzystwa Rezonansu Magnetycznego, Bydgoszcz 2002.

- [4] M. Tanasiewicz, W.P. Węglarz, T. Kupka, Z. Sułek, M. Gibas, A. Jasiński, XXXV Ogólnopolskie Seminarium na Temat Magnetycznego Rezonansu Jądrowego i Jego Zastosowań, Kraków 2002.
- [5] M. Tanasiewicz, *Magazyn Stomatologiczny*, 2003, XIII, 3, 64-68.
- [6] M. Tanasiewicz, T.W. Kupka, W.P. Węglarz, A. Jasiński, M. Gibas, *Journal of Dental Research* 2003, vol. 82, special issue B, 3047.
- [7] W.P. Węglarz, M. Tanasiewicz, T. Kupka, T. Skórka, Z. Sułek, A. Jasiński, *Solid State NMR*, **25**, 84-87 (2004).

THEORETICAL CALCULATIONS OF ^{15}N NMR CHEMICAL SHIFTS OF 6-BENZYLAMINOPURINE DERIVATIVES

Jaromír Toušek^a, and Radek Marek^b

^a *Department of Theoretical and Physical Chemistry, Faculty of Science, Masaryk University, Kotlářská 2, CZ-611 37 Brno, Czech Republic*

^b *National Center for Biomolecular Research, Faculty of Science, Masaryk University, Kotlářská 2, CZ-611 37 Brno, Czech Republic*

Biogenetic purine bases play central roles in most biological processes¹. The proper characterization of the tautomeric equilibria of the variously substituted purine derivatives under diverse conditions is of great importance and significance. The tautomeric equilibria can be described using NMR spectroscopy and quantum chemical calculations of chemical shielding constants. Due to the formation of hydrogen bonds of purine molecule with the molecule of the solvent (in solution) or with other purine molecules (in solid phase) calculations can not be reliably performed with the isolated molecule and intermolecular interactions must be included². The aim of this work is to calculate ^{15}N chemical shifts of 6-(2-chlorobenzylamino)purine and to determine the influence of the intermolecular interactions on the values of chemical shifts. Calculated chemical shifts for liquid and solid phase were compared with the experimental values. The values of ^{15}N NMR chemical shifts calculated for isolated molecule differ significantly from the experimental values (rmsd(s) = 10.74 ppm for solid phase and rmsd(l) = 5.23 ppm for liquid). The agreement of the experimental and calculated values improve, when the intermolecular effects are included (rmsd(s) = 3.89 ppm and rmsd(l) = 4.53 ppm). The improvement is especially significant for the solid phase.

The geometries of the molecules were optimized using RHF/6-31G** method, chemical shifts were calculated using B3LYP/6-31G** method. Calculations were performed with Gaussian 98 software.

This project was supported by MSMT grant (LN00A016).

References:

1. Mok D. W. S., Mok M. (eds) in: *Cytokinins: Chemistry, Activity and Functions*, CRC Press: Boca Raton, FL, 1994.
2. Facelli J. C., Pugmire R. J., Grant D. M.: *J. Am. Chem. Soc.* *118*, 5488 (1996).

^1H MAS AND ^{13}C CP/MAS NMR STUDIES OF URINARY STONES

Monika Uniczko¹, Zdzisław Durski², and Waclaw Kolodziejcki¹

¹*Department of Inorganic and Analytical Chemistry, Medical University of Warsaw,
ul. Banacha 1, 02-097 Warsaw, Poland*

²*Department of Inorganic Chemistry, Warsaw University of Technology,
ul. Noakowskiego 3, 00-664 Warsaw, Poland*

Urinary stones usually contain various components: uric acid, calcium oxalate, struvite, brushite, hydroxyapatite and carbonate apatite. The main purpose of this research is to develop a procedure of qualitative and quantitative analysis of urinary stones by means of high resolution-solid state NMR. The first step in the project is to measure spectra of most abundant components, so adequate „one-component” urinary stones have been selected on the basis of powder X-ray diffractograms from a large collection of various urinary stones. In the poster, we present their proton and carbon-13 spectra recorded under magic-angle spinning (MAS), with 30 and 7.5 kHz spinning rates, respectively. For carbon-13, cross-polarization (CP) from protons was used. The spectra are interpreted and discussed in relation to the literature results. We conclude that it is possible to identify various components of complex urinary stones by high-resolution solid-state NMR.

APPLICATION OF FMRI IN ESTIMATION OF THE NEURAL PROCESSING OF THE AFFECTIVE VISUAL STIMULI

Andrzej Urbanik, Michał Kuniecki¹, Liliana Podsiadlo, Barbara Sobiecka, and Justyna Kozub

Department of Radiology, Collegium Medicum, Jagellonian University, Kraków, Poland

¹Department of Psychophysiology, Jagellonian University, Kraków, Poland

Purpose:

The central mechanisms underlying emotional appraisal of incoming stimuli has been extensively studied both in animal and human subjects. Despite the fact that understanding of this issue is increasing, some specific questions remain to be answered. In the following study, using fMRI technique, we examined how the brain processes emotionally loaded (positively and negatively) visual information.

Materials and Methods:

Sixteen male volunteers were examined in the Signa 1.5T MR system (BOLD). Each experimental session consisted of five activation periods, three of which constituted baseline and two experimental conditions. In experimental condition subjects were shown slides selected on the basis of high score on Arousal and Valence scale from standardized IAPS picture set, while in the baseline condition custom prepared color checkerboards were presented. There were two runs, in the first run subjects saw only negatively valenced pictures, during the second run only positive pictures were shown.

Results:

For the positive stimuli we detected significant activation in the bilateral occipito-temporal cortex, as well as left anterior insular cortex. For the negative stimuli, in addition to the previous structures, we also observed activation of the right amygdala.

Conclusion:

Activation of bilateral occipito-temporal cortex proves enhancement of visual processing of negative slides as compared to neutral checkerboards. This might be attributed to top-down processes. Such hypothesis is further supported by apparent activation of amygdala which maintain connections with visual cortex. Amygdala is a structure commonly described as being involved in processing of negative stimuli. Activation of insular cortex is probably related to autonomic arousal accompanying watching emotional content.

ESTIMATION OF SPEECH REGIONS IN BILINGUAL SUBJECTS IN FMRI

Andrzej Urbanik, Marek Binder¹, Barbara Sobiecka, Justyna Kozub, and Amira Bryll

Department of Radiology, Collegium Medicum of Jagellonian University, Kraków, Poland

¹Department of Psychophysiology, Jagellonian University, Kraków, Poland

Purpose:

The aim of this study was to identify the functional anatomy of the cerebral speech regions involved in speaking in native and foreign language in the same subject.

Material and methods:

Twelve neurologically healthy, right-handed volunteers (12 women and eight men) were examined in the Signa Horizon 1.5 T MR system (GEMS), using BOLD technique. Experimental design consisted of two activation runs. Each of them included two kinds of tasks arranged in series of five blocks lasting for 30s. In the experimental condition of the first run subjects were required to speak in their native language and in the second run the task was to speak in the foreign language. In both runs baseline condition was the same and subjects were supposed to lie silently in the bore.

Results:

All subjects showed greater activation in the left hemisphere areas when speaking in native language. The most active region was Broca's area (BA44). The other active areas were auditory cortex (with more significant activation shown in the left hemisphere) and frontal areas bilaterally. When subjects spoke in foreign languages, the pattern of activity was more distributed and varied individually. Active areas covered the right homologue of the Broca's area, left parietal cortex, and frontal cortices bilaterally.

Conclusions:

Obtained results show that activity of the brain regions correlated with speaking in the foreign and in the native language appears to be differently localized. Activation of Broca's area when speaking in native language is probably genetically determined. Distributed pattern of activity in the foreign language condition reflects individual strategies in acquiring and speaking in foreign language.

FMRI IN ESTIMATION OF INFLUENCE OF DIFFICULTY OF A COGNITIVE TASK ON THE PATTERNS OF BRAIN ACTIVITY

Andrzej Urbanik, Marek Binder¹, Justyna Kozub, and Barbara Sobiecka

Department of Radiology, Collegium Medicum, Jagellonian University, Kraków, Poland

¹Department of Psychophysiology, Jagellonian University, Kraków, Poland

Purpose:

The aim of the study was to examine the effects of the difficulty of the cognitive task on the changes of the patterns of the brain activity. We also determined whether the higher level of difficulty affects in the same way task based on verbal and nonverbal material.

Materials and methods:

Twelve volunteers were examined in the Signa Horizon 1.5T MR (BOLD). Experimental design consisted of four activation runs.

During the first and the second run subjects were required to remember the changing sequences of letters. In the third and the fourth run subjects were asked to remember changing sequences of abstract pictures. Statistical analyses were carried out using SPM99 software.

Results:

The most significant increase associated with difficulty was observed in the dorsolateral prefrontal areas, (verbal and nonverbal tasks). Furthermore, there were separate activation sites for the nonverbal (parietal cortex) and verbal tasks (precentral gyrus, left parietal cortex), not sensitive to the task difficulty.

Conclusions:

Areas responsible for aspects of cognitive function were differently activated by the level of cognitive demand. Regions responsible for manipulation showed increase of activity, which was dependent of the level of difficulty. This was not observed for the areas whose activity was dependent of the type of the task.

NEURAL CORRELATES OF WORKING MEMORY ACTIVITY DURING PERFORMANCE OF VERBAL AND NONVERBAL TASKS

Andrzej Urbanik, Marek Binder¹, Justyna Kozub, and Barbara Sobiecka

Department of Radiology, Collegium Medicum, Jagellonian University

¹*Department of Psychophysiology, Jagellonian University*

Purpose:

Working memory is considered to be a cognitive system responsible for the temporary storage and manipulation of different kinds of information. The aim of the study was the attempt to answer the question whether there are specialized brain structures that support working memory functions associated with performance of verbal and non-verbal tasks.

Materials and methods:

Twelve neurologically healthy, right-handed volunteers were examined in the Signa 1.5T MR system (Signa Horizon, GEMS) using BOLD technique. Experimental design consisted of two activation runs. Each of them included different task. During the first run subjects were required to remember the changing sequences of letters, and during the second run they were asked to remember changing sequences of abstract pictures. Statistical analyses were carried out using SPM99 software.

Results:

For both verbal and nonverbal task, localization of the several active areas partially overlapped, and the common activated areas were situated in the prefrontal cortex: dorsal-lateral prefrontal cortex bilaterally, ventral-lateral prefrontal cortex in the left hemisphere and the anterior cingulate gyrus.

Furthermore, there were separate activation sites for the nonverbal and verbal tasks, which were observed in the left parietal cortex for the verbal task and the frontal cortex for the nonverbal task.

Conclusion:

In our study we observed separate areas responsible for different aspects of working memory performance, namely, manipulation (update and monitoring) and storage of information. Regions responsible for manipulation were independent of the task, and localization of regions responsible for storage was associated with the type of stimulus (verbal or nonverbal).

THE ASSESSMENT OF DEMENTIA CHANGES WITH HMRS METHOD

Andrzej Urbanik, Jerzy Walecki¹, Andrzej Jasiński², Justyna Kozub, Barbara Sobiecka, Maria Orłowiejska³, Rafał Motyl³, and Andrzej Szczudlik³

Department of Radiology, Collegium Medicum, Jagellonian University, Kraków, Poland

¹Department of Imaging Diagnostic, Hospital MSWiA, Warszawa, Poland

²Institute of Nuclear Physics, Kraków, Poland

³Department of Neurology, Collegium Medicum, Jagellonian University, Kraków, Poland

Objective:

The assessment of dementia changes with HMRS method (MR proton spectroscopy).

Material and Method:

With the MR Signa Horizon 1.5 T (GEMS) system MRI and HMRS research have been performed for 108 people with clinical dementia diagnosis; Alzheimer type (47), ischemic vascular (49) and mixed (15). As control groups (physiological ageing) the healthy people were examined; 32 young people (17-31) and 44 old ones (57-85). The analysis of relative concentration ratio of NAA/Cr, Cho/Cr, ml/Cr and NAA/ml in four selected brain areas was performed, depending on age, sex and clinical condition.

Results:

In Alzheimer dementia the statistically essential increase of ml/Cr and decrease of NAA/ml and NAA/Cr. It was proved that the quantity and quality analysis of spectra might facilitate the process of Alzheimer type dementia differentiation. The statistically essential decrease of NAA/Cr proved to be a physiological ageing determinant of the brain, mainly in the crown-occiput area.

Conclusions:

HMRS makes it possible to assess the brain physiological ageing process as well as Alzheimer type dementia.

APPLICATION OF ^{13}C -NMR TO THE STUDY OF POLYOFIN PYROLIS PRODUCTS

Grzegorz Urbanowicz¹, Jerzy Ossowski¹, and Marek Matlengiewicz^{1,2}

¹ *Department of Environmental Chemistry and Technology, Silesian University,
ul. Szkolna 9, 40-006 KATOWICE, Poland*

² *Institute of Coal Chemistry, Polish Academy of Sciences, ul. Sowińskiego 5,
44-121 GLIWICE, Poland*

Noncatalytic pyrolysis of polyolefins yields a complex mixture of liquid hydrocarbons. The crude mixture obtained from such a pyrolysis of commercial polypropylene at 300°C in pressureless steel reactor was separated by distillation into 30 narrow fractions with boiling points from 56 to 300°C. The fractions were analyzed by means of. The 100 MHz ^{13}C NMR spectra of individual fractions are well separated into the lines of individual hydrocarbons hence the analysis of individual components of the mixtures can be performed using our own spectra library of pure hydrocarbons, even though the spectrum for each fraction can contain up to about 200 lines. The attribution based on the chemical shifts of the individual hydrocarbons was subsequently verified with the literature data of their boiling points. The results obtained indicate that despite separation of the initial mixture into very narrow distillation fraction the composition of subsequent fractions is very close to each other. The neighboring fractions have similar composition which changes gradually with the increase of the distillation temperature. The lower fractions are composed mainly of short-chain linear hydrocarbons. Starting from the fraction boiling at 68 till 195°C cyclic hydrocarbons can be observed. Above 150°C more and more branched chains are present and only small quantities of aromatic hydrocarbons can be determined. In the fractions collected above 220°C dominate the compounds having long linear chains with some branches but with complete lack of cyclic and aromatic structures. It can be seen from this study that ^{13}C NMR spectroscopy can be positively applied to the analysis of individual compounds even in the case of very complex hydrocarbon mixtures derived from pyrolysis of olefins.

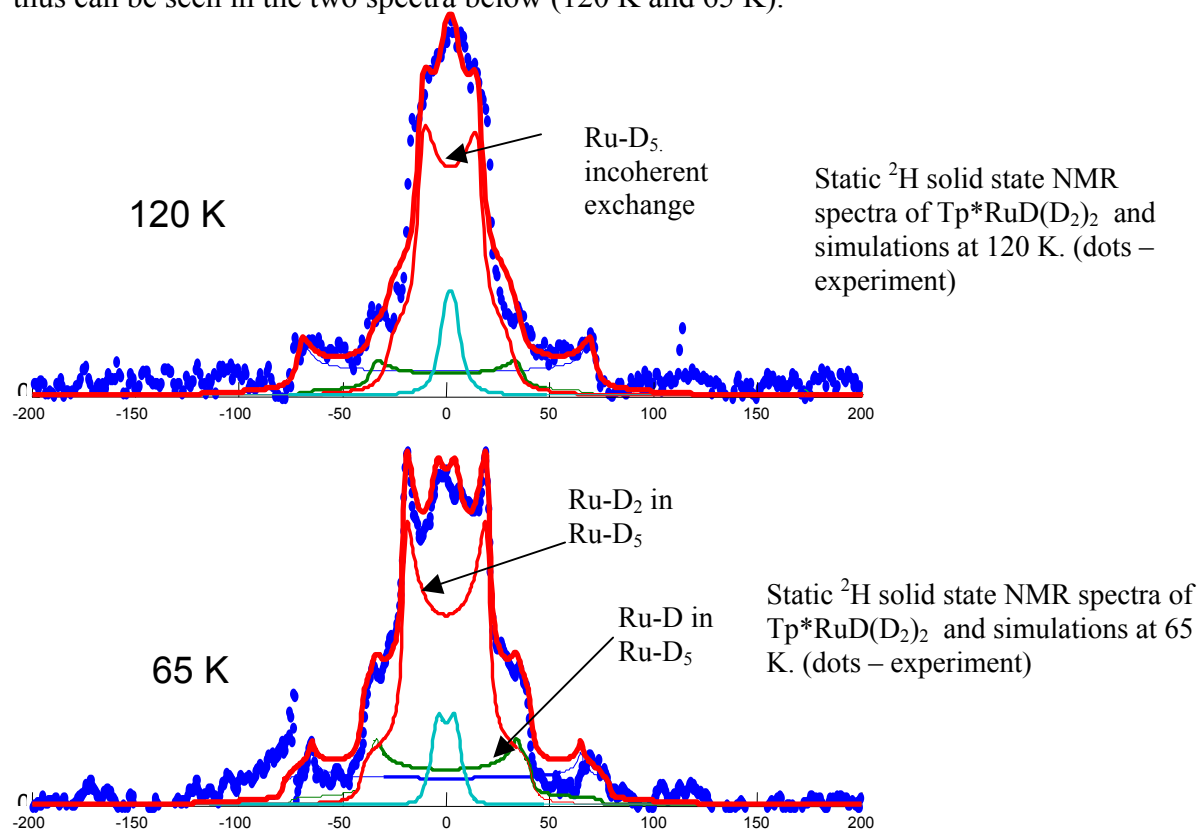
DEUTERIUM ON Ru NANOPARTICLES AND IN THE MODEL COMPLEXES: STUDIES OF BINDING AND MOBILITY BY NMR

Bernadeta Walaszek[§], Tal Pery[§], Karine Philippot[⊥], Bruno Chaudret[⊥], Hans-Heinrich Limbach[§], and Gerd Buntkowsky[§]

[§] *Institut für Physikalische und Theoretische Chemie, Freie Universität Berlin, Takustr.3, D-14195 Berlin, Germany*

[⊥] *Laboratoire de Chimie de Coordination du CNRS, 205, Route de Narbonne, 31077 Toulouse Cedex 04, France*

Ruthenium Nanoparticles have a very large surface area and therefore they are very active for numerous catalytic processes. D₂ adsorbed on the surface of Nanoparticles or adsorbed in model complexes are of great importance in studying catalysis. The investigation of mobility of these molecules on the surface of Ruthenium Nanoparticles and model complexes like Tp**Ru*D(D₂)₂ is presented in this work. These studies have been performed with solid state NMR techniques. D₂ solid state NMR is a very good tool to investigate deuterium exchange, because the anisotropy of the quadrupole interaction typically found for these nuclei, gives us a lot of information about any nuclear motions inside the sample. By line shape analysis one can determine the quadrupole coupling constants, which can be used in solid state NMR as chemical shifts in liquid state NMR are used. In the model complexes the values of quadrupole coupling constants are equal for Ru-D 70 kHz, Ru-D₅ 34 kHz, Ru-D₂ 42 kHz and C-D 120 kHz. In these complexes we have frozen out the incoherent exchange thus can be seen in the two spectra below (120 K and 65 K).



DIAGNOSTIC IMPORTANCE OF MAGNETIZATION TRANSFER IN MRI MULTIPLE SCLEROSIS MONITORING

Wicher Magdalena¹, Kluczevska Aneta¹, Konopka Marek², Kieltyka Aleksandra²,
Drzazga Zofia¹, Pilch-Kowalczyk Marek², Hartel Marcin², and Filippi Massimo³

¹*Institute of Physics, Department of Medical Physics, Silesian University, Katowice, Poland*

²*Silesian Diagnostic Imaging Center "HELIMED", Katowice, Poland*

³*Department of Neurology, Scientific Institute Ospedale San Raffaele, University of Milan, Milan, Italy*

Multiple Sclerosis (MS) is a chronic disease of the central nervous system, predominantly affecting young adults in their most productive years. SM plaques are the most important diagnostic landmarks of this disease. The plaques can be divided to active ("fresh plaques") and inactive ("old plaques"), which can be distinguished by contrast enhancement.

Magnetization transfer (MT) can provide additional information leading to earlier detection of these abnormalities than conventional MRI. The first application of the MT technique *in vivo* was performed by Wolff and Balaban [1]. In the last decade MTI has been intensely developed in clinical radiology [2, 3, 4], particularly in neuroradiology.

Water in biological tissues can be separated in two pools, water in relatively free state (Hf) and restricted motion state or bound state (Hr). Off-resonance RF pulse causes saturation of the energy level of bound water protons thus differentiating them from free water protons. Magnetization Transfer Imaging (MTI) allows simultaneous evaluation of differences in exchange and relaxation behavior over a relatively large region of interest. Due to the interactions between the macromolecules and water proton pool, a reduction of the magnetization of water proton is observed.

When a MT saturation pulse is combined with an imaging sequence, the diminished magnetization of the free water proton pool reduces signal intensity of the imaged tissue.

MT can be quantified by calculation of the magnetization transfer ratio (MTR) according to following formula:

$$MTR = \frac{M_0 - M_s}{M_0} * 100\%$$

where: M_s – intensity of a region of interest (ROI) with MT impulse,

M_0 – intensity of the same region of interest (ROI) without MT impulse.

This paper presents application of magnetization transfer (MT) histograms studies of brain tissue multiple sclerosis.

The investigations were performed in 18 patients with clinically defined MS and in 6 volunteers with normal appearing brain tissue.

MR images were obtained using 1,5 T scanner (GE Medical Systems Signa Echo Speed) in axial planes. All examinations consisted of SE T1-weighted images before and SE T1, T2, PD-weighted ones after contrast medium administration, also of GRE T2-weighted images with and without MT impulse (1,2kHz frequency).

The set of the 20 slices for each patient was analyzed using *DispImage v. 4.9*, *VTK CISC Registration Toolkit* and *MTC v. 1.0* software.

The results were elaborated in nonparametric ANOVA Friedman's, Wald-Wolfitz's, U-Manna-Whitney's tests with $p < 0.05$.

The average MTR histograms derived from MS patient population and control subject are presented at *Figure 1*:

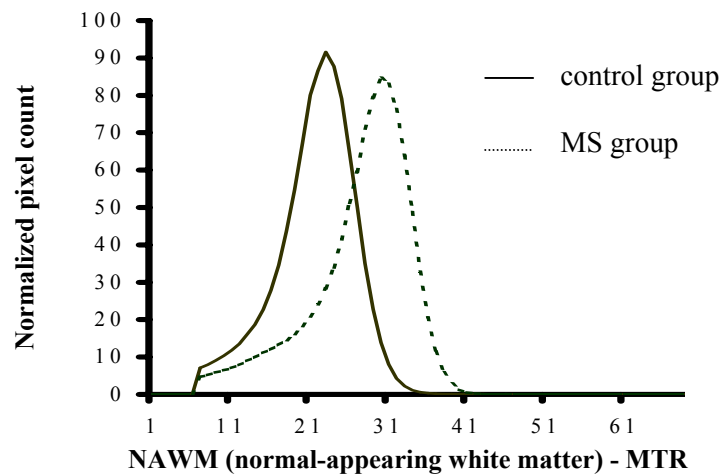


Figure 1. Normal-appearing brain tissue magnetization transfer ratio (MTR) histograms from MS and control population.

It should be noted that patients with MS had lower histogram peak height than for control subject. MTR histograms are correlated with clinical manifestations. Group of MS patients was not homogenous in activity of plaques (7 patients and 11 patients with active and inactive form MS, respectively).

The statistical analysis showed:

- 1) MR with application of magnetization transfer is a quantitative method able to discover demyelination process, yet not seen in conventional MRI,
- 2) there is statistically significant difference in MTR between control group and MS group,
- 3) no statistically significant difference in MTR between active and inactive demyelination plaques has been found,
- 4) MTR value is not related to diameter of the MS plaques.

MR with magnetization transfer provides valuable information on SM process and thus can become useful method in monitoring white matter abnormalities.

References:

- [1] R.S. Balaban, S.D. Wolff, *Magnetic Resonance in Medicine*, 10 (1989) 135
- [2] J.C. McGovan, M. Filippi, A. Campi, R. Grossman, *Journal of Neurology and Psychiatry*, 64 (1998) 66
- [3] M.A. van Buchem, *Journal of Computer Assisted Tomography*, 23 (1999) 9
- [4] M. Filippi, *Neurology*, 54 (2000) 186

¹³C CP MAS STUDIES OF BAICALEIN AND ITS DERIVATIVES

Michał Wolniak¹, Jan Oszmiański², Sebastian Olejniczak³, and Iwona Wawer¹

¹Department of Physical Chemistry, Faculty of Pharmacy, Medical University of Warsaw, Banacha 1, 02-097 Warsaw, Poland

²Department of Fruit and Vegetable Processing, Agricultural University, Norwida 25, 50-375 Wrocław, Poland.

³Polish Academy of Sciences, Center of Molecular and Macromolecular Studies, 90-363 Łódź, Sienkiewicza 112, Poland

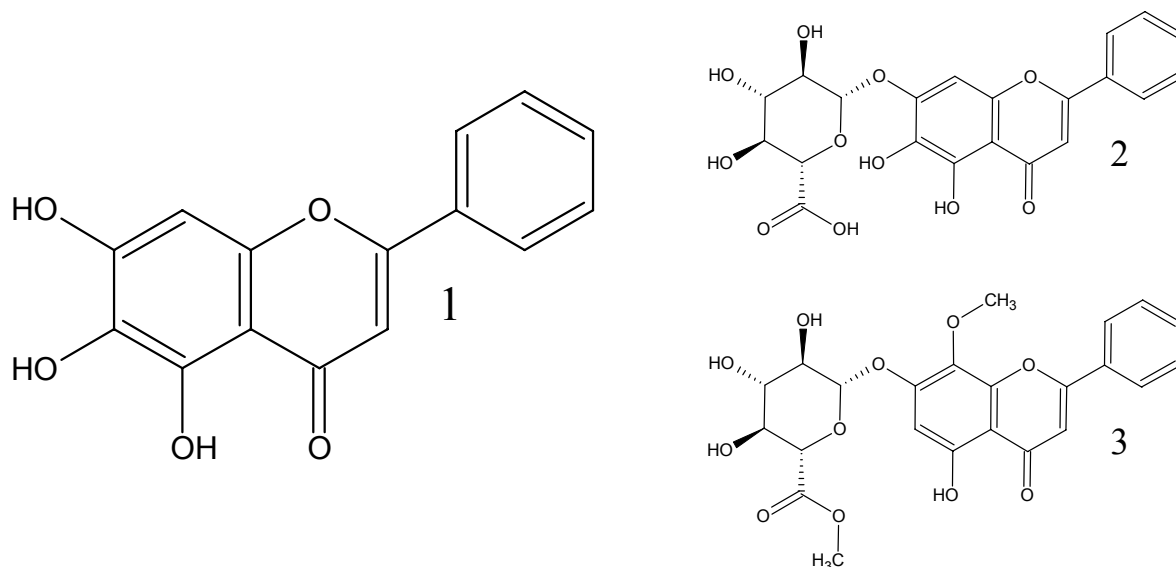
Flavonoids are widely distributed in the plant kingdom, and recently became appreciated as important constituents of human diet [1]. One of the interesting representative is baicalin, mainly because of its strong antioxidative properties and high accumulation (20%) in the roots of chinese medicinal plant *Scutellaria baicalensis* Georgi [2]. Apart from the health promoting effects, some flavonoids were found to be toxic and cancerogenic [3]. It seemed interesting to examine molecular structure of flavonoids of *Scutellaria* in the solid state and to get information on their bio-active conformations.

The studied compounds: baicalein, baicalin, wogonoside were isolated from the roots of *Scutellaria baicalensis* Georgi.

NMR spectrometers: cross-polarization (CP) magic-angle spinning (MAS) solid-state ¹³C NMR spectra were recorded on a Bruker AVANCE DSX-400 instrument at 100.61 MHz. The samples were spun at 8-10 kHz in 4mm ZrO₂ rotor. ¹H and ¹³C NMR spectra for the samples in methanol were recorded on a Bruker Avance 500 MHz spectrometer equipped with an inverse detection probe. The experiments were run using standard Bruker software. Chemical shift anisotropy was measured using PASS-2D method [4,5] with the sample spinning at 1500Hz.

The computers & programs: the calculations were run on Cray SV1ex-1-32 supercomputer at ICM UW, Warsaw using Gaussian 98 package.

The structure of baicalein and its derivatives:



1.baicalein; 2.baicalin; 3.wogonoside.

^{13}C NMR spectra of **1-3** were recorded for solution and solid state. Some signals in the ^{13}C CPMAS spectra were identified using dipolar dephasing and short contact time sequences. However, the correct assignment of all resonances cannot be done by direct comparison of solution and solid state data. The 1D and 2D NMR spectra (COSY, HETCOR, HMBC) were analyzed in order to obtain complete assignment of ^1H and ^{13}C chemical shifts. In some experiments the pulse field gradient (PFG) system was used in order to reduce the time of measurement and to improve the quality of NMR spectra. The analysis of the ^{13}C δ_{iso} and the anisotropic values for the chemical shift tensors δ_{ii} supplied information on the molecular structure. Additionally, NMR shielding constants were calculated using GIAO DFT method, and the theoretical shielding parameters σ_{iso} and σ_{ii} were compared with experimental results.

References:

1. Havsteen, B.H. The biochemistry and medical significance of the flavonoids. *Pharmacol. Therapeut.* **96**: 67-202; 2002.
2. Lu, H.; Jiang, Y.; Chen, F. Application of high-speed counter-current chromatography to the preparative separation and purification of baicalin from the Chinese medicinal plant *Scutellaria baicalensis*. *J. Chromatogr. A.* **1017**: 117-123; 2003.
3. Metodiewa, D.; Jaiswal, A.K.; Cenas, N.; Dickancaite, E.; Segura-Aguilar, J. Quercetin may act as a cytotoxic prooxidant after its metabolic activation to semiquinone and quinoidal product. *Free Radic. Biol. Med.* **26**: 107-116; 1999.
4. Olejniczak, S.; Potrzebowski, J. Solid state studies and density functional theory (DFT) calculations of conformers of quercetin. *Org. Biomol. Chem.* **2**: 001-008; 2004.
5. Olejniczak, S.; Ganicz, K.; Tomczykowa, M.; Gudej, J.; Potrzebowski, J. Structural studies of 2-(3',4'-dihydroxyphenyl)-7- β -D-glucopyranos-1-O-yl-8-hydroxychroman-4-one in the liquid and solid states by means of 2D NMR spectroscopy and DFT calculations. *J. Chem. Soc., Perkin Transactions 2* **6**: 1059-1065; 2002.

ORDERING EFFECTS IN COMPUTER-SIMULATED BLOCK COPOLYMER MELTS

Sebastian Wołoszczuk, Michał Banaszak, and Stefan Jurga

Monte Carlo simulations, using the Cooperative Motion Algorithm, have been performed to investigate the behavior of symmetric diblock [3,4] and the corresponding A-B-A triblock [1,2,4] copolymer melts. In one of our recent works [1] we showed that at low temperature regimes (below T_{ODT}) slow cooling process gives the results which conflicts with the experimental data and with the theory. Such a thermal treatment leads to lamellar spacing and orientation trapping as the temperature decreases. We decided to use an alternative method – quenching – where the system is instantaneously cooled down to the required temperature from the athermal state. The results obtained from the quenched simulation are in agreement with the theory and experimental investigations. Moreover, we noticed an extra low temperature effects which were not observed in slow cooling scheme, such as an extra peak in specific heat, abrupt decrease of the energy and also corresponding increase of the chain mean squared end-to-end distance and of the periodicity. All these effects were associated with an interfacial ordering from a strongly segregated but still a little diffused lamellar phase to a more strongly segregated phase with a smooth and sharp interface. We described that ordering quantitatively.

Besides the results from the simulation of the triblocks we also present the results obtained for the symmetric diblock copolymer melts (degree of polymerization $N=16$). Such as in the case of A-B-A triblocks, we performed quenches instead of slow cooling method and the low-temperature effects, observed earlier for the triblocks, are also present. We used a set of four different lattice sizes in order to explore the corresponding size effects. The low temperature interfacial ordering is described quantitatively as it was done for the triblocks [1]. All mentioned effects are present independently of size of the simulation box. The lattice size affects the temperature where these effects appear, but only as a small shifts close to definite value. In the case of triblocks (degree of polymerization $N=30$) we reported that temperature as $T^*/N=0.08$. Here we obtained $T^*/N=0.15$ and it stays in agreement with the value for the corresponding triblocks. We found, what is not surprising because of fitting between the simulation box and the lamellar periodicity, that the lattice size affects the way the system reaches the low temperature state.

Summarizing all our work we can say that the low temperature effects are present both for the diblocks and the triblocks independently of the simulation box size. We have to point that there is still a necessity to perform a non-lattice molecular dynamics simulation to arbitrate how the lattice environment influences an observed low temperature behaviour.

References:

- [1] M. Banaszak, S. Wołoszczuk, S. Jurga, T. Pakuła, J. Chem. Phys., 119(21), 11451-11457 (2003)
- [2] M. Banaszak, S. Wołoszczuk, T. Pakuła, S. Jurga, Phys. Rev. E, 66, 031804 (2002)
- [3] S. Wołoszczuk, M. Banaszak, S. Jurga, T. Pakuła, M. Radosz, J. Chem. Phys., (in press 2004)
- [4] S. Wołoszczuk, M. Banaszak, S. Jurga, M. Radosz, Computational Methods in Science and Technology, (submitted 2004)
- [5] T. Pakula, K. Karatasos, S. H. Anastasiadis, and G. Fytas, Macromolecules, 26, 8463 (1997)
- [6] L. Leibler, Macromolecules, 13, 1602 (1980).

³¹P NMR STUDIES OF HIV-INFECTED HUMAN CELLS

Krzysztof Wroblewski¹, Tomasz Rozmyslowicz², and Glen N. Gaulton²

¹*Department of Radiology, University of Pennsylvania School of Medicine, Philadelphia, PA 19104, USA*

²*Department of Pathology and Laboratory Medicine, University of Pennsylvania School of Medicine, Philadelphia, PA 19104, USA*

Perchloric acid extraction, when performed under strict conditions of temperature and pH, is claimed to be a reliable method of providing cytosolic composition without quantitative or qualitative changes. This method is widely employed to follow functional changes in heart and kidney cells during disease states such as myocarditis and nephropathy, and may be used for monitoring bone marrow abnormalities where NMR-registered changes in cell metabolite production were proposed to serve as prognostic variables in disease progression. Using PCA extracts instead of live cells also saves us from manipulating HIV-infected cells outside of specially designated areas.

Thymocytes were isolated from fresh neonatal thymic tissue obtained from routine thoracic surgeries. SupT1 and CEM cells (uninfected and chronically infected) were obtained from Dr. James Hoxie, CFAR, University of Pennsylvania; U87/CD4+ and MAGI/CD4+ cell lines were obtained from Dr. Francisco Gonzales Sacrano, Department of Neurology, University of Pennsylvania. Cells were infected with 89.6 or IIIB viral stocks. To confirm infection and viral replication, p24 ELISA was performed. The cell pellet was placed on ice and extracted with ice-cold PCA solution. Subsequently KHCO₃-neutralized solution was centrifuged and lyophilized. The lyophilizate was dissolved in 2ml of D₂O, the pH was adjusted with HCl, and standard 1D phosphorus spectra were acquired.

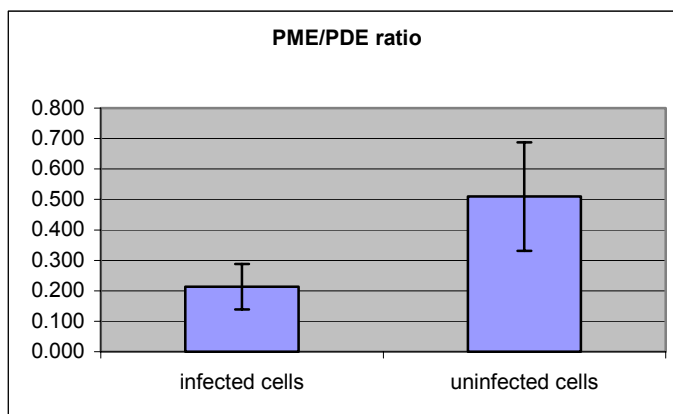


Figure 1. PME/PDE ratio measured in PCA extracts obtained from HIV infected and uninfected cells.

All spectra were obtained and processed on a Bruker AMX-500 NMR spectrometer using standard Bruker equipment. Obtained FID was Fourier-transformed after Gaussian/exponential line broadening. Areas of PME and PDE signals were measured after Gaussian/Lorentzian curve fitting to the experimental data.

As shown in the Figure 1, the phosphomonoester (PME) to phosphodiester (PDE) ratio in uninfected cells is two times higher than in HIV infected ones. The PME signals include

mainly phosphocholine and phosphoethanolamine while PDE was identified mainly as glycerophosphorylcholine. Presence of these metabolites is controlled by the catabolic pathways of phospholipids, which involve phospholipases as well as phosphodiesterases. The mechanisms that determine the content of phosphodiesterases and their modulation by the presence of HIV comprise another target for future investigation.

It is clear however that presented results indicate essential differences in control and regulation of the synthesis and breakdown of phospholipids between HIV-infected and normal cells of the same origin, and a relatively easy to measure PME/PDE ratio can be used for monitoring of the degree of infection and functional changes in the HIV-1 infected cells and tissues.

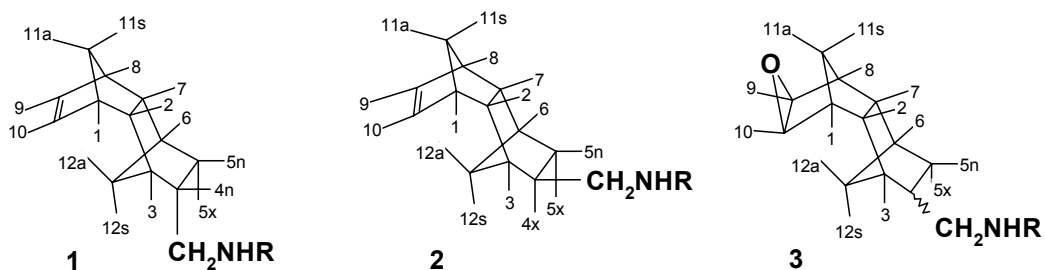
DETERMINATION OF TETRACYCLIC AMINE DERIVATIVES STRUCTURE USING ^1H , ^{13}C , 2D NMR

Olga W. Yuzlenko¹ and Lilia I. Kasyan²

¹ Department of Technology and Biotechnology of Drugs, Jagellonian University, Medical College, Kraków, Poland; ² Department of Organic Chemistry, Dniepropetrovsk National University, Faculty of Chemistry, Dniepropetrovsk, Ukraine,
e-mail: olga_yuzlenko@yahoo.com

On the background of actively investigated bicyclic and adamantane amines [1] there are independently less accessible compounds with tetracyclic carbon skeleton - products of interaction between substituted norbornenes with a new molecule of cyclopentadiene. The polycyclic structure of bis-adducts till now precisely is not determined, usually, experimental researches were carried out with a stereoisomeric mixture.

Our work deals with the search for tetracyclic amine derivatives and determination of their structure [2]. We made an attempt to synthesise stereoisomeric pure exo-(**1**) and endo-4-methylaminotetracyclo[6.2.1.1^{3,6}.0^{2,7}]dodec-9-ene (**2**) derivatives and their epoxides (**3**) to investigate their structure and reactivity. ^1H , ^{13}C , 2D Spectroscopy was applied to determine the spatial structure and substituents orientation.



NMR spectra were useful to determine:

- bicyclic fragments and methylene bridges orientation in tetracyclic (H^2 and H^7 shifts are 2.43 and 1.95 ppm; vicinal coupling constant for protons H^2 and H^7 is $J_{2,7}^2=8.2$ Hz, geminal coupling constants are $J_{2,1/7,8}^3=4.3/4.5$ Hz; proton shifts for H^{11a} and H^{11s} are nearly equivalent, although protons H^{12a} and H^{12s} are shifted with $\Delta\delta\approx 1.5$ ppm);
- criteria for exo- stereoisomers (equivalent shifts for H^9 and H^{10} ; different shifts for paired protons H^2 and H^7 , H^3 and H^6 with $\Delta\delta\approx 0.02$ ppm; shifts for H^{4n} are about 1.45-1.65 ppm; shifts for H^{5n} are $\delta=0.86-0.96$ ppm);
- criteria for endo- stereoisomers (different shifts for H^9 and H^{10} with $\Delta\delta\approx 0.06$ ppm, H^2 and H^7 ; equivalent shifts for protons H^3 and H^6 ; shifts for H^{4x} are $\delta=2.10-2.20$ ppm; shifts for H^{5n} are $\delta=0.49-0.55$ ppm);
- regiochemistry of reactions between epoxides and amines ($\delta(\text{NHCH}_2\text{CHOH})=4.69$ ppm; $\delta(\text{NHCH}_2\text{CHOH})=2.52$ and 2.86 ppm);
- epoxidation pathway and epoxide ring orientation in tetracyclic compounds (shifts for H^9 and H^{10} are nearly 3.10 ppm; shifts for proton H^{11a} are $\delta\approx 0.72$ ppm, and $\delta\approx 1.44$ ppm for proton H^{11s}).

The similar tendencies in ^{13}C NMR spectra shifts were observed. 2D NMR Spectra ($^{13}\text{C}\{^1\text{H}\}$ and $^1\text{H}\{^1\text{H}\}$) were helpful for signal shifts coincidence.

References:

1. Kasyan L.I. Tarabara I.N, Savel'eva O.A., Kasyan A.O. Azabrendanes. III. Synthesis of Stereoisomeric Exo- and Endo-5-Acylaminomethyl-exo-2,3-epoxybicyclo[2.2.1]heptanes and their Reductions by Lithium Aluminium Hydride. *Journal of Heteroatom Chemistry*. **2001**; Vol. 82(3): 119-130.
2. Kasyan A.O., Golodaeva E.A., Yuzlenko O.V., Shyshkina S.V., Shyshkin O.V., Kasyan L.I. Synthesis and stereochemistry of exo-4-methylaminotetracyclo[6.2.1.1^{3,6}.0^{2,7}]dodec-9-ene. *Russian Journal of Organic Chemistry*. **2003**; Vol. 39(12): 1724-11732(9).

NMR STUDY OF Mo AND Re MAGNETISM IN DOUBLE PEROVSKITES

**Dariusz Zając^{a,b}, Czesław Kapusta^a, Peter C. Riedi^c, Marcin Sikora^a, Colin J. Oates^a,
Damian Rybicki^a, Jose Maria DeTeresa^b, David Serrate^b, Clara Marquina^b,
M. Ricardo Ibarra^b, and Javier Blasco^b**

^a *Department of Solid State Physics, Faculty of Physics and Applied Computer Science, AGH University of Science and Technology, Cracow, Poland*

^b *Instituto de Ciencia de Materiales de Aragon, Universidad de Zaragoza - CSIC, Zaragoza, Spain*

^c *Department of Physics and Astronomy, University of St. Andrews, St. Andrews, Scotland, UK*

Double perovskites of the formula $A_2BB'O_6$ are known for their negative high field magnetoresistance at magnetic ordering temperatures, termed “colossal magnetoresistance” (CMR), as well as for a considerable low field magnetoresistance, called giant magnetoresistance (GMR). They also possess relatively high T_C compared with other magnetic perovskites, which altogether makes them good candidates for applications e.g. in spin electronics. In order to study the magnetism of 4d (Mo) and 5d (Re) elements in the Fe-Mo and Fe-Re (as B and B' elements) compounds with different alkaline earth and La substitution (A elements), nuclear magnetic resonance (NMR) measurements have been carried out.

The frequency swept NMR spin echo spectra and relaxation times T_2 have been measured at no applied magnetic field at 4.2 K on polycrystalline powder samples of Ba_2FeMoO_6 , Sr_2FeMoO_6 , Ca_2FeMoO_6 , Ba_2FeReO_6 , Sr_2FeReO_6 and Ca_2FeMoO_6 as well as on the La doped “constant bandwidth” $Sr_{1-3x}Ba_{1+x}La_{2x}FeMoO_6$ ($x=0.1, 0.2, 0.3$) series. The resonant lines observed in the range 30-80 MHz in the case of Mo compounds correspond to ^{95}Mo and ^{97}Mo resonances and the lines at 800-950 MHz in Re based compounds are attributed to ^{185}Re and ^{187}Re resonances. Due to very close gyromagnetic ratios of Mo and Re isotopes their resonances are unresolved. The values of the Mo and Re hyperfine fields (B_{HF}) derived from the spectra amounts to: 19(1)T, 24(1)T, 23(1)T, 87(4)T, 94(1)T and 95(3)T for Ba_2FeMoO_6 , Sr_2FeMoO_6 , Ca_2FeMoO_6 , Ba_2FeReO_6 , Sr_2FeReO_6 and Ca_2FeMoO_6 , respectively. Their relatively large magnitude, too high for the sole “transferred” origin, indicates presence of magnetic moments of $0.6 \mu_B$ at molybdenum and of $1 \mu_B$ at rhenium ions. The measurement in the applied magnetic field shows the shift of the main Mo resonance line toward higher frequencies according to full gyromagnetic ratio. As the dominant Fermi contact contribution to the hyperfine field is antiparallel to the magnetic moment of the parent ion, this means an antiparallel orientation of the Mo (Re) moments to the Fe moments dominating in the magnetisation of the compounds. The results confirm the model of the double exchange like coupling between the minority Fe and majority Mo (Re) spins via antibonding oxygen orbitals, which explains magnetic properties and half metallicity of the compounds.

The values of Mo B_{HF} agree very well with those obtained from theoretical calculations, Figure 1. A departure of the experimental B_{HF} values from theoretical ones for Re is attributed to the presence of an unquenched orbital moment on Re ions, which is confirmed by our measurements with X-ray magnetic circular dichroism method. A comparison of the values of Mo and Re magnetic moments (B_{HF}) with Curie temperatures, T_C of the compounds in the A_2FeMoO_6 and A_2FeReO_6 series as well as in the “constant bandwidth” $Sr_{1-3x}Ba_{1+x}La_{2x}FeMoO_6$ (Fig.2) series shows their linear proportionality. The results mean that the strength of magnetic coupling in the compounds is proportional to the magnetic moment

of Mo (Re) ions, which in turn is proportional to the electron density at these sites. A satellite pattern in the spectra of the La doped compounds reveals a local character of electron doping and the contribution from one La neighbour to the magnetic moment at the adjacent Mo site amounts to $0.043\mu_B$.

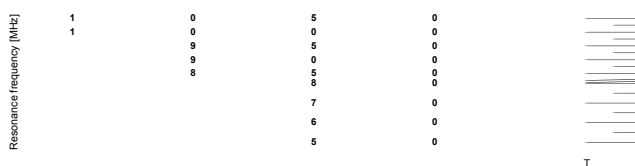


Figure 1. NMR resonance frequencies of the main line for A_2FeMoO_6 and A_2FeReO_6 perovskites (open triangles and diamonds) and theoretical calculations of total and spin magnetic moments (filled points).

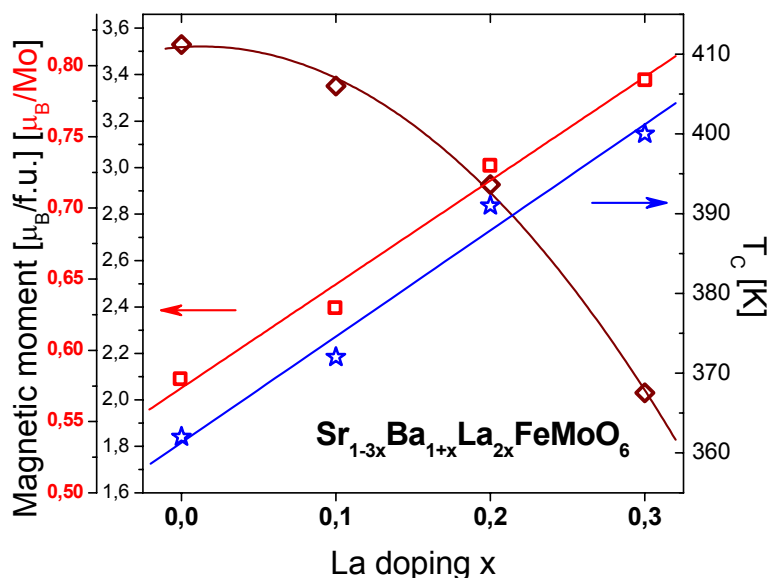


Figure 2. The bulk magnetization (brown diamonds), the magnetic moment at Mo (red squares) and T_C (blue stars) in function of the La doping, for the constant bandwidth series.

IMAGING AND T_2 RELAXATION MAPPING OF ARTICULAR CARTILAGE USING NUCLEAR MAGNETIC RESONANCE

**Tomasz Zalewski, Sławomir Kuśmia, Przemysław Lubiatowski*,
Jacek Kruczyński*, and Stefan Jurga**

Institute of Physics, Adam Mickiewicz University, Umultowska 85, PL-61614, Poznan, Poland

** Department of Orthopaedics, University of Medical Science in Poznan,
June 28, 1956 no 135/147*

The high incidences of cartilage lesions have necessitated the development of techniques for accurate treatment and monitoring of these lesions. Non-invasive assessment of the cartilage properties, especially cartilage organization, could lead to discovery of new therapeutic methods. In our study we are using relaxation time measurements and magnetic resonance imaging methods. Transverse relaxation time T_2 has potential to detect laminar appearance of articular cartilage. T_2 values were measured at 9,4 T in several systems: 1) articular cartilage with scaffold (PLGA - Poly-Lactic-co-Glycolic Acid), 2) articular cartilage with scaffold (PLGA) containing chondrocytes, 3) articular cartilage with artificially induced defects. All articular cartilage specimens were T_2 mapped and the results from magnetic resonance measurements were compared with results obtained from optical microscopy. We suppose that this analysis permits us to correlate spectroscopic findings and histology assessments of articular cartilage organization.

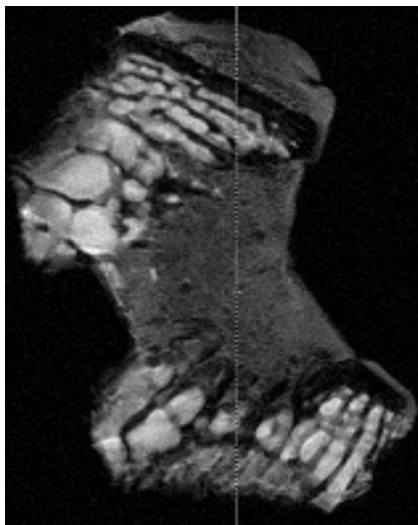


Fig. 1 Articular cartilage with scaffold (PLGA)

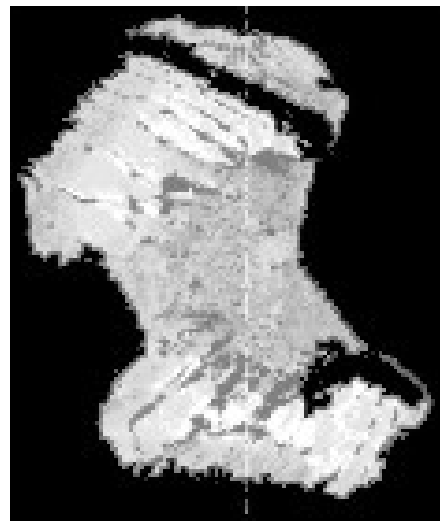


Fig. 2 T_2 map of articular cartilage with scaffold PLGA

References:

- [1] Nina M. Menezes, Martha L. Gray, James R. Hartke, Deborah Burstein, T_2 and $T_{1\rho}$ MRI in Articular Cartilage Systems, *Magn Reson Med* 51(2004): 503-509
- [2] Yang Xia, Heterogeneity of Cartilage Laminae in MR Imaging, *Journal of Magnetic Resonance Imaging* 11(2000):686-693

**THREE-DIMENSIONAL STRUCTURE AND BACKBONE DYNAMICS
OF THE MIXED DISULFIDE OF BOVINE *apo*-S100A1 PROTEIN
WITH β -MERCAPTOETHANOL**

Zhukov I.¹, Ejchart A.¹, and Bierzyński A.²

¹ *Laboratory of Biological NMR, IBB PAS*

² *Department of Biophysics, IBB PAS*

S100A1, a member of the S100 protein family, is a homodimeric Ca^{2+} -binding protein containing 93 residues per subunit. Each subunit of S100A1 has two helix-loop-helix calcium-binding domains and the dimer is stabilized by non-covalent interactions. The protein regulates, in a calcium-dependent manner, a large number of biological processes. Recently, we have discovered that formation of mixed disulfides with glutathione, cysteine and mercaptoethanol increases, by several orders of magnitude, the affinity of S100A1 for calcium. Structural studies have been undertaken to elucidate the mechanism of this phenomenon.

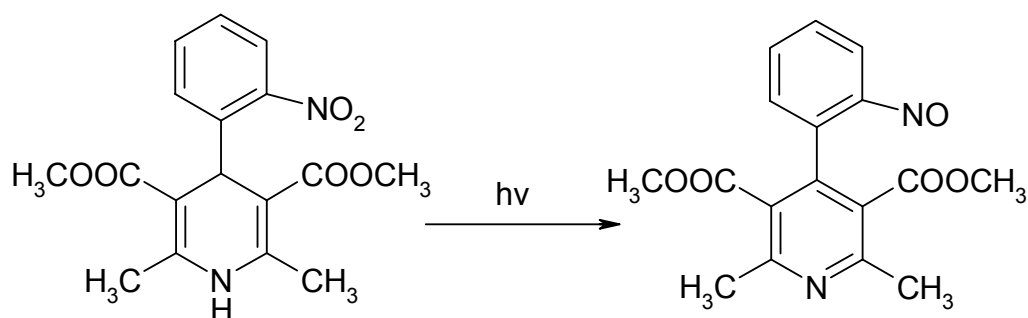
The three-dimensional structure of bovine *apo*-S100A1 with the SH group of cysteine C85 blocked with β -mercaptoethanol was determined by NMR spectroscopy using 2780 NOE distance constraints, 328 dihedral angle constraints, and 148 hydrogen bond constraints (*ca.* 17.5 constraints per residue) derived from a series of 2D and 3D NMR measurements. The final structure was found to be globular and compact with the four helices and a small antiparallel β -sheet in each subunit. The backbone r.m.s.d. value was equal to 1.80 ± 0.38 Å for 12 lowest energy structures. Additionally, S100A1 backbone dynamics was studied by ^{15}N nuclear magnetic relaxation at 11.7 T. Longitudinal relaxation rates, transverse relaxation rates, and $^{15}\text{N}/^1\text{H}$ nuclear Overhauser enhancements were determined for 92 out of 93 backbone amide groups. Results were analyzed using a model-free approach. An overall correlation time, τ_{R} , was equal to 8.1 ns and the internal mobilities of residues in helices I and IV forming dimer interface were found to be more restricted than those in helices II and III, as judged from the generalized order parameter values; $S^2_{\text{I}} = 0.82$ and $S^2_{\text{IV}} = 0.81$ vs. $S^2_{\text{II}} = 0.74$ and $S^2_{\text{III}} = 0.73$.

¹³C CPMAS NMR STUDIES OF NIFEDIPINE AND ITS ANALOGUES

Monika Zielińska and Iwona Wawer

Department of Physical Chemistry, Faculty of Pharmacy, The Medical University of Warsaw, Banacha 1, 02-097 Warsaw, Poland

Nifedipine and its analogues belong to the family of 1,4-dihydropyridine (DHP) derivatives that can modulate calcium permeability across the cell membrane (so-called calcium channels blockers). This group of drugs has been extensively used in the treatment of cardiovascular disorders. Besides nifedipine, nitrendipine and felodipine have been introduced to the pharmaceutical market.



Unfortunately those substances are unstable under daylight conditions. Photochemical decomposition is accompanied by alteration in their activities and the loss of therapeutic effects [1].

The aim of our study was to follow this process by means of solid state NMR.

¹³C CPMAS NMR spectra of were recorded on the Bruker 300 and 400 MHz instruments, the samples were spun in 4mm ZrO₂ rotor at 8 kHz.

Nifedipine and its photodegradation product as well as nitrendipine and felodipine were investigated. On illumination nifedipine converts to 2-nitrosophenyl derivative and ¹³C CPMAS chemical shifts reflect this structural change. Characteristic feature of nifedipine and its analogues is the configuration of the ester groups with the antiperiplanar or synperiplanar location of carbonyl [2]. The analysis of solution-to-solid state chemical shifts indicated that carbonyl groups are involved in hydrogen bonding .

References:

1. A. Hilgeroth, G. Hempel, U. Baumeister, D. Reichert; *Solid State NMR* 13 (1999) 231-243.
2. R. Fossheim, A. Joslyn, A.J. Solo, E. Luchowski, A. Rutledge, D.J. Triggle; *J. Med. Chem.* 31 (1988) 300-305.

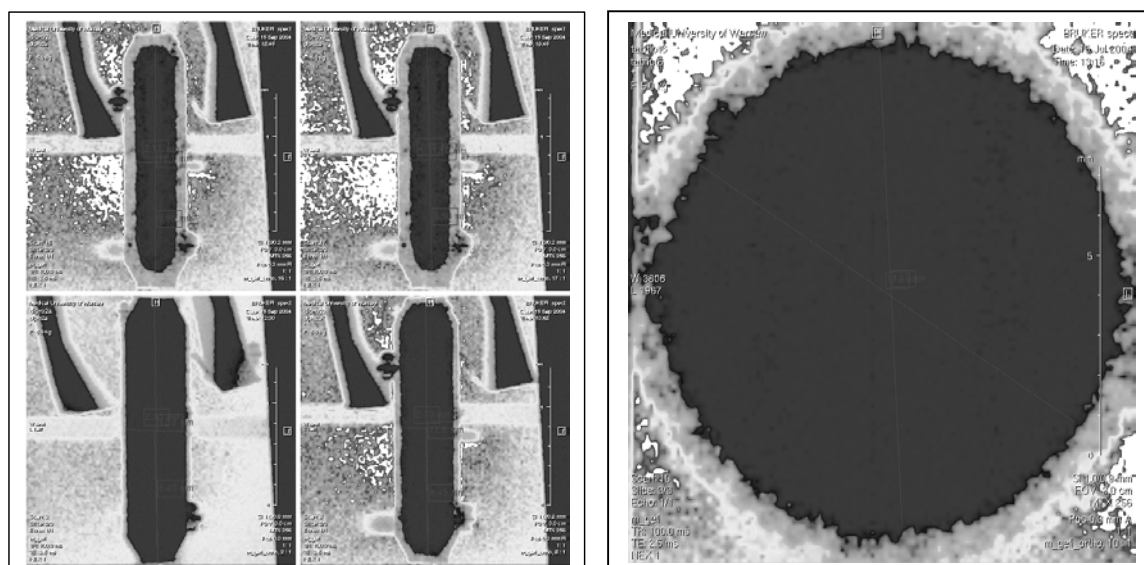
MRI STUDIES OF TABLETS

Monika Zielińska^a, Bożena Kwiatkowska^b, and Michał Dera^b

^aDepartment of Physical Chemistry, ^bDepartment of Applied Pharmacy, Faculty of Pharmacy, Medical University of Warsaw, Banacha 1, 02-097 Warsaw, Poland

NMR imaging, a non-invasive technique, has been used to study porosity of tablets in 1995 [1]. Water mobility in the gel layer of different HMPC tablets was studied [2,3]. The disintegration rate of bromhexin tablets is within 1-30 min, therefore fast imaging method FLASH with spoiling gradients was used to obtain images in short time intervals [4]. MRI allowed studying the disintegration of paracetamol tablets under acidic gastric pH conditions [5], which may help to predict their behavior in the stomach after oral administration.

It seemed worth to extend the studies into some new, promising type of tablets, such as floating one. The floating tablets are designed to prolong the gastric residence time, to increased the drug bioavailability and diminish the side effects of irritating drugs.



The measurements were performed on a Bruker AVANCE 400 MHz NMR wide bore spectrometer equipped with micro imaging probehead 20mm. The kinetic of water penetration was followed using gradient echo fast imaging (mgefiortho) sequence with repetition time 100 ms and echo time 2,5 ms. The selected images of floating tablet with paracetamol as active substance are illustrated above.

References:

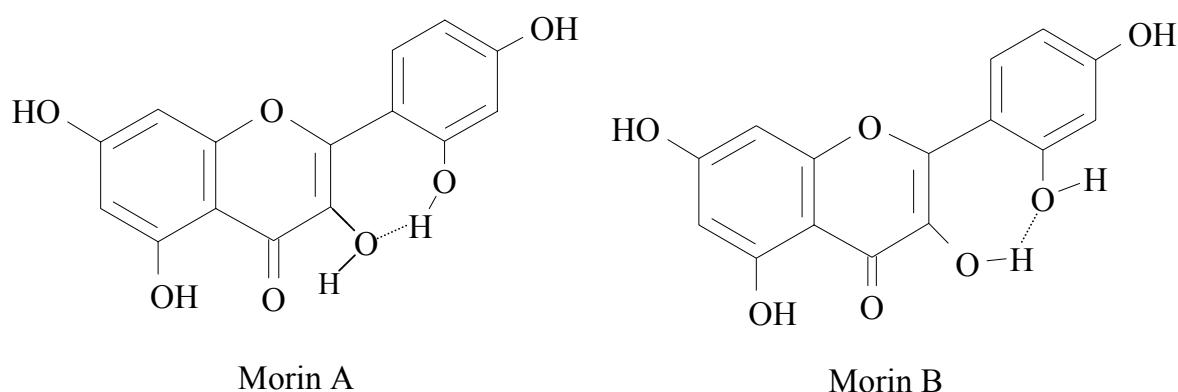
1. G. Nebgen, D. Gross V. Lehmann, F. Muller; J. Pharm. Sc. Vol.84, No 3, 1995.
2. J. Tritt-Goc, N.Pislewski; J. Control. Release 80 (2002) 79-86.
3. A.R. Rajabi-Siahboomi, R.W. Bowtell, P. Mansfield, M.C. Davies, C.D. Melia; Pharm. Res. Vol.13, No. 3, 1996.
4. S. Kwieciński, M. Weychert, A. Jasiński, P. Kulinowski, I. Wawer, E. Sieradzki; Appl. Magn. Reson. 22, 23-29 (2002).
5. J. Tritt-Goc, J. Kowalczyk; Eur. J. Pharm. Sci. 15 (2002) 341-346.

POLYMORPHISM OF MORIN (2',3,4',5,7-PENTAHYDROXYFLAVONE) – ¹³C CPMAS NMR AND GIAO CHF CALCULATIONS

Agnieszka Zielińska, Katarzyna Paradowska, Jacek Jakowski, and Iwona Wawer

Department of Physical Chemistry, Faculty of Pharmacy, Medical University of Warsaw,
02-097 Warsaw, Banacha 1

The crystal structure of morin has been studied by x-ray diffraction in 1994 [1] and the results showed the presence of two molecules (A and B) in the asymmetric unit cell. The most interesting feature of these structures is their pattern of hydrogen bonding. It can be characterized as “clockwise” and “anticlockwise”, according to the orientation of hydroxyl groups. It encouraged us to study solid morin by MAS NMR.



¹³C CPMAS NMR spectra were recorded on a BRUKER AVANCE DSX-400 spectrometer; the powder sample was packed in a 4 mm ZrO₂ rotor and spun at 8 kHz. Besides standard spectrum, also delayed decoupling and short contact time experiments were performed in order to separate the signals of quaternary and protonated carbons.

The ¹³C CPMAS spectrum of morin contains two sets of resonances, as expected. The assignments were made using information from solution-state NMR, however it is impossible to definitely assign carbons that have the same numbers of protons and similar chemical shifts. Theoretical studies on particular conformers supply additional information and shed light on the problem how the orientation of hydroxyl groups and phenyl ring influence the shielding of aromatic carbons. The DFT method was used to calculate shielding constants for morin A and B, the geometry was optimized with 6-31G (d,p) base, starting from crystallographic data. The relationships between CPMAS chemical shifts for all carbons of the molecule and their theoretical shielding constants are fairly good, although only intramolecular interactions are reproduced. Significant differences $\Delta = \sigma_{\text{DFT}}(\text{A}) - \sigma_{\text{DFT}}(\text{B})$ between two conformations of morin appear for C2, C3 and C2'. The shielding constants reflect different orientations of C2'-OH and C3-OH hydroxyls.

Reference:

1. V. Cody, J.R. Luft, Conformational analysis of flavonoids: crystal and molecular structures of morin hydrate and myricetin (1:2) triphenylphosphine oxide complex, *J. Mol. Struct.* 317 (1994) 89-97

¹ L. Kozerski, A.P. Mazurek, R. Kawêcki, W. Bocian, P. Krajewski, E. Bednarek, J. Sitkowski, M.P. Williamson, A.J.G. Moir, P.E. Hansen, *Nucleic Acids Res.* (2001), **29**, 1132.